PARAMETRIC STUDY IN SOIL STRUCTURE INTERACTION OF A DIAPHRAGM WALL TYPE BERTHING STRUCTURE

Thesis

Submitted in partial fulfillment of the requirements for the degree of

DOCTOR OF PHILOSOPHY

By

YAJNHESWARAN.B

DEPARTMENT OF APPLIED MECHANICS AND HYDRAULICS
NATIONAL INSTITUTE OF TECHNOLOGY KARNATAKA
SURATHKAL, MANGALORE- 575 025

DECEMBER 2017

PARAMETRIC STUDY IN SOIL STRUCTURE INTERACTION OF A DIAPHRAGM WALL TYPE BERTHING STRUCTURE

Thesis

Submitted in partial fulfillment of the requirements for the degree of

DOCTOR OF PHILOSOPHY

By

YAJNHESWARAN.B
(AM11P03)

Department of Applied Mechanics & Hydraulics
NITK, Surathkal

DEPARTMENT OF APPLIED MECHANICS AND HYDRAULICS
NATIONAL INSTITUTE OF TECHNOLOGY KARNATAKA
SURATHKAL, MANGALORE- 575 025

DECEMBER 2017

D E C L A R A T I O N

By the Ph.D. Research Scholar

I hereby *declare* that the Research Thesis entitled **"Parametric Study in Soil Structure Interaction of a Diaphragm wall type Berthing Structure",** which is being submitted to the **National Institute of Technology Karnataka, Surathkal** in partial fulfilment of the requirements for the award of the **Degree of Doctor of Philosophy** in the **Department of Applied Mechanics and Hydraulics** is a *bonafide report of the research work carried out by me*. The material contained in this Research Thesis has not been submitted to any University or Institution for the award of any degree.

YAJNHESWARAN.B
(Register Number: 110635 AM11P03)
Department of Applied Mechanics and Hydraulics
National Institute of Technology Karnataka, India

Place: NITK Surathkal
Date: 27-12-2017

C E R T I F I C A T E

This is to *certify* that the Research Thesis entitled **"Parametric study in soil structure interaction of a diaphragm wall type berthing structure",** submitted by **Yajnheswaran. B** (Register Number: 110635 AM11P03) as the record of the research work carried out by him, is *accepted as the Research Thesis submission* in partial fulfilment of the requirements for the award of degree of **Doctor of Philosophy**.

Prof. Subba Rao
(Research Guide)
Department of Applied Mechanics and Hydraulics
National Institute of Technology Karnataka, India

Prof. Amai Mahesha
(Chairman – DRPC)
Department of Applied Mechanics and Hydraulics
National Institute of Technology Karnataka, India

ABSTRACT

Berthing structure is one of the most essential facility required in ports and harbours. Diaphragm wall provides structural support and water tightness to the berthing structure by retaining the back fill soil. Large earth pressure and water loads result massive and costly construction. It is required to examine an innovative wall system that is more cost effective than traditional wall systems. The study of soil-structure interaction is essential to understand the behaviour of wall under static and dynamic loading conditions.

The performance of the anchored diaphragm wall depends on the wall stiffness, embedded depth of wall, type of anchor and its location and the type of loads acting on the wall. Study of the effect of construction stages on the performance of wall is important for the safer wall installation. The difference in stiffness of the wall causes redistribution of stresses and consequent reduction in displacement and bending moment. The present study analyses the diaphragm wall without anchor, and with anchor at varying locations for static and dynamic loading conditions. The study is also extended for a diaphragm wall with varying stiffness.

To study such behavior, finite element based software Plaxis 2D and 3D are adopted in the present study. In Plaxis 2D static and dynamic analysis are carried out to obtain the maximum displacement, shear force and bending moment of a diaphragm wall with and without anchor. Similarly, in Plaxis 3D, static analysis are carried to find maximum displacement, shear force and bending moment for the diaphragm wall with and without anchor. Analysis is undertaken to study the effects of construction sequences and effect of stiffness by varying the stiffness of the wall within the sections. To study the effect of stiffness on the behavior of diaphragm wall, static analysis is carried on uniform and non-uniform sections. Seven different diaphragm wall sections, section1 and sections 2, 3, 4, 5, 6 & 7, having uniform and non-uniform configurations respectively, are modelled and the results are compared with the actual section.

In Plaxis 2D static analysis, the maximum displacement, shear force and bending moment are reduced by 91.79%, 11.69% & 57% respectively, when anchor is

introduced in the diaphragm wall. In Plaxis 2D dynamic analysis for the case with anchor, the maximum value of displacement, shear force and bending moment are increased by 7.2%, 10% & 13.5%) with respect to static analysis.

The maximum values of displacement, shear force & bending moment obtained in Plaxis 2D are higher by 22.82%, 15.43% & 17.98% when compared with Plaxis 3D results. The maximum bending moment obtained in Plaxis 3D analysis for anchored diaphragm wall for the case without considering the construction stage is reduced by 59.6% and in Plaxis 2D, it is 54.41%, when compared to the maximum bending moment obtained by considering the construction stage for the anchor location at +4.5 m.

Even though the stiffness of section 1 is 83.77% less than that of actual section, displacement for section 1 is increased by 70.2%, and bending moment is reduced by 46.44% when compared with the actual section. Maximum displacement and bending moment are found corresponding to anchor location +4.5 m. Both displacement and bending moment are found minimum at anchor location -6 m.

The displacement of the T section is reduced by 47.9%, 43.5% & 38.4% for anchor location +4.5m, +2.5m and 0 m respectively when compared to actual section. Similarly, the bending moment for T section is reduced by 82.6%, 80.14% & 81.6% respectively, for the same anchor locations.

The analysis of section 4 & 5 shows that rigid concrete panel is susceptible to higher bending moment when flexible pile is introduced in between rigid RCC wall. When the two sections of different stiffness are coupled to form a single section, the stiffer member is taking higher bending moment.

In the present investigation validation of analysis, results are carried by comparing the results obtained by empirical models, case studies having analytical and numerical results and field measured data of similar case studies.

Keywords: berthing structure, diaphragm wall, static, dynamic, stiffness, different sections, anchor, excavation, cantilever, propped, displacement, shear force, bending moment and redistribution.

ACKNOWLEDGEMENTS

With deep sense of gratitude, I express my heartfelt thanks to Prof. Subba Rao, Professor, Department of Applied Mechanics and Hydraulics, NITK, Surathkal for his elucidative and comprehensive guidance and encouragement at every stage of this work. He has been a source of inspiration to me in academics as well as in my career. His moral support and critical guidance has been priceless which has given me an invaluable opportunity to publish my research work in many international / national journals/conferences which is a matter of great pride and satisfaction to me. The easily approachable nature and ever helpful attitude of Prof. Subba Rao will always be admired, valued and cherished.

I thank the former Directors of NITK, Surathkal, Prof. Sandeep Sancheti, Prof. Swapan Bhattacharya, Prof. K.N Lokesh and the present Director, Prof. Karanam Uma Maheshwar Rao for granting me the permission to use the institutional infrastructure facilities, without which research work would have been impossible.

I am greatly indebted to Prof. M K. Nagaraja, Prof. Subba Rao and Prof. G. S. Dwarakish, former Heads of the Department of Applied Mechanics and Hydraulics, NITK, Surathkal, and Prof. A. Mahesha, the present Head of the Department for granting me the permission to use the departmental computing and laboratory facilities available for necessary research work to the maximum extend which was very vital for the completion of the computational aspects relevant to this research.

I am also thankful to Prof. A U Ravi Shankar, Prof. D. Venkat Reddy, former Heads of the Department of Civil Engineering, NITK, Surathkal, and Prof. George Varghese, the present Head of the Department for granting me the permission to use the departmental computing and laboratory facilities available for necessary research work.

I am grateful to Research Progress Committee members, Prof. Katta Venkataramana, Dept. of Civil Engineering and Dr. Dattatraya N. Gaonkar Dept. of Electrical & Electronics Engineering, for their critical evaluation and useful suggestions during the progress of the work.

I sincerely acknowledge the help and support rendered by all the Professors, Associate Professors and Assistant Professors of Department of Applied Mechanics and Hydraulics.

I gratefully acknowledge the support and all help rendered by the Post Graduate students Ms Parvathi, Sri Ranjan and Sri. Akshay during the research work.

I thank former foreman Mr. Jagadish, and the present foreman Mr. Seetaram, and his supporting staff, Mr, Anand Devadiga, Mr Gopala Krishna, Mr. Padmanabha and Mr. Padmanabha Acharya for their help and support.

I thank Mr. Balakrishna, Literary Assistant, NITK, Surathkal, for all help rendered without which it was impossible for me to complete this work on time.

I express heartfelt gratitude to authors of all those research publications which have been referred in this thesis.

A number of people have helped directly and indirectly in the course of this work. I wish to convey the deepest thanks to everyone who has contributed towards this thesis, without whom its completion would have been impossible.

Finally, I wish to express my gratitude, love and affection to my family members, mother Devaki Amma, wife K.N Sunitha, son Nandakishor. E. N and my colleagues for their continuous and invaluable encouragement on the road to the completion of my research. I also thank my late father K Vasudeva Holla, and I dedicate all my gains to his soul.

Above all, I would like to thank Almighty God for the completion of this thesis.

Yajnheswaran. Bhagithimar

CONTENTS

LIST OF FIGURES

LIST OF TABLES

NOMENCLATURE

Symbols	Explanation
EA	Axial modulus
EI	Flexural rigidity
μ	Poisson's Ratio
γ_{sat}	Saturated density
c	Cohesion
∅	Friction angle
R	Correlation coefficient
δh	Maximum displacement
γ_w	unit weight of water
h_{avg}.	Average support spacing
H_e	Excavation depth
t	Thickness of diaphragm wall
$\underline{\underline{L}}^T$	Transpose of a differential operator
$\underline{\sigma}$	Vector with stress component.
$\underline{b}$	body force
ψ	Dilatancy angle
σ	Normal stress
ε	Strain
E	Modulus of Elasticity
$\sigma_x, \sigma_y, \sigma_z$	Stress components
$\tau_{xy}, \tau_{yz}, \tau_{zx}$	Shear stress components
$\varepsilon_x, \varepsilon_y, \varepsilon_z$	Strain components
$\gamma_{xy}, \gamma_{yz}, \gamma_{zx}$	Shear strain components
K	Shear modulus
E_{oed}	Oedometer modulus
$f_{1a}, f_{1b}, f_{2a}, f_{2b}, f_{3a}, f_{3b}$	Yield functions
$\sigma_1, \sigma_3, \sigma_2$	Major. Minor, intermediate principal stresses

M	Mass matrix
ü	Acceleration
u	displacement
C	Damping coefficient
K	Stiffness matrix
F	Load vector
Vp	Compression wave velocity
Vs	Shear wave velocity
γ	Unit weight
α and β	Rayleigh coefficients
ξ_i	Damping ratio
ω_i	Frequencies
V_R	Rayleigh wave
g	Acceleration due to gravity
u_x, u_y and u_z	Translational degrees of freedom
$\emptyset_x, \emptyset_y, \emptyset_z$	Rotational degrees of freedom
m	Meter
f_{ck}	Characteristic compressive strength of concrete
h_1, h_2 and h_3	Strut spacing

CHAPTER 1

INTRODUCTION

1.1 SOIL - STRUCTURE INTERACTION (SSI)

The real behavior of structures in contact with the ground involves an interactive process beginning with the construction phase and ending with a state of balance after a period of adjustment of stresses and strains with in the structures and within the ground influenced by the structure (IStructE, 1989). Most of the civil engineering structures involve some type of structural element with direct contact with soil. The process in which the response of the soil influences the motion of the structure and the motion of the structure influences the response of the soil is termed as soil-structure interaction (SSI) (Tuladhar, 2008). Two broad objectives of analysing soil structure interaction problems are: i) estimation of displacements ii) calculating the distribution of internal stresses. Neglecting the effects of soil structure interaction is not advisable for heavy structures resting on relatively soft soils. In order to consider the forces acting and the safety against failure in the structure, calculation of earth-pressures are performed based on loads and soil conditions at the site (Bjureland, 2013). Serviceability limit state is adopted to calculate deformations and forces acting on the retaining structure and the surrounding environment. Calculations are performed using characteristic values on both earth-pressures and material strength parameters. Deformations can be studied in different ways, by using empirical relations based on data from measurements, performed by Terzaghi and Peck and presented by Peck (1969), to get an estimate of the expected ground movements or by performing numerical calculations using soil models implemented in a Finite Element Methods (Ryner et al. 1999).

Recent trends in earthquake engineering include analyzing the displacement that a structure undergoes during an earthquake, and considering the structural as well as nonstructural damage that it causes. Even though soil-structure interaction increases damping, which is

beneficial, it can also cause additional displacement to the overall structure. This displacement of the structure in some cases have detrimental effects. In structures founded on softer soil, the interaction can cause large increase in the natural period of the structure, leading to much larger relative displacements. The motion experienced by the base of a structure founded on rock is essentially identical to that occurring in the same point before the structure built. The seismic analysis can thus be restricted to the structure excited by this specified motion. Yegian et al. (2001) described a wide variety of applications of dynamic soil structure interaction in geotechnical engineering practice. Ingale et al. (2015) concluded from the laboratory investigation that, the earth pressure obtained by seismic cases are higher than that of static cases.

1.2 BERTHING STRUCTURE

In ports and harbours to provide facilities for berthing and mooring of vessels, transporting cargos, debark and leaving the passengers and vehicles, berthing structures are required. One of the most expensive structures in the ports is berthing structure. In this structure, lateral forces are caused by impact of berthing ships, pull from mooring ropes, pressure of wind, current, wave and floating ice, seismic force, earth pressure, differential water pressure and live load on the structure.

Berthing structure is classified as open type or vertical face type. Open type structure (Fig. 1.1) consists of a rigid deck supported over vertical piles or combination of vertical and raker piles. The slope underneath the structure, established either by dredging or by filling should be constructed prior to the pile driving to avoid lateral forces to be developed on the piles due to the lateral movement of soil. In vertical type structures, sheet pile walls, block wall, caissons and diaphragm walls are used.

1.2.1 Diaphragm walls.

Diaphragm walls are one of the soil retaining structures, which provide structural support and water tightness to the berthing structure. The reinforced concrete diaphragm walls are also called slurry trench walls. In general, the thickness and width of diaphragm wall panel varies from 0.6 m to 1.1 m and 2.5 m to 6.0 m respectively. The wall is constructed panel by panel in full depth. Short widths of 2.5 m are selected in less stable soils, under very

high surcharge or for very deep walls. Different panel sections other than the conventional rectangular sections; T and composite sections are possible according to the requirement and site suitability.

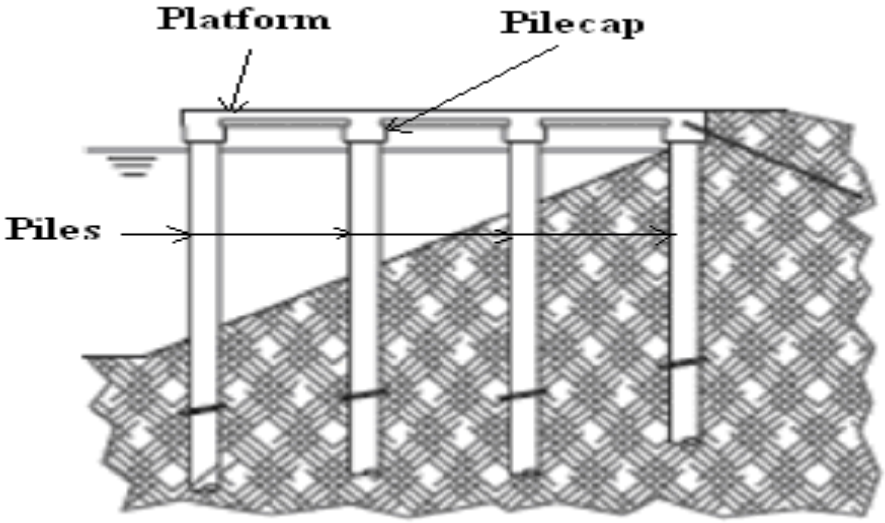

Fig. 1.1 Open type structure (Gaythwaite, 1981)

Anchored diaphragm walls (tie back wall) provide the support of vertical or near vertical excavations (Fig. 1.2). A tieback is a horizontal wire or rod, or a helical anchor, used to reinforce retaining walls for stability by fixing one end to the wall and the other end to a stable structure, such as a concrete deadman which has been embedded into the ground or anchored into earth with sufficient resistance. The tie rod anchors are provided in order to strengthen the structure and to resist the lateral loads and their by reduce the deflection largely. The use of tie rod anchors in diaphragm wall will reduce the bending moment and lateral deflection and thus the required cross sectional area of the wall and the amount of reinforcement will be reduced resulting in an economical design of the structure. In general, excavation in soil mass causes unloading and local yielding of the soil. If the opening is deep enough, a shear surface develops, resulting in some form of shear failure. A retaining wall is constructed against the excavation face to limit unloading of the soft ground and inhibit formation of a failure surface. An active stress environment acts upon the wall, and unless it is stable, a resisting force must be introduced, for example, in the form of anchors, to provide the conditions of stability. On the other hand, movement (vertical or horizontal) must be restrained and confined within allowable limits.

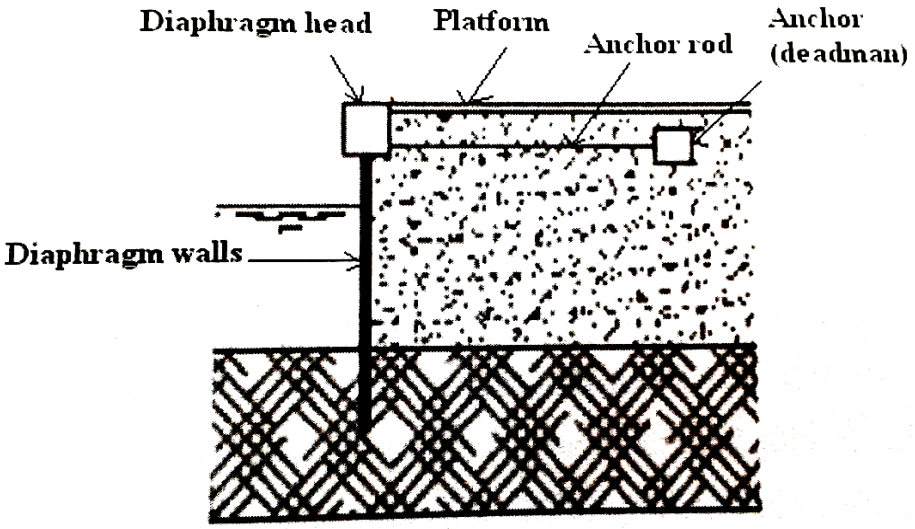

Fig. 1.2 Anchored diaphragm wall (Gaythwaite, 1981)

The mechanism of an anchored wall is thus complex since the ground, wall and anchors must interact and work together in order to resist earth pressure loads and surcharges developing during and after construction, and restrict deformations to acceptable values. As the wall deflects toward the excavation under the lateral loading, the anchor stretches and initiates the load transfer in the fixed zone.

1.2.2 Soil Arching and 3-D Effects on Diaphragm wall

When there is a difference of the stiffness between the installed structure and the surrounding soil, arching occurs. If the structure is stiffer than the soil then load arches onto the structure. Otherwise, if the structure is less stiff than the soil then load arches away from the structure. For instance, if part of a rigid support of soil mass yields, the adjoining particles move with respect to the remainder of the soil mass. This movement is resisted by shearing stresses, which reduce the pressure on the yielding portion of the support. Terzaghi (1959) observed that arching also takes place if one part of a yielding support moves out more than the other part. Differing stiffness of wall components may lead a three dimensional stress flow in the surrounding soil. The 3-D soil pressure transfer from a yielding mass in the out of plane direction is referred as soil arching. Current conventional design procedures for flexible or rigid diaphragm walls do not take in to account the 3-D

stress flow in the surrounding soil mass. These phenomena have significant effect on distribution of earth pressure and consequently bending moments and shear forces acting on a structure. Arching involves stress transfer from yielding part of the soil to the unyielding part of the soil. It depends on shear strength of soil and yielding of soil.

Numerical models involving FEM can offer several approximations to predict true solutions in problems of soil structure interaction. The accuracy of these approximations depends on the modeler's ability to interpret what is happening in the field. Often the problem being modelled is complex and has to be simplified to obtain a solution. Finite element method has become more popular as a tool to predict the soil response. This has led to increased pressure on researchers to develop comprehensive descriptions for soil behavior, which in turn leads to more complex constitutive relationship. A constitutive model to be satisfactory it must be able to: (i) define the material behaviour for all stress paths; (ii) identify model parameters by means of standard material tests; and (iii) physically represent the material response to changes in applied stress or strain (Prevost & Popescu, 1996). Previous studies have explored constitutive models and found that the use of isotropic models such as elasto plastic Mohr–Coulomb and Drucker–Prager models are sufficiently accurate.

1.2.3 Methods of Analyzing Soil-Structure Interaction of a Diaphragm wall

There are several methods to analyse the soil structure interaction of a diaphragm wall structure. Some of the methods are; a) Equivalent Beam Method, b) Beam on Elastic Foundation Method, c) Finite Element Method, d) Mobilized Strength Design method (MSD) etc. The methods of soil structure interaction under earth quake are; a) Pseudo static methods and empirical correlations, b) simplified dynamic analysis, c) fully coupled numerical analysis, d) performance based design, e) finite element methods etc.

1.3 OBJECTIVES AND SCOPE OF THE WORK

In the present study, it is proposed to perform FEM analysis to asses 2D and 3D aspects of diaphragm wall type berthing structure. For the analysis, the anchored diaphragm wall of multy purpose deep draft berth of NMPT is considered. The investigation thus has been the following objectives,

- ✓ To perform Engineering assessment of 2D & 3D soil structure interaction of diaphragm wall with and without anchors.
- ✓ To analyse the effect of dredging on the diaphragm wall**.**
- ✓ To Analysis the diaphragm wall considering seismic forces.
- ✓ To study the effect of anchor and its location in the diaphragm wall.
- ✓ To study behavior of diaphragm wall during the different stages of construction.
- ✓ To Study the stiffness effect by varying the diaphragm wall sections and to develop a data base of flexible wall and stiff wall system.
- ✓ To validate the results by comparing with case studies and design charts.

1.3.1 Scope

Construction of piles and diaphragm wall supporting open type berthing structure on marine soils results in the development of time dependent vertical and horizontal sub soil displacement. Whereas the landside of the berthing structure may generate axial and lateral loads on the piles and diaphragm walls during dredging. Because of the complexity in soil behavior, the accurate prediction and conclusion of actual displacement is difficult while following the conventional design procedures of berthing structure. A common practice in design of diaphragm wall is to design a thick section of uniform stiffness throughout. However, it may not be economical always. The present study investigates the deformations and corresponding bending moments resulting from the interaction between the structure and the soil, which are not, included in simplified 2-D design procedures. Results of the 2D & 3-D analyses are compared with case studies having full-scale field test results. The study also includes the behavior of structure under varying the stiffness. The assessment of soil structure interaction of a diaphragm wall is useful in sizing of the structural members, spacing of the structural members, to get the exposed height of the wall, and to assess the depth of embedment of wall etc.

1.4 FORMAT OF PRESENTATION

The thesis is presented in eight chapters. **Chapter 1** introduces the basic concepts of soil structure interaction, different tie back wall systems, importance of study of SSI of

diaphragm wall, soil arching and 3-D effects on diaphragm wall and scope & objectives of the study. **Chapter 2** gives a review of the literature of previous research and the problem formulation & objectives of the present research work. **Chapter 3** explains current design methods for tieback wall system, description of software, methodology, study area and data collection. **Chapter 4** includes 2D analysis of diaphragm wall with respect to static and dynamic loading. In **Chapter 5,** 3D analysis of diaphragm wall for static loading and construction sequence analysis of diaphragm wall is included. **Chapter 6** includes 3-D analysis of diaphragm wall with different cross sections. In **Chapter7** validation of results by comparing case studies and design charts are included. **Chapter 8** represents the summary of present study with the main conclusions listed and the scope for future work.

CHAPTER 2

LITERATURE REVIEW

2.1 SOIL – STRUCTURE INTERACTION

A review of related research in the area of soil structure interaction (SSI) of diaphragm wall is presented in the chapter. The focus of the review is SSI of flexible and rigid wall system. The major findings include,1) lateral response of diaphragm wall during dredging, 2) construction sequences, 3) field model study, 4) FEM and computer based analytical studies, 4) numerical studies on retaining walls, 5) laboratory model studies, 6) seismic response of retaining wall etc.

Tschebotarioff (1948) modified Equivalent Beam Method by conducting extensive large-scale (1:10) model tests at Princeton University in New Jersey on flexible wall. Sand was used as backfill for these tests. In one series of tests strain gauges were used to measure bending moments. Bending moments obtained from the strain measurements were less than those from conventional methods. It was noted the point of contraflexure occurred at or near the dredge line. He developed a design procedure which was a modification of the Equivalent Beam Method, based on information gained in the model tests. The design procedure was based on the assumption that a hinge is formed at the dredge line. The study also investigated the effect of the method of construction on earth pressures.

Rowe (1957) performed approximately 900 small-scale model tests on anchored sheet pile walls. He conducted two types of tests denoted as pressure tests and flexibility tests. The pressure tests were conducted to obtain the pressure distribution existing on a sheet-pile wall undergoing movement. The flexibility tests were carried out to study the influence of pile flexibility on design factor. Rowe concluded when backfilling was complete, the distribution of earth pressure followed Coulomb's theory of active earth pressures with no wall friction. During dredging, the pressure at the tie rod level increased. This increase continued until passive failure, provided no yield at the anchor was allowed. Outward yield

of the tie rods caused a breakdown of the arching. The yield necessary to completely relieve the arching at the tie rod level varied with the amount of surcharge and the tie rod depth. A maximum tie rod yield H/1000 (where H is the wall height) was sufficient to relieve the arching in all test cases. The major part of moment reduction was due to flexure below the dredge line. The test also realized that, increase in flexibility of the wall leads greater moment reduction and the moment reduction depends upon the location of dredge line and the density of the sand. The test also showed the reduction in wall flexibility below the dredge level reduced the tie rod force.

Mana and Clough (1981) carried out parametric studies on the effect of wall stiffness and strut spacing, the effect of strut stiffness and excavation geometry such as excavation width and depth of the underlying firm layer, the effect of strut preloading and calculation of elastic soil stiffness on excavation induced deformation.

The study concludes;

1) Increasing the wall bending stiffness or decreasing strut spacing decreases movement. This effect is more significant when the factor of safety is low.
2) Increasing the strut stiffness reduces movement, though the effect shows diminishing return at very high stiffness.
3) Movement increases as excavation width and depth to an underlying firm layer increases. Use of preloads in the struts reduces movement, although there is a diminishing returns effect at higher preloads.
4) Movement levels are strongly influenced by the soil modulus. Higher modulus leads to smaller movement.

Clough & Rourke (1990) proposed a semi-empirical procedure for estimating movement in the excavation of clay in which the maximum lateral wall movement δ_{hm} is evaluated relative to factor of safety (FS) and system stiffness, which is defined as follows: System stiffness $(\eta) = EI/\gamma_w h^4$

Where EI is the flexure rigidity per unit width of the retaining wall, γ_w is the unit weight of water and h, the average support spacing. The factor of safety (FS) is defined according to Terzaghi (1943), the system stiffness is defined as a function of the wall flexural stiffness, average vertical separation of supports, and unit weight of water, which is used as a normalizing parameter. Fig. 2.1 shows δ_{hm} plotted relative to system stiffness for various FS. The family of curves in the figure is based on average condition, good workmanship, and the assumption that cantilever deformation of the wall contributes only a small fraction

of the total movement. A method for estimating cantilever movement is also recommended by Clough & Rourke (1990) to be added directly to those predicted by the Fig. 2.1.

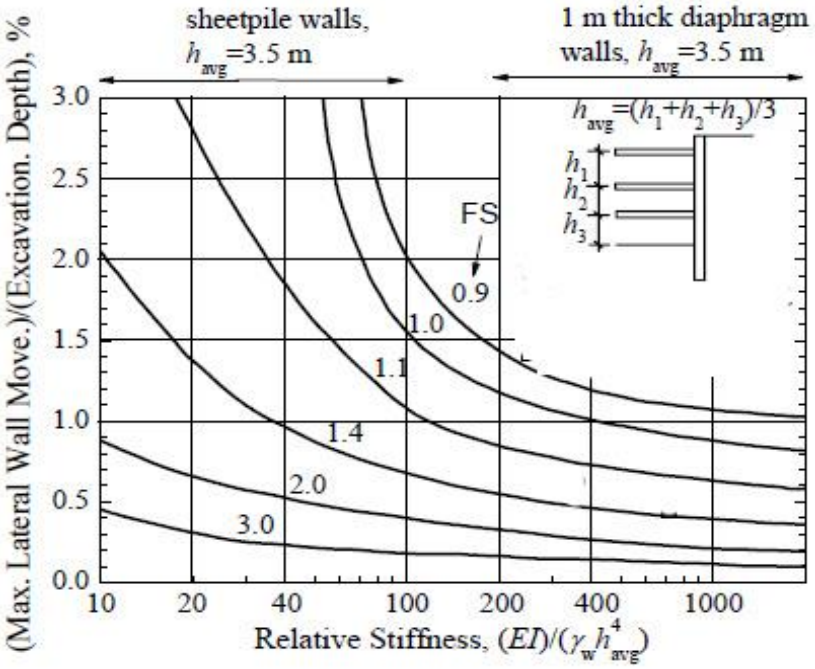

Fig. 2.1 Design chart for estimating maximum lateral wall movement in soft to medium clays (Clough and O'Rourke 1990).

Tie-back behavior of wall under service conditions were studied by Spiros Costopoulos (1988) with the aid of a detailed physical model and verified by a simple numerical model. Test results were then extrapolated to realize the practical aspects of the experimental data. A small scale physical model test was conducted to study soil and wall movements, variation in anchor pre-stress as well as sand stresses on the wall. Numerical parametric analysis of soil structure interactions based on a winkler model were also made by varying soil stiffness and anchor pre-stress values to fit the model tests. From the study it was concluded the soil-wall-anchor interaction under "service conditions" was governed by the wall penetration depth and the anchor pre-stress, the stabilizing action of which was a function of the displacement inside the sand mass.

Mosher and Knowles (1990) conducted an analytical study of a 50 feet high temporary tieback reinforced concrete diaphragm wall at Bonneville Lock and dam on the Columbia River. The wall was installed by the slurry trench method of construction. This temporary wall was used to retain soil from the excavation for the construction of a new lock at the site and to retain the foundation soil of the Union Pacific Railroad

that was adjacent to the wall. The design of the wall had come under scrutiny due to the close proximity to the railroad line. This temporary wall was designed to limit settlement of the soil behind the wall upon which the adjacent railroad tracks were founded. This study focused on three objectives: (a) to provide a means for additional confirmation of procedures used in the design of the wall, (b) to predict potential wall performance during excavation and tieback installation, and (c) to assist in the interpretation of instrumentation results. To ensure that the wall would perform as designed, it was evaluated using FEA. The FEA provided analytical measures of wall and soil behavior. The FEA results were used as a means to evaluate the wall design and instrumentation data. The computer program SOILSTRUCT was used to perform the 2-D analytical analysis. The initial FEA in general showed qualitatively that the wall responded satisfactory. The soil stiffness's used in the initial analyses were conservative values so that the deflections predicted by the analysis should be greater than those actually experienced by the wall. The final phase of the study was to perform parametric studies to obtain values of soil stiffness. The parametric studies indicated that the relative value of the hyperbolic soil stiffness modulus was an influential parameter in the results of the FEA. Increase of the modulus values for primary and unload-reload provided results that closely approached the observed behavior. There was close agreement between the observed wall deflections and bending moments and the analytical results.

Powrie and Li (1991) have carried out a series of numerical analyses on excavations of singly propped at the crest of the retaining wall. The effect of soil, wall and prop stiffness and pre-excavation pressure coefficient were investigated. As the structure investigated was very stiff, the magnitude of soil and wall movements were governed by the stiffness of the soil rather than that of the wall. A reduction in soil stiffness by a factor of 2 resulted in an increase in wall deformation almost by the same order of magnitude. On the other hand, wall movement was little affected by a 40% reduction in bending stiffness when the thickness of the wall was reduced from 1.5m to 1.25m. The assumed pre-excavation lateral earth pressure significantly affected the prop loads.

Potts et al. (1991) have studied about the effect of wall stiffness on bending moments of retaining walls. Numerical analysis is carried out on wall stiffness and soil stress distribution by considering three typical excavations in stiff clay. The geometry of the wall and soil parameters considered that of Bell common Tunnel (UK).The Imperial College Finite Element Program was used to perform analysis. Eight nodded 2-D elements were

used to model the soil and 1-D beam elements were used to model the wall. The wall installation effects were not considered. From the analysis it concluded, that the soil structure interaction plays a dominant role in the behavior of soil supporting walls. It also concluded that maximum bending moment in the structure had a great relation in wall stiffness. Approximately five times reduction in maximum bending moment occurred when the wall stiffness was reduced from that of one meter to concrete thickness section to Frodingham 1N sheet pile. But the wall displacement increase could be tolerated by propping or anchoring. It was also observed 25% to 40% cost saving while using flexible wall.

Neelakantan et al. (1992) investigated whether substantial wall displacements or failures preceded liquefaction. Mononobe-Okabe seismic earth pressure equations were performed to determine whether failures lead to the general failure of anchored retaining walls during seismic events. Results of shaking table tests on aluminum walls with cohesionless soil as the back fill confirm the analytical methodology. Based on the limit analysis, a balanced seismic design concept for anchored retaining wall was presented. They concluded that the balanced design procedure provided a method, whereby the additional forces required to be carried by the anchor to improve the seismic stability of the retaining wall system. But the study has not considered wall material property, flexibility, and three dimensional stress flow.

Anestis et al. (1997) carried evaluation on dynamic response of cantilever retaining walls. Study involves to assess the magnitude and distribution of the dynamic displacements, pressures and forces induced by horizontal ground shaking in walls that are both flexible and elastically constrained against rotation at their base and also to assess the effects and relative importance of the factors involved. The system examined a semi-infinite, uniform layer of visco-elastic material of height H that is free at its upper surface, is bonded to a rigid base, and is retained along one of its vertical boundaries by a uniform, flexible cantilever wall that is elastically constrained against rotation at its base. The bases of both the wall and the soil stratum are presumed to experience a space-invariant horizontal motion, the acceleration of which at any time t is I_g (t), and its maximum value is Xg. Material damping for the medium is considered to be of the constant hysteretic type. Study concluded that increasing flexibility reduces the horizontal extensional stiffness of the

retained medium relative to its shearing stiffness and this reduction decreases the proportion of the soil inertia forces that gets transferred to the wall.

Gourvenec and Powrie (2000) carried out a series of 3-D finite element analyses to investigate the effect of the removal of sections of an earth berm supporting an embedded retaining diaphragm wall. For the selected wall- berm geometry and soil conditions considered in the analyses, relationships between the wall movement, the length of berm section removed, the spacing between successive unsupported sections, and the time elapsed following excavation were investigated. The finite element analyses (FEA) were carried out using the computer program CRISP (Britto and Gunn, 1987). Each analysis modeled at 7.5m deep cutting retained by a 15m deep and 1m thick diaphragm wall. The analysis started with the wall already in place. The 3-D finite element mesh used in the analyses was composed of 720 linear strain brick elements. Separate analyses were carried out for each excavation geometry rather than modeling excavation progressively in a single analysis so that the wall displacements calculated over a given time period could be compared directly. The results of the FEA showed that the removal of a section of an earth berm resulted in localized displacements near the unsupported section of the wall. The maximum wall movement occurred at the center of the unsupported section. Additionally the magnitude of wall movements and the extent of the wall affected by the removal of a section of berm.

Yegian et al. (2001) described a wide variety of applications of dynamic soil structure interaction in geotechnical engineering practice. The paper mentioned the development in the field of SSI under seismic waves.

Poh et al. (2001) studied the ground movement with wall construction by considering four case histories on the adjacent ground response to the construction of diaphragm wall panels. The aspects of performance monitored included lateral soil movements and soil settlements. The monitoring results indicated that the lateral soil movements caused by the construction of wall panels increased with increasing wall dimension. These results suggest that the magnitude of the lateral soil movements could be minimized by reducing the dimensions of the wall panels. The results also suggest that the use of high slurry levels during the construction of the wall panels would help to minimize the lateral soil movements. The maximum inward lateral soil movements appear to increase with the increasing longitudinal cross-sectional area of the wall panels. The study recommends the

scope of additional studies to better understand the aspect of slurry wall deformations with respect to longitudinal cross-sectional area.

Long (2001) analyzed 296 case histories. The database shows that for excavations in stiff clay and soft clay, the normalized maximum lateral wall displacements are in the range of δ_{hm}/H = 0.05% - 0.5% and up to 3.2% respectively. His studies largely focused on validating results of Clough and Rourke (1990).

Mitew (2002) Carried numerical analysis and parametric studies on displacements of a diaphragm wall using Geo4-Sheeting analysis and Rido – software and Geo4-FEM and Plaxis 7.2 and results of numerical analysis had been compared with the results of in-situ measurements. From the study it is concluded that, maximum theoretical displacements of the wall estimated in all FEM analysis, in general, are very close to the value of maximum real displacement measured during construction. All calculation sequences showed a significant diaphragm wall displacement towards the excavation in the span above the foundation slab in last two construction phases, which has not been observed in-situ. Relatively best results had been obtained when the soil parameters were based on the results of pressuremeter investigations.

A full scale field study was conducted by Muthukumaran et al. (2002) on a berthing structure with diaphragm wall to estimate the axial load distribution during axial loading and the lateral displacement during dredging. After construction of the berth, it was decided to conduct a full scale axial load test on a single pile and monitor the lateral movements of the berth during and after dredging. A shallow water berth at Jawaharlal Nehru Port Trust (JNPT), Mumbai was recently constructed and comprised of a diaphragm wall and pile rows to support the deck structure was considered for the study. When the dredging work was undertaken, it was decided to monitor the lateral movements of the berth. For this purpose, one inclinometer tube was installed in one panel of the diaphragm wall and in one of the piles of the structure. From the study it is concluded that the total settlement of 3.9 mm was within the settlement limit of 12 mm as per IS 2911 (Part-4) 1985, which indicates that the pile has not reached its capacity. The weathered rock at the site offered substantial frictional resistance, i.e. about 20% to 45% of the total resistance. A maximum of 75% load is mobilized by frictional resistance and the remaining 25% load is mobilized by the end bearing resistance.

Mohammad et al. (2003) evaluated the effect of deep excavation on lateral deformation of diaphragm walls and on the ground surface settlement adjacent to the excavation in five

metro stations in the southwestern section of the Ahwaz metro in Iran. In one of these stations (Kargar Square Station) the ground surface settlement around the station and the lateral deformation of the top of the diaphragm wall were measured in three stages during excavation to a depth of 5 m. After construction work was suspended in this section of the metro, numerical methods were used to predict the ground surface settlement and the lateral wall deformation that would be caused by excavation at depths between 5 m and 17.2 m. The measured data were used to back calculate soil parameters required for this analysis. The ground surface settlement and the lateral deformation of the wall in all these stations that would result from excavation to a final depth of 17.2 m below ground were predicted using the back calculated parameters. The relationship between the maximum ground surface settlement and the distance to the wall for all five stations of the Ahwaz metro was predicted. The predicted maximum lateral deformation (δ_{hm}) due to excavation in the southern stations of the Ahwaz metro is between 0.5% H_e and 0.7% H_e (H_e: depth of excavation). The ratio of the predicted maximum settlement of the ground surface (δ_{vm}) to the depth of excavation is in the range of δ_{hm} /H_e = (0.25– 0.35) %.

Sakas, and Tazaki (2003) studied the development and applications of diaphragm wall with special section steel NS-Box composite section. NS Box steel and concrete is developed to meet the demand for strong, stiff wall of reduced thickness to save space on congested sites and to achieve manpower savings by maximizing prefabrication.

Small scale model tests was conducted by Anwar Hossain et al. (2004) and studied the behavior aspects of the composite wall and its components including load- deflection response, strength, stiffness, failure modes, stress condition and sheet concrete interactions. The effect of modes of applications of load on the behavior of composite walls was also investigated. It was concluded the strain conditions in a composite walls was affected by the initial bonding of steel concrete interface, initial concrete cracking with subsequent propagation of cracks and initial buckling of profiled steel sheeting. Composite walls are found to provide shear strength and shear stiffness higher than the summation of the individual contributions.

Moormann (2004) had carried out extensive empirical studies by taking 530 case histories of retaining wall and ground movement due to excavation in soft soil (cu<75kpa) into account. It is concluded that the maximum horizontal wall displacement (δ_{hm}) lies between 0.5% H and 1.0 % H, on average at 0.87% H. The location of maximum horizontal displacement is at 0.5H to 1.0H below the ground.

Jacques Monnet et al. (2006) did an interpretation of field measurements using pressure meter results and finite element analysis for a diaphragm wall with the help of finite element program Cesar-Lcpc Dubouchet 1992 and calculated the horizontal displacements and the bending moment on the wall. The mesh was made of 220 quadrilateral elements with eight nodes. The diaphragm wall was modeled with two layers of elements. The program used an elasto-plastic Mohr- Coulomb model. The diaphragm wall had a total height of 14 m for an embedded part of 3 m and an excavation of 11 m. A horizontal strut was fixed at 2.67 m below the top of the wall. The finite element calculation was not adjusted on the experimental results. Measurements were made by inclinometer to find the bending deformation of the wall and the horizontal displacements. For a 14 m height diaphragm wall, the theoretical displacements found by finite element calculation are 4 mm larger than the measured displacements .The bending moment matched with the experiment with a 15% over estimation and gave a good prediction of the behavior of the wall. The predicted force in the strut was 668 kN for a measured effort of 570 kN.

Psarropoulos et al. (2005) developed a more general finite element method of solution, the results of which were shown to be in agreement with the available analytical results for the distribution of dynamic earth pressures on rigid and flexible walls. Both homogeneous and inhomogeneous retained soil were considered, while a second soil layer was introduced as the foundation of the retaining system. Modeling was extended to account for: (a) soil in homogeneity of the retained soil, and (b) translational flexibility of the wall foundation. The results confirmed the crude convergence between Mononobe–Okabe and elasticity-based solutions for structurally or rotationally flexible walls.

Jacques Monnet et al. (2006) did an interpretation of field measurements using pressure meter results and finite element analysis for a diaphragm Wall with the help of finite element program Cesar-Lcpc Dubouchet 1992 and calculated the horizontal displacements and the bending moment on the wall. The mesh was made of 220 quadrilateral elements with eight nodes. The diaphragm wall was modeled with two layers of elements. The program used an elasto-plastic Mohr- Coulomb model. The diaphragm wall had a total height of 14 m for an embedded part of 3 m and an excavation of 11 m. A horizontal strut was fixed at 2.67 m below the top of the wall. Measurements were made by inclinometer to find the bending deformation of the wall and the horizontal displacements. For a 14 m height diaphragm wall, the theoretical displacements found by finite element calculation are 4 mm larger than the measured displacements. The bending moment matched with the

experiment with a 15% over estimation and gave a good prediction of the behavior of the wall.

Diao Yu et al. (2008) carried numerical analysis of effect of friction between diaphragm wall and soil on braced excavation. A plane strain finite element model was established to investigate the effect of friction between diaphragm wall and soil on braced excavation. The behavior of interface between diaphragm wall and soil was simulated with the interface model of ABAQUS. The study were made to take wall-soil interface into account when numerical simulations of excavation was performed to predict wall deflection and ground surface settlement distribution. The results show that deflection of diaphragm wall and ground surface settlement decreases with the decrease of friction angle.

Niggar (2010) carried parametric study using finite element program for the enhancement of steel sheet-piling quay walls using grouted anchors. An extensive parametric study through the finite element program, Plaxis, version 8.2 was carried out to investigate the enhancement of using grouted anchors technique on the load response of sheet-piling quay wall. The influence of sheet-pile wall geometry, grout-ties inclination and location, length of grout, dredging depth and backfill soil angle of internal friction are analyzed and the results are presented. The study concluded that the rehabilitation of steel sheet piling quay walls using additional grouting tie-rods had a significant role on the performance of anchored quay wall system. The anchored wall and surrounding soil showed more stabilized behavior when the grouted anchors were used. Both the maximum bending moment and horizontal displacement exerted along the sheet pile wall had been considerably reduced. Also, the maximum ground surface settlement and force in the original system anchor had been reduced. Results also show that the optimal length of the grout falls between; 0.40 and 0.50 of the quay wall original height. Furthermore, the grout-ties inclination has a great effect on the system's performance.

Hsii Sheng Hsieh et al. (2011) studied the performance of T-shaped diaphragm wall in a large scale excavation. The T-shaped diaphragm wall had a relatively high rigidity that can withstand lateral earth pressure without excessive wall movement. 1-D analysis was carried using RIDO software to calculate the lateral displacement. The observed lateral displacement of T-shaped diaphragm wall was less than 1.5 cm for excavation depth of 9.6 meter. Additional side frictions developed along buttress surfaces of the T-shaped wall is believed to help in significantly reducing wall displacement. While casting the T-shaped diaphragm wall, the T shape had to cast in one integral unit. The flexural stiffness of T-

shaped wall would be dramatically reduced if the perimeter wall and buttress wall were separately cast. Overlapping of the primary and secondary panels is also achieved by using a special joint that further increases the overall stiffness of the retaining system. Side frictions developed along the buttresses were not incorporated in the 1-D analyses. A proper 3-D analysis will provide a more realistic estimate on the lateral displacement of T-shaped wall.

Arablouei et al. (2011) carried out numerical study on dynamic response of quay wall during earthquake and soil structure interactions were conducted using ADINA finite element program. A typical configuration of caisson type quay wall was used for analysis and seven real earth quake records along with one harmonic excitation were applied as base acceleration. The results showed that the influence of seawater structure interactions on the permanent displacement of a Caisson type quay wall constructed on relatively non-liquefiable site was not significant. Vertical component of earthquake waves can considerably affect the hydrodynamic response of seawater. Frequency content of ground motion plays a key role on residual displacement of wall.

Premalatha et al. (2011) conducted a series of laboratory test with single row of instrumented piles in a berthing structure reduced to a modal scale. The experiments were carried out by applying both berthing and mooring forces with and without considering the seabed slope angle. Tie rods were introduced in the frame of the berthing structure and its effects is studied. From the study it was concluded that mooring force was much critical compared to the other lateral loads acting on the structure. Tie rod was effective in reducing the deflection of the structure and there by controlling the forces that goes to the piles.

Premalatha et al. (2011) carried out a numerical study on pile group supporting berthing structures subjected to berthing and mooing forces and the forces raised due to dredging operations. A 2D Finite element model developed using Plaxis and validated using the theoretical solutions. Three different soil slopes such as 1V:3H, 1V:2H and 1V:1.5H were considered to simulate the actual field condition in berthing structure. The effect of berthing /mooring forces and the effect due to dredging operations on the pile groups were investigated with and without tie-rod anchors. It was concluded that lateral deflection of berthing structure due to mooring and pulling force was more when compared to berthing force. Among the three slopes (viz 1V:3H, 1V:2H and 1V:1.5H), slope 1V:3H was

normally stable by itself and had the least deflection. Effect of tie played a major role in reducing the deflection of the berthing structure.

Subha (2012) carried finite element approach for analyzing the lateral response of pile and diaphragm wall during dredging and seismic loading on the dredged soil. In this study model tests were analyzed using a plane strain finite element approach with the piles represented as equivalent sheet pile wall. Soil strata were represented by 15 node triangular elements of elastic-plastic Mohr-Coulomb model. Soil structure interaction was modeled by means of bilinear Mohr-Coulomb model and Plaxis was used for the study. ANZA earthquake data were considered for earth quake analysis. The analysis concluded that the lateral response of the berthing structure was significantly affected by dredging under earth quake conditions.

Bolton et al. (2014) studied ground movements associated with braced excavations in Shanghai and found that conventional design charts fail to take account either of the characteristics of soil deformability or the relevant deformation mechanisms. The study recommends a new method which provides a set of design charts that clarify the influence of soil deformability, wall stiffness, and the geometry of the excavation in relation to the depth of soft ground.

Yong Tan and Dalong (2015) examined the structural behaviors of the multi-propped diaphragm wall for excavation of the 17.85-m deep rectangular pit. The study concentrated on the structural behaviors of the multi-propped earth retaining systems, which included the comparison of field measurement of wall movement and numerical analysis. Inclinometers were used to measure the wall displacement. The comparison between the field data and the design analysis results shows that the theoretical beam on-elastic-foundation design models can make a relative reasonable estimation on the wall deflections for the unpropped circular diaphragm wall, but highly underestimated the wall deflections of the multi-propped rectangular diaphragm wall.

Ingale et al. (2015) did a laboratory investigation in soft & hard, murum & black cotton soil to study the static and dynamic earth pressure behind the retaining wall. The static earth pressure study was based on Rankine and Coulomb methods and dynamic earth pressure was based on Mononobe-Okabe and IS code method. From the study concluded that if a retaining wall is subjected to above backfills (soft murrum, hard murrum, black cotton soil) the earth pressure obtained by seismic case higher than static cases. The percentage difference between static and dynamic earth pressure ranging in between 9.35% to 10.66%.

Lee et al. (2016) conducted three-dimensional nonlinear soil-structure interaction analysis to study the dynamic behavior of structures established in flexible ground. In this study, a three-dimensional time- domain formulation of perfectly matched discrete layers (PMDLs) is developed. The developed PMDL formulation can minimize the modeling region. A procedure to determine the parameters of the three- dimensional PMDLs to model a layered half-space effectively and accurately proposed. The study concluded that The dynamic behavior of structures established in flexible ground can be greatly influenced by soil-structure interaction.

Orabi et al. (2017) proposed the inverted U-Shape reinforced- concrete wall configuration that provides an alternative to gravity wall system in areas with limited base width. The proposed wall configuration consists of a stem embedded at the toe and extending to an optimized intermediate height, a relief floor acting as a tie-back, a dead-man, and a limited height gravity wall extending above the stem for the remaining wall height. Authors studied the performance of the proposed wall system in terms of global stability, induced straining actions, and wall movement. The parametric study was conducted using the 2-D finite element software PLAXIS and 2-D limit equilibrium (LE) analyses are also conducted using SLIDE software. The results showed that the critical failure surface is forming an active wedge against the dead-man, and a passive wedge against the stem with the surface intersecting both toes at points of high shear strains. It was observed that introducing the dead man resulted in up to 35 % reduction in horizontal deflections and up to 50% reduction in vertical settlements. The authors showed an alternative gravity wall system, which showed a satisfactory performance of stability and serviceability.

Kavitha and Sundaravadivelu (2017) conducted numerical study in soil-structure interaction analysis of a berthing structure under lateral loading. The finite element modeling and analysis have been carried out using PLAXIS 3D software. The soil domain is 60m long, 24m wide and 45m deep. The soil model accommodates diaphragm wall and the four rows of piles behind the wall connected by top beam. The excavation is 20m deep and is carried out in 7 stages and the whole process is modeled in 10 phases. The diaphragm wall and piles are modeled as beam elements interconnected by nodes. The study concluded that lateral response of the berthing structure is significantly affected by dredging.

Popa et al. (2017) investigated the effect of using various constitutive laws on displacements for numerical modeling of diaphragm wall. A 2D numerical modelling using

finite element method (PLAXIS V8, 2D) for an anchored diaphragm wall for a deep excavation was analysed using following soil constitutive laws: Mohr - Coulomb Model, Hardening Soil Model and Hardening Soil Model with Small Strain Stiffness. The modeled retaining wall was built in Bucharest, Romania for a deep excavation of 66 x 127 m and a maximum depth of over 16 m. The retaining structure consisted of diaphragm walls 80 cm thick and 20 - 24 m long. Numerical results were validated with the inclinometric measurements. The major conclusions drawn by the authors are: (i) wall and ground displacements determined using Mohr-Coulomb criterion are exaggerated and even the shape of the deformation curve is not realistic (ii) computations using Hardening Soil criterion indicated a substantial improvement of results. Even if displacements are still high, it can be observed that the wall deformation shape is closer to the measured one (iii) the results obtained using the Hardening Soil Model with Small Strain Stiffness are close to the field measurements. However, the input model parameters required dynamic laboratory or in situ tests.

Shahin et al. (2017) conducted finite element analyses of anchor type retaining wall in the braced excavation. First, the authors have conducted some model tests using the mass of aluminum rods as model ground. The size of the model ground was 680mm in width and 450mm in height. The retaining wall was 300mm in length, 60mm in width and 0.5mm in thickness, which was a plate of aluminum material. Using the results obtained from the model tests, authors have validated their own finite element code called FEMtij-2D. The FEMtij-2D uses an elasto-plastic constitutive model called the sub loading tj model. After the validation, authors have simulated a field observation of an anchor type retaining wall by finite element code. The results obtained by the FEMtij-2D and field observed values were in good agreement. It was concluded that longer anchor in the lower parts of the excavation produces a significant supporting effect resisting wall displacement of the backfill ground. In addition, it was observed that the supporting effect of the anchor in braced excavation could be achieved, if the anchor block is setup outside the assumed slip surface developed during excavation.

2.2 SUMMARY OF LITERATURE REVIEW AND PROBLEM FORMULATION

The assessment of SSI aspects of the retaining wall systems takes into consideration of the following design issues. sizing of the structural members, spacing of structural members,

exposed (free) height of the walls, depth of embedment of the walls, soil types, range in parameters for the constitutive model of typical soil. Construction of piles and diaphragm wall supporting open type berthing structure on marine soils results in development of vertical and horizontal sub soil displacement. The sub soil displacement may generate axial and lateral loads on the piles and diaphragm walls during dredging which is not actually considered in the conventional design procedures of berthing structure. There will be additional lateral loads derived from landside earth pressure during dredging.

Large earth pressure and water loads result massive and costly construction. It is required to examine an innovative wall system that is more cost effective than traditional wall systems. From the literature it is found that as wall flexibility increases the stresses imposed by the surrounding soil redistribute and reduce the structural forces in the wall. But these beneficial effects are accompanied by greater wall and soil movements.

In composite wall system individual deformations will not be the same due to difference in stiffness. The wall displacements are likely to be sufficient to fully mobilize the shear resistance of the retained soil (Bolton, 2006). The deformation of the individual component of the composite section depend the bending stiffness EI, where E is the modulus of elasticity of material and I is the moment of inertia of the section. So the bending stiffness of the member depends the geometry and the material property of the member. Therefore the deformation in the composite wall is the summation of individual deformation and it will vary according to the bending stiffness of the individual member. The difference in stiffness of the wall components contributes three dimensional stress flows in the surrounding soil and it may have a significant effect on the distribution of earth pressures and subsequent bending moments and shear forces acting on a structure (Abraham, 2007). The three dimensional stress flows may have a significant effect on the distribution of earth pressures and subsequent bending moments and shear forces acting on a structure. From the literature it is also found that the use of tie rod anchors in berthing structures will reduce the bending moment and lateral deflection and thus the required cross sectional area of the wall and the amount of reinforcement can be reduced resulting in an economical design.

The 2D conventional design procedure does not take in to account 3D stress flow in the surrounding soil. No current design procedure is available for the innovative composite wall system accounting three dimensional stresses. Very few research works have been carried on 2-D and 3-D analysis on diaphragm wall which is one of the structural members

of a berthing structure and assessed the engineering parameters. So there is good scope for the parametric study of SSI of a diaphragm wall by 2-D and 3D analysis and performing engineering assessment and also studying three dimensional stress flow of the retained soil around the composite wall system having varying wall stiffness. Hence the present study investigates the effect of lateral loads on diaphragm wall of uniform as well as varying sections with tie rod anchor.

CHAPTER 3

CURRENT DESIGN METHODS, METHODOLOGY AND DATA COLLECTION

3. 1 GENERAL

Some of the methods used in the analysis and design of tieback wall systems, described in Strom and Ebeling (2001) are listed as:

1 Beam on rigid supports (RIGID) method.

2 Beam on elastic supports (WINKLER) method.

3 Linear-elastic finite element (LEFEM) method.

4 Nonlinear finite element-soil structure interaction (NLFEM) method.

Bolton et al. (1989, 1990a, 1990b, 2004, 2006) suggested a new design approach for un-drained clays based on the theory of plasticity. The method is known as,

5 Mobilized Strength Design method (MSD).

3.1.1 Beam on Rigid Supports (RIGID) Method

The terminology of RIGID analysis is in accordance with that used by Kerr and Tamaro (1990).

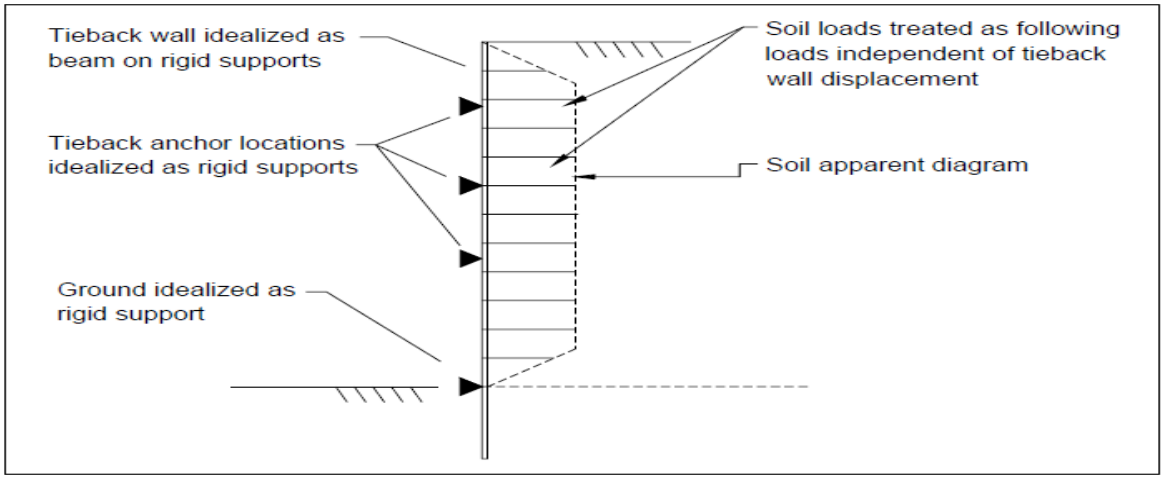

Fig. 3.1. Equivalent beam on rigid supports method (RIGID)

The tieback wall is assumed to be a continuous elastic member (with a constant value of EI) supported on fixed ground anchors. In the RIGID method, the soil loads are pre-

determined and considered to be following loads that are independent of wall displacements. Thus, in this method the redistribution of earth pressures due to wall movements is not considered. The soil loading can have a trapezoidal distribution (from apparent earth pressure envelopes) or typical triangular distribution from conventional equilibrium procedures. The foundation soil on the front side of the wall is assumed to act as a fictitious support at the point of zero net pressure that prevents translation of the wall. The RIGID analysis method is illustrated in Fig. 3.1.

3.1.2 WINKLER Method

The WINKLER method is a beam on elastic foundation method of analysis. This method is based on a one-dimensional (1-D) finite element representation of the wall/soil system. The tieback wall is considered continuous flexural member with stiffness EI and is modelled as linearly elastic beam-column elements. The wall is supported by a set of infinitely closely spaced distributed nonlinear springs with stiffness (k) to represent the soil, and discrete nonlinear preloaded concentrated springs to model the anchors. The soil springs are preloaded to at-rest pressure conditions to represent the condition that exists prior to excavation.

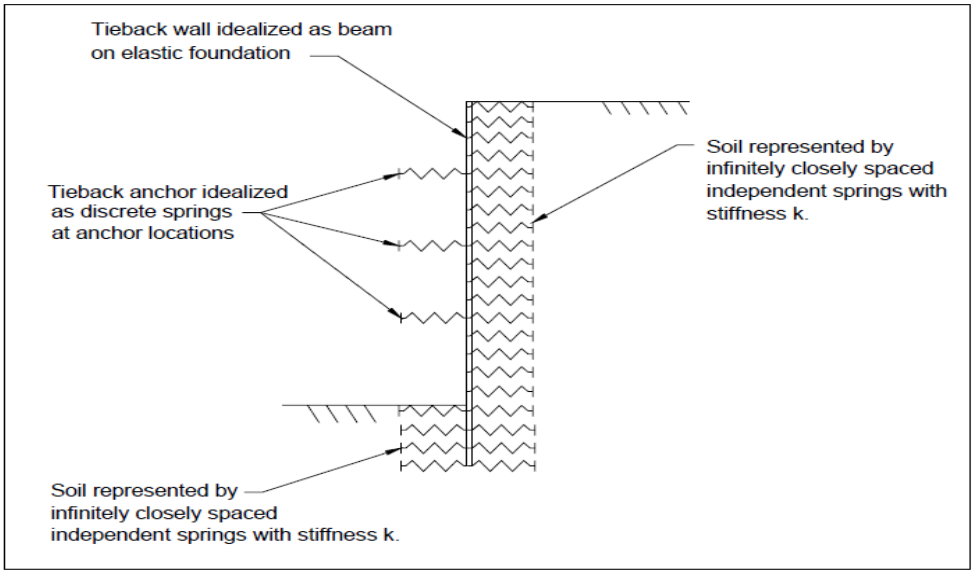

Fig. 3.2 Beam on elastic foundation method (WINKLER)

As the excavation occurs (i.e., removal of soil springs in the excavation region), the wall moves toward the excavation. This movement is the result of the preload in the soil on the backside (unexcavated) of the wall. The soil springs on the excavation side must carry more

load than at-rest loads in order to help keeping the wall system in equilibrium. Additionally, at the ground anchor locations, the tiebacks represented by a preload anchor springs also contribute to the equilibrium of the overall system. The fundamental assumption in the WINKLER spring analysis method is that each spring used to represent the soil acts independently (i.e., the behavior of one spring has no effect on the behavior of adjacent springs). The WINKLER analysis method as represented in Fig. 3.2 can be used in a staged excavation analysis without consideration of system displacements that occurred during each stage of construction.

3.1.3 Linear Elastic Finite Element Method (LEFEM)

A linear material is described as material behavior in which the magnitude of the response of a material is directly proportional to the magnitude of the loads applied to the material. This behavior can be visualized by a stress-strain curve shown in Fig. 3.3. Elastic materials undergo only recoverable deformations, i.e., they return to their initial state when the load is removed. These materials have a unique stress-strain relationship given by Hooke's law that may be written as;

$$\sigma = E\,\varepsilon \qquad (3.1)$$

Where σ is stress, ε is strain, and E is the modulus of elasticity. To model SSI problems as linear elastic problems the following assumptions are made (Liu, 1998)

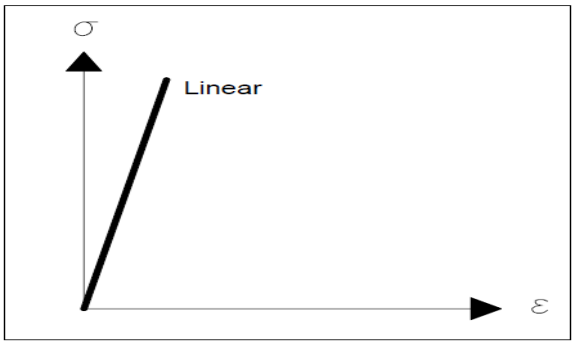

Fig. 3.3 Illustration of linear stress-strain relationship.

1. Material behavior is elastic.
2. Small deformation (loading pattern is not changed due to the deformed shape)

LEFEM has been used in a stage excavation analysis to evaluate displacement, bending moment and anchor loads in diaphragm walls. A linear analysis can provide important information about the behavior of a structure, and can be a good approximation of the

behavior a structure in many cases. Linear analysis is also the basis for most nonlinear analysis. A finite element mesh was used to model the diaphragm wall to capture plate bending effects for stage excavation analysis, and to capture anchor load redistribution effects.

Fig. 3.4 illustrates the LEFEM in combination with linear WINKLER springs with respect to a staged excavation analysis. Linear elastic finite element method analyses are sometimes used to model diaphragm (continuous) wall systems in combination with linear Winkler soil springs (Strom and Ebeling, 2001). In the linear elastic model, the soil and water on the unexcavated side of the wall are modeled as loads, and the soil on the excavation side is modeled as linear elastic (Winkler) springs preloaded to at-rest pressure conditions. The forces in the springs are monitored during a staged excavation analysis to determine if they exceed passive pressure resistance. If this occurs, a passive pressure force replaces the spring. In more sophisticated LEFEM analyses, bilinear excavation side springs are used, with the plastic region of the bilinear curve representing the passive limit state of the soil. On the active (unexcavated) side, the pressures on the wall are applied as distributed loads. The soil active pressure is assumed to be unchanged throughout the entire sequence of excavation.

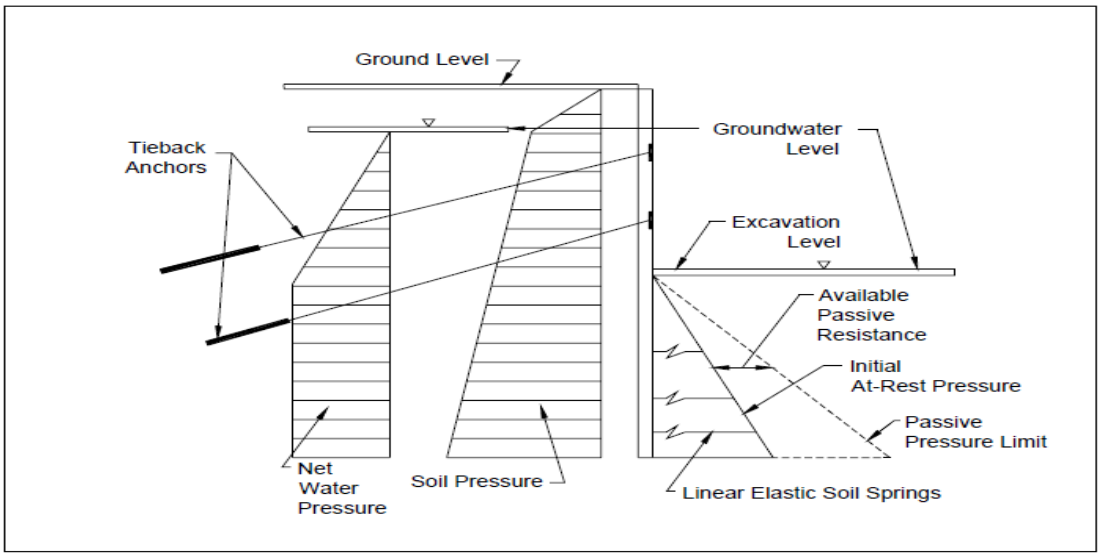

Fig. 3.4. Linear elastic finite element model (LEFEM) of diaphragm wall in combination with linear Winkler soil springs.

One of the major advantages of this recently approved method is, its economical attractiveness. Computer programs are capable to analyze simple as well as more

complicated structural elements within a very short timeframe compared to manual calculations. Besides, the required amount of reinforcement which follows from the linear elastic finite element method is more economical compared to the regular design methods.

3.1.4 Nonlinear Finite Element Method (NLFEM)

A nonlinear material is described as material behavior in which the magnitude of the response of a material is not directly proportional to the magnitude of the loads applied to the material. A nonlinear material behavior can be visualized on a stress vs. strain plot as shown in Fig. 3.5. The Nonlinear Finite Element Method (NLFEM) has been used in sequence of construction analyses to capture soil-structure interaction effects. The actual stress- strain response of soil and soil-to-structure interfaces in these analyses is nonlinear and stress path dependent. In these analyses, soil nonlinearities can be evaluated and soil pressures can be allowed to vary as a result of the structural and related soil deformations.

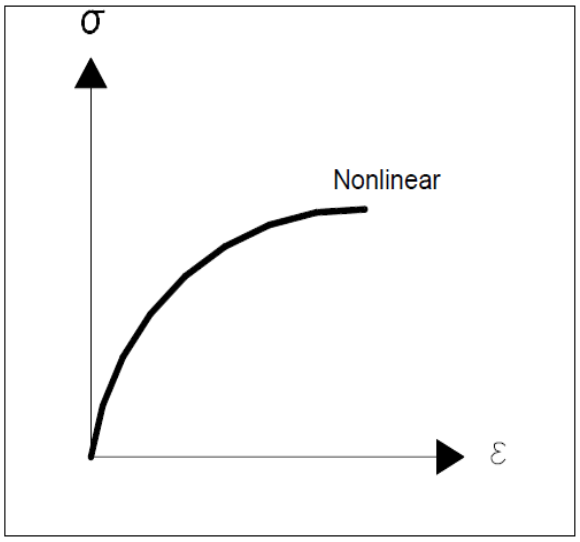

Fig. 3.5 Illustration of nonlinear stress-strain relationship

Nonlinearity is natural in physical problems. In fact, the linear assumptions we make are only valid in special circumstances and usually involve some measure of "smallness", for example, small strains, small displacements, small rotations, small changes in temperature, and so on. We use linear approximations not because they are more correct but because linear solutions are easier to compute. The computational cost is smaller. Solutions can be superposed on each other. However, linear analysis is not adequate and nonlinear analysis is necessary when designing high performance components. Establishing the causes of

failure. Simulating true material behavior. Trying to gain a better understanding of physical phenomena.

3.1.5 Mobilized Strength Design (MSD)

The method of MSD was introduced to achieve a general unified simple design methodology, which could satisfy both safety and serviceability in some simple steps of calculation, as an alternative to the standard limit state design methodology which separate design issues into stability and serviceability problems. In the MSD method, the design strength limiting the deformation and satisfying equilibrium is selected according to actual stress-strain data without the use of empirical factors. Basically, two concepts of the approach are:

1) Simple deformation mechanisms are used, which represent the working state of the geotechnical problem. The mechanisms represent the equilibrium and displacement of the various soil bodies, especially at their junction with the superstructure.

2) Stress-strain data from soil tests on undisturbed samples taken from representative elements are used directly to link stress and displacements under working conditions. The use of constitutive laws and soil parameters are avoided.

The approach has been successfully implemented by Osman and Bolton (2006) on geotechnical problems such as shallow foundations, cantilever retaining walls, tunneling induced displacements and also deep excavations inducing wall displacements and ground deformation. This approach has the advantage that one can use a single stress-strain curve from a single soil test, together with a simple hand calculation, to estimate both stability and soil deformation without the need for complex computer simulation. In this method for deep excavation problem the total wall deformation could be taken as the sum of the cantilever movement and the bulging movement.

3.2 METHODOLOGY

A series of nonlinear analysis are performed to assess the behavior of diaphragm wall. To perform 2D and 3D analysis, finite element software Plaxis is used. The performance of the diaphragm wall is assessed based on the investigation issues such as effect of dredging on wall displacement, effect of displacement with varying anchor locations, construction sequence effects on wall displacement, effect of stiffness by varying wall configuration etc. To investigate such issues a diaphragm wall is modelled using Plaxis 2D software and static

and dynamic analysis is performed. The soil data and structural element details considered are of the existing deep draft berth of New Mangalore Port Trust. As second phase of investigation 3D static analysis is performed for the same structure to compare the results of 2D analysis. The third phase of study is concentrated on the 3D analysis of the wall with different configurations to study the stiffness effects and the results are compared with the results of the actual diaphragm wall section. The final phase of the investigation deals with validation of present result by comparing with the results of case studies collected from literature.

3.3 SOFTWARE

Plaxis-2-D and 3-D finite element computer programs are used to perform deformation and stability analyses for various types of geotechnical structures. The software is specially used to evaluate soil structure interaction problems. Real situations may be modeled either by a plane strain or an axisymmetric model. The program uses a convenient graphical user interface that enables users to quickly generate a geometry model and finite element mesh based on a representative vertical cross-section of the structure. Plaxis supports various models to simulate the behaviour of soil and other continuum.

3.3.1 Plaxis 2D.

Plaxis 2D is a special purpose two-dimensional finite element computer program used to perform deformation and stability analyses for various types of geotechnical applications. Real situations may be modelled either by a plane strain or an axisymmetric model. The program uses a convenient graphical user interface that enables users to quickly generate a geometry model and finite element mesh based on a representative vertical cross-section of the situation at hand. The user interface consists of four sub-programs (input, calculations, output and curves).The Plaxis 2-D includes the following models,

a. Linear elastic model:

b.User-define soil model

c. Jointed rock model

d. Hardening soil model

e. Soft soil model

f. Soft soil creep model

g. Mohr-Coulomb model

Plaxis offers for each soil model a choice of three types of behaviour, (a) drained behaviour, (b) undrained behavior, (c) non-porous behaviour. Using the drained behavior settings no excess pore pressure are generated and it is for the case of dry soils. Undrained settings are used for full development of excess pore pressure. In non-porous behavior neither initial nor excess pore pressure will be taken in to account. For modelling of concrete behavior non-porous setting may be adopted. In the present study undrained behavior of soil is considered because of the presence of water may significantly influence the soil response.

3.3.2 Model

The generation of a two dimensional finite element model in Plaxis is based on a geometry model. This geometry model is created in the x-y plane of the global coordinate system as shown in the Fig. 3.6, whereas the z-direction is out-of–plane direction. In the global coordinate system the positive z-direction is pointing towards the user. In a plane strain analysis σ_{zz} is the out-of-plane stress.

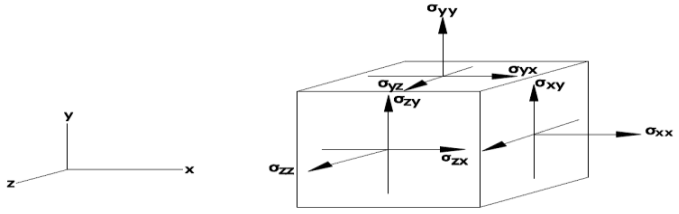

Fig. 3.6 Coordinate system and indication of positive stress component

A plane strain model Fig. 3.7 (a) is used for geometries with a uniform cross section. Displacements and strains in z-direction are assumed to be zero. Normal stresses in z-direction are fully taken in to account

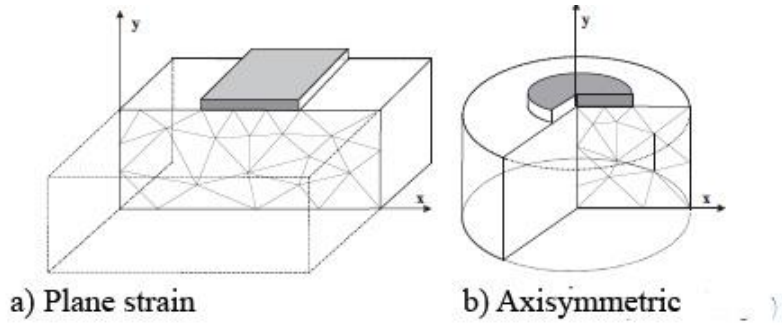

Fig. 3.7 Examples of a plane strain and axisymmetric problem in 2D

In plane strain analysis with two-dimensional FEM model there exist two translational degrees of freedom per node (x-and y- direction).

An axisymmetric model Fig. 3.7 (b) is used for circular structures with a uniform radial cross section and loading around the central axis. The x-coordinate represents the radius and y-coordinates corresponds to the axial line of symmetry.

3.3.3 Elements

There are either 6-nodes or 15-node triangular elements to model soil layer and other volume clusters in Plaxis.

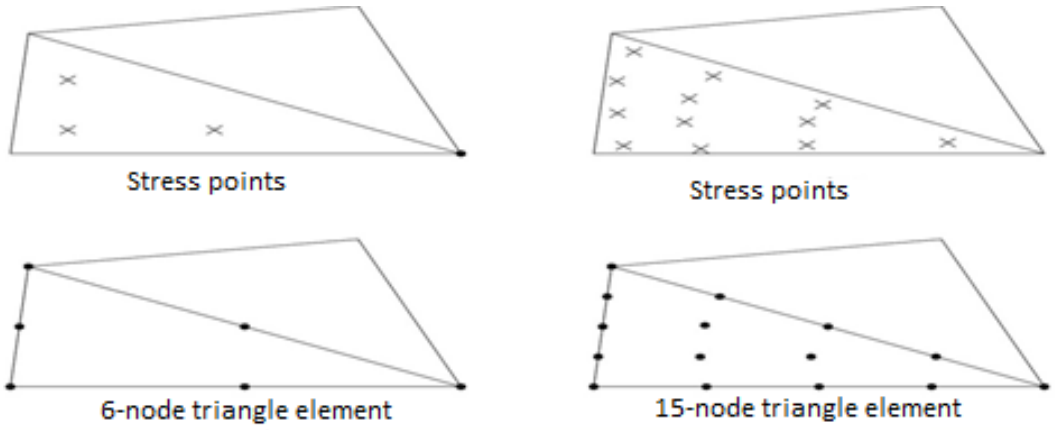

Fig. 3.8 Position of nodes and stress points in soil elements.

The 15-noded triangular element provides the fourth order interpolation and numerical integration involves twelve stress points. The 6-node triangular element provides second order interpolation and numerical integration involves three stress points. In the analysis 15-noded triangular elements are considered because it can produce accurate stress results for different problems. The Fig. 3.8 shows the stress points and nodes in the soil elements.

3.3.4 Plates

Plates are structural objects used to model slender structures with a significant bending stiffness and a normal stiffness. Plates can be used to simulate the wall, shell or line elements which extends in z-direction. Hence plate element is used to model diaphragm wall. The most important parameters for the plate element are the flexural rigidity EI and the axial stiffness EA. Plate thickness d_{eq} is calculated from the equation.

$$d_{req.} = \sqrt{\frac{12EI}{EA}} \qquad (3.2)$$

3.3.5 Beam Elements

Plates in the 2D Finite Element Model are composed of beam elements with three degrees of freedom per node: two translational degrees of freedom (u_x,u_y) and one rotational degrees of freedom(rotation in the x-y plane). The beam element is based on Mindline beam theory. This theory allows for beam deflections due to shearing as well as bending. Beam elements can become plastic, if a prescribed maximum bending moment or maximum axial force is reached. Bending moments and axial forces are evaluated from the stresses at the stress points. 3-node beam element contains two pairs of stress points and 5-node beam element contains four pairs of stress points as shown in Fig. 3.9

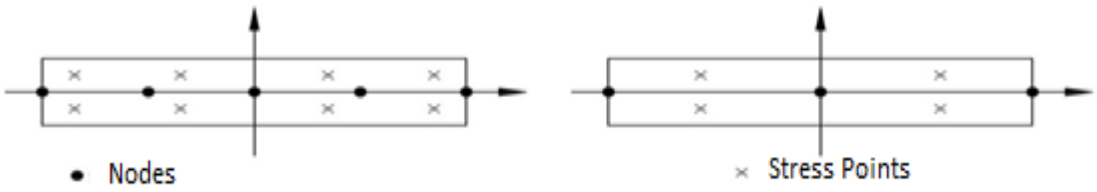

Fig. 3.9 Position of nodes and stress points in a 3-node and 5 node element.

3.3.6 Interface Elements

Interfaces are composed of interface elements which are connected to soil element as shown in the Fig. 3.10. Each interface is assigned with a virtual thickness, which is an imaginary dimension used to define the material properties of the interface. In general interface elements are supposed to generate very little elastic deformation and therefore the virtual thickness should be small. In any soil-structure interaction situation relative movement of the structure with respect to the soil can occur. The use of continuum 2D elements with compatibility in a finite element analysis of these situations prohibits relative movement at the soil-structure interface. Nodal compatibility of the finite element method constrains the adjacent structural and soil elements to move together. Interface or joint elements can be used to model the soil-structure boundary such as the sides of a wall or pile, or the underside of a footing. Particular advantages being the ability to vary the constitutive behaviour of the soil-structure interface (e.g. the maximum wall friction angle) and to allow differential movement of the soil and the structure, i.e. slip and separation.

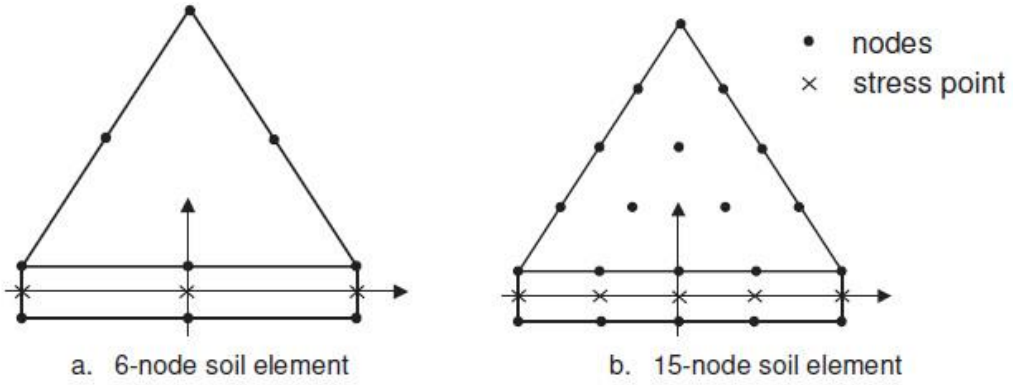

Fig. 3.10 Distribution of nodes and stress points in interface elements and their connection to the soil elements.

The virtual thickness is calculated as the virtual thickness factor times the average element size. The average element size is determined by the global coarseness settings for the mesh generation. The standard value of the virtual thickness factor is 0.1. When using 15-node soil elements, the corresponding interface elements are five pairs of nodes as shown in Fig. 3.10 (b)

3.3.7 Basic Equations of Continuum Deformation

The static equilibrium of a continuum can be formulated as:

$$\underline{\underline{L}}^T \underline{\sigma} + \underline{b} = \underline{0} \qquad (3.3)$$

The equation (3.3) relates the spatial derivatives of the six stress components, assembled in vector $\underline{\sigma}$, to the three compents of the body forces, assembled in vector $\underline{b}$. $\underline{\underline{L}}^T$ is the transpose of a differential operator;

$$\underline{\underline{L}}^T = \begin{bmatrix} \frac{\partial}{\partial x} & 0 & 0 & \frac{\partial}{\partial y} & 0 & \frac{\partial}{\partial z} \\ 0 & \frac{\partial}{\partial y} & 0 & \frac{\partial}{\partial x} & \frac{\partial}{\partial z} & 0 \\ 0 & 0 & \frac{\partial}{\partial z} & 0 & \frac{\partial}{\partial y} & \frac{\partial}{\partial x} \end{bmatrix} \qquad (3.4)$$

Where, $\underline{b}$ is the vector containing the body force, $\underline{\underline{L}}^T$ is the differential operator, $\underline{\sigma}$ is the vector with stress components.
The nonlinear and linear continuum mechanism deals with kinematics, stress and equilibrium, and constitutive behavior. In the linear case, an assumption is made that deformation is sufficiently small to enable the effect of changes in the geometrical

configuration of the solid to be ignored, whereas in nonlinear case the magnitude of the deformation is unrestricted.

3.3.8 Modeling of soil behavior

The linear elastic perfectly- plastic Mohr-Coulomb model is considered for the study and this model requires five basic input parameters, namely Young's modulus (E), Poisson's ratio (ν), Cohesion (c), Friction angle (φ), and Dilatancy angle (ψ). To understand the five basic parameters, typical stress-strain curves obtained from standard triaxial tests can be used. Fig. 3.10 shows the results from standard drained triaxial tests, (a) elastic and (b) elasto-plastic model.

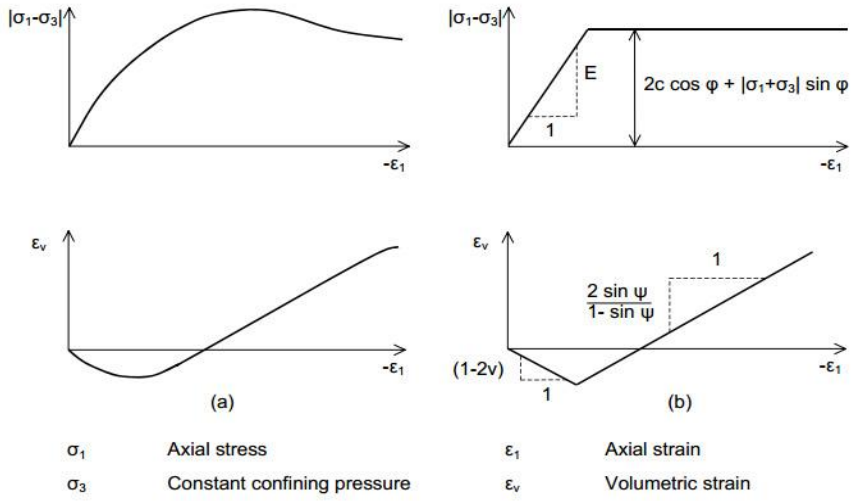

Fig. 3.11 Results from standard drained tests.

3.3.9 Constitutive Models

A constitutive model refers to relation between the stress and strain in a material. Displacements are related to the strain through kinematics, the forces are related to the stress through the equilibrium equations and equations related to the stress to strain are the constitutive relations.

The relationship between stress and strain is an important aspect of finite programs since, the programs compute stresses or deformation in a soil continuum subjected to external loading. The simplest relationship between stress and strain is the linear relationship known as Hooke's Law.

$$\sigma = E\varepsilon \qquad (3.5)$$

Where σ is stress, E is Modulus of Elasticity, and ε is strain.

This relationship is for ideal conditions and may be applicable for some materials, but most soils do not behave in accordance with this model. Soil is heterogeneous, exhibits non-

linear stress strain behaviour and has a strength limit, and is sensitive to water moving through its pores. Therefore the simple Hooke's Law stress-strain representation of soil is not always sufficient. Researchers have attempted to emulate the behaviour of soil by means of constitutive models. Comprehensive mathematical formulations have been developed instead of the simple "E" in Hooke's Law. In these formulations, the soil stiffness may change as the sample is strained in shear or hydrostatically instead of having a constant stiffness. It should be noted that most geotechnical finite element programs contain a basic linear-elastic model. This model is often used in preliminary analyses or when very little soil information is available.

3.3.10 Linear Elastic Perfectly- Plastic Mohr-Coulomb Model

Soils behave rather non-linear when subjected to changes of stress or strain. The linear elastic part of the Mohr-Coulomb model is based on Hooke's law of isotropic elasticity. The perfectly plastic part is based on the Mohr-Coulomb failure criterion. Hooke's law can be given by the equation:

$$\{\sigma\} = [C]\{\varepsilon\} \tag{3.6}$$

$$\begin{Bmatrix} \sigma_x \\ \sigma_y \\ \sigma_z \\ \tau_{xy} \\ \tau_{yz} \\ \tau_{zx} \end{Bmatrix} = \frac{E}{(1+\upsilon)(1-2\upsilon)} \begin{bmatrix} 1-\upsilon & \upsilon & \upsilon & 0 & 0 & 0 \\ \upsilon & 1-\upsilon & \upsilon & 0 & 0 & 0 \\ \upsilon & \upsilon & 1-\upsilon & 0 & 0 & 0 \\ 0 & 0 & 0 & \frac{1-2\upsilon}{2} & 0 & 0 \\ 0 & 0 & 0 & 0 & \frac{1-2\upsilon}{2} & 0 \\ 0 & 0 & 0 & 0 & 0 & \frac{1-2\upsilon}{2} \end{bmatrix} \begin{Bmatrix} \varepsilon_x \\ \varepsilon_y \\ \varepsilon_z \\ \gamma_{xy} \\ \gamma_{yz} \\ \gamma_{zx} \end{Bmatrix} \tag{3.7}$$

Where,

$\sigma_x, \sigma_y, \sigma_z$ are stress components,

$\tau_{xy,} \tau_{yz,} \tau_{zx}$ are shear stress components,

$\varepsilon_x, \varepsilon_y, \varepsilon_z$ are strain components,

$\gamma_{xy}, \gamma_{yz}, \gamma_{zx}$ are shear strain components

υ is Poisson's ratio and E is Young's modulus.

The relationship between Young's modulus E, shear modulus K and oedometer modulus are given by

$$G = \frac{E}{2(1+\upsilon)} \tag{3.8}$$

$$K = \frac{E}{3(1-2\upsilon)} \tag{3.9}$$

$$E_{oed} = \frac{(1-\upsilon)E}{(1-2\upsilon)(1+\upsilon)} \tag{3.10}$$

According to the classical theory of plasticity (Hill, 1950), plastic strain rates are proportional to the derivative of the yield function with respect to the stresses.

Mohr (1900) hypothesized a criterion of failure for real materials in which he stated that materials fail when the shear stress on the failure plane at failure reaches some unique function of the normal stress on that plane.

$$\tau_{ff} = f(\sigma_{ff}) \tag{3.11}$$

Where τ is the shear stress and σ is the normal stress. The first subscript (f) refers to the plane on which the stress acts (in this case the failure plane) and the second (f) means "at failure." Coulomb's equation is,

$$\tau_f = \sigma \tan\phi + c \tag{3.12}$$

Mohr-Coulomb failure criterion represents the linear envelops that is obtained from a plot of the shear strength of a material vs applied normal stress.

$$\tau_{ff} = \sigma_{ff} \tan\phi + c \tag{3.13}$$

Where τ is the shear strength, σ is the normal stress, c is the intercept of the failure envelop with the τ axis, ϕ is the slope of the failure envelope.

The Mohr-Coulomb yield conditions consists of six yield functions, when formulated in terms of principal stresses (Smith & Griffiths, 1982). Yield function is a function of stress and strain. Fig. 3.12 shows Mohr-Coulomb failure surface in principal stress plane. The failure surface in this case depends on type of loading (triaxial compression and triaxial extension etc.).The equations for the failure surface are the following:

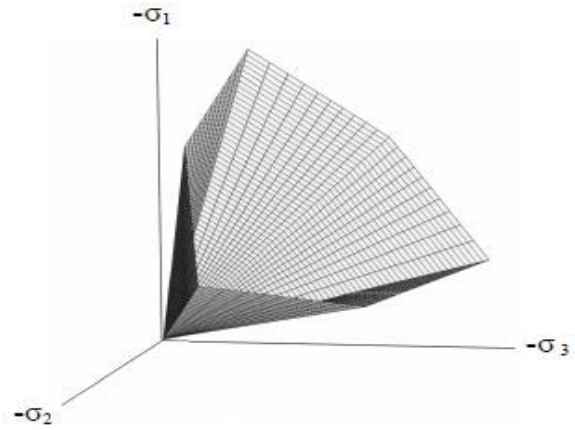

Fig. 3.12 Mohr-Coulomb yield surface in principal stress space

$$f_{1a} = \frac{1}{2}(\sigma_{2} - \sigma_3) + \frac{1}{2}(\sigma_2 + \sigma_3)\sin\phi - c\cos\phi \le 0 \qquad (3.14)$$

$$f_{1b} = \frac{1}{2}(\sigma_3 - \sigma_2) + \frac{1}{2}(\sigma_2 + \sigma_3)\sin\phi - c\cos\phi \le 0 \qquad (3.15)$$

$$f_{2a} = \frac{1}{2}(\sigma_3 - \sigma_1) + \frac{1}{2}(\sigma_3 + \sigma_1)\sin\phi - c\cos\phi \le 0 \qquad (3.16)$$

$$f_{2b} = \frac{1}{2}(\sigma_1 - \sigma_3) + \frac{1}{2}(\sigma_1 + \sigma_3)\sin\phi - c\cos\phi \le 0 \qquad (3.17)$$

$$f_{3a} = \frac{1}{2}(\sigma_1 - \sigma_2) + \frac{1}{2}(\sigma_1 + \sigma_2)\sin\phi - c\cos\phi \le 0 \qquad (3.18)$$

$$f_{3b} = \frac{1}{2}(\sigma_2 - \sigma_1) + \frac{1}{2}(\sigma_2 + \sigma_1)\sin\phi - c\cos\phi \le 0 \qquad (3.19)$$

Where ϕ and c are the friction angle and cohesion.

Where σ_1 = major principal stresses, σ_3 = minor principal stresses, σ_2 = intermediate principal stresses and 1, 2, 3 represents the plane on which stress acts, f_1, f_2 and f_3 are the yield functions, a, b and c represents the failure plane.

3.4 STATIC ANALYSIS

The two dimensional finite element program Plaxis 2D is used for the analysis. Plane strain finite element approach is used for the analysis of the berthing structure. In this analysis equivalent sheet pile walls are modeled as beam column elements and soil strata is represented by 15-noded triangular elements of elasto-plastic Mohr-Coulomb model. The different nodes are connected by bilinear Mohr-Coulomb interface elements. The different parameters to be inputted into the software include the structural details of the different

elements and also the properties of the different soil layers. All the details to be inputted are collected from New Mangalore Port Trust (NMPT).

The program uses a convenient graphical user interface that enables the user to quickly generate a geometry model and finite element mesh based on a representative vertical cross-section of the situation at hand. The user interface consists of three sub-programs (input, calculations and output data processing).

3.4.1 Input Pre-Processing

To carry out a finite element analysis using Plaxis, the user has to create a finite element model and specify the material properties and boundary conditions. This is done in the Input program. To set up a finite element model, the user must create a two-dimensional geometry model composed of points, lines and other components in the x-y plane. The generation of an appropriate finite element mesh and the generation of properties and boundary conditions on an element level is automatically performed by the Plaxis mesh generator based on the input of the geometry model. Users may also customize the finite element mesh in order to gain optimum performance. The final part of the input comprises the generation of water pressures and initial effective stresses to set the initial state.

When a geometry model is created in the input program it is suggested that the different input items are selected in the order given by the second tool bar. In principle, first draw the geometry contour, then add the soil layers, then structural objects, then construction layers, then boundary conditions and then loadings.

3.4.1.1 Input Program

The input program contains all facilities to create and to modify a geometry model, to generate a corresponding finite element and to generate initial conditions. The generation of the initial conditions is done in a separate mode of the input program (initial conditions mode).

3.4.1.2 Model

PLAXIS Version 8 is used to carry out two-dimensional finite element analyses. Finite element models may be either Plane strain or Axisymmetric. The default setting of the Model parameter is Plain strain. A plane strain model is used for geometries with a (more or less) uniform cross section and corresponding stress state and loading scheme over a certain length perpendicular to the cross section (z-direction). Displacements and strains in

z-direction are assumed to be zero. However, normal stresses in z-direction are fully taken into account.

An axisymmetric model is used for circular structures with a (more or less) uniform radial cross section and loading scheme around the central axis, where the deformation and stress state are assumed to be identical in any radial direction.

The selection of plane strain or axisymmetric results in a two dimensional finite element model with only two translational degrees of freedom per node (x- and y-direction).

3.4.1.3 Elements

The user may select either 6-node or 15-node triangular elements to model soil layers and other volume clusters. The 15 node triangle element provides a fourth order interpolation for displacements and the numerical integration involves twelve Gauss points (stress points). For the 6-node triangle the order of interpolation is two and the numerical integration involves three Gauss points. The element type used in the present study is 15-node triangular element.

3.4.1.4 Geometry

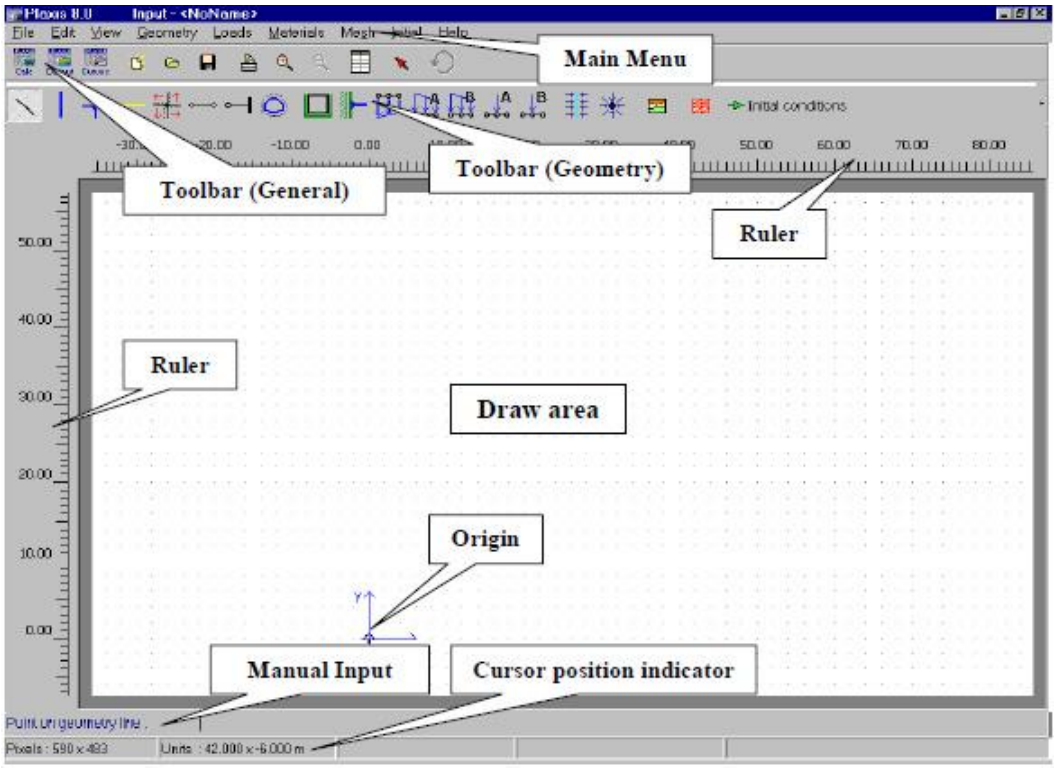

Fig. 3.13 Main window of the input program

A geometry model consists of points, Points and the user enters lines, whereas the program generates clusters. In addition to these basic components, structural objects or special conditions can be assigned to the geometry model to simulate tunnel linings, walls etc. Fig. 3.13 shows the main window of the input program. The generation of a finite element model begins with the creation of a geometry model, which is a representation of the problem of interest.

3.4.1.5 Loads and Boundary Conditions

The loads sub-menu contains the options to introduce distributed loads, line loads or point loads and prescribed displacements in the geometry model. Loads and prescribed displacements can be applied at the model boundaries as well as inside the model.

Prescribed displacements are special conditions that can be imposed on the model to control the displacements of certain points. Fixities are prescribed displacements equal to zero. Rotation fixities are used to fix the rotational degree of freedom of a plate around the z-axis. Drains are used to prescribe lines inside the geometry model where pore pressures are set to zero.

3.4.1.6 Material Properties

In PLAXIS, soil properties and material properties of structures are stored in material data sets. There are four different types of material sets: data sets for soil and interfaces, plates, geogrids and anchors. All data sets are stored in a material data base.

3.4.1.7 Material Model

The soil strata is represented by 15-node triangular elements of elasto-plastic Mohr-Coulomb model. Plate element is used to model diaphragm wall.

3.4.1.8 Type of material behavior (Material type)

In principle, all model parameters in Plaxis are meant to represent the effective soil response, i.e. the relation between the stresses and strains associated with the soil skeleton. To enable incorporation of the water-skeleton interaction in the soil response, Plaxis offers drained, undrained and non-porous behavioures for each soil model.

3.4.1.9 Mesh Generation

When the geometry model is fully defined and material properties are assigned to all clusters and structural objects, the geometry has to be divided into finite elements in order to perform finite element calculations. A composition of finite elements is called a mesh. The basic type of mesh element are the 15-node and 6-node triangular elements.

3.4.1.10 Initial Conditions

Once the geometry model has been created and the finite element mesh has been generated, the initial stress state and the initial configuration must be specified. This is done in the initial conditions part of the input program. With the generation of initial stresses, the generation of the initial situation of the finite element model is complete. By clicking the calculate button in the tool bar, the program goes to the next stage which is the calculations stage.

3.4.2 Calculations

After the generation of a finite element model, the actual finite element calculations can be executed. It is necessary to define which types of calculations are to be performed and which types of loadings or construction stages are to be activated during the calculations. This is done in the calculations program.

3.4.2.1 Defining a Calculation Phase

Consider a new project for which no calculation phase has yet been defined. In this case, the calculations list contains only one line, indicated as 'initial phase' with phase number 0. This line represents the initial situation of the project as defined in the initial conditions mode of the input program. The 'Initial phase' is the starting point for further calculations. To introduce the first calculation phase for the current project, the next button should be pressed after which a new line appears.

3.4.2.2 Calculation Types

The type of calculation of a phase is primarily defined in the combo box. Distinction is made between four basic types of calculations: a Plastic calculation, a Consolidation analysis, ∅-c reduction and Dynamic analysis.

3.4.2.3 Execution of the Calculation Process

When calculation phases have been defined and points for curves have been selected, then the calculation process can be executed.

3.4.2.4 Selecting Calculation Phases for Output

On selecting a finished calculation phase and clicking on the output button, the results of the selected phase are directly displayed in the output program. In this way, results of different calculation phases can be easily compared.

3.4.3 Output Data Post Processing

The main output quantities of a finite element calculation are the displacements at the nodes and the stresses at the stress points. In addition, when a finite element model involves structural elements, structural forces are calculated in these elements. The moments and forces, which are induced in these elements and the displacements of these elements, are obtained in this stage.

3.5 DYNAMIC ANALYSIS

The dynamic analysis of the structure is similar in most stages to the static analysis. Here also plane strain finite element approach is used for the analysis of the berthing structure. In this analysis equivalent sheet pile walls are modeled as beam column elements and soil strata is represented by 15-noded triangular elements of elastic-plastic Mohr-Coulomb model.

The input and soil parameters are similar to that used during static analysis. The different nodes are connected by bilinear Mohr-Coulomb interface elements. The stratigraphy is represented using finite elements. The self-weight load is applied to the mesh for generating the initial stress condition, allowing the excavation (dredging) procedure to be modeled. In addition to this, the earthquake data also need to be inputted into the program. The earthquake response spectrum used in this analysis is the acceleration-time details of the Imperial Valley earthquake, California (1987). The peak acceleration considered in this case is -307.053 cm/s^2 at 2.15 s. The response spectrum of the earthquake is shown in Fig. 3.14.

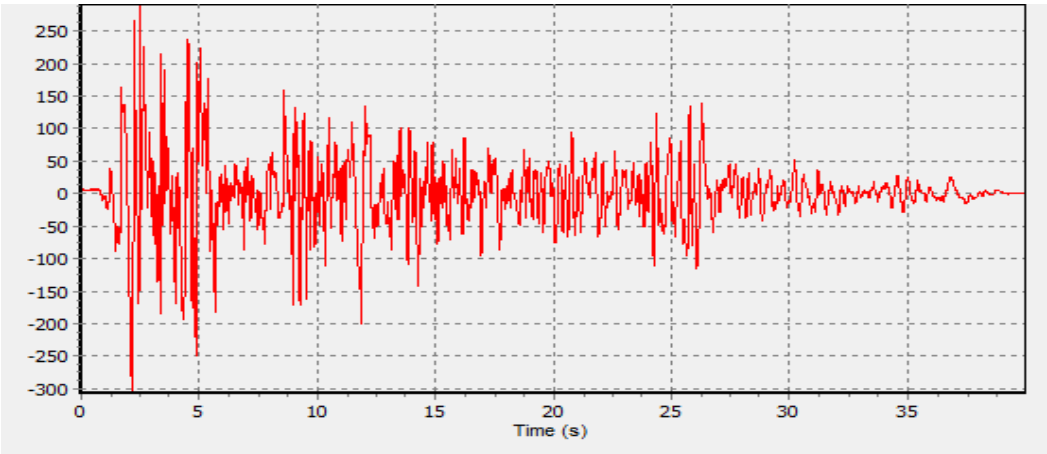

Fig. 3.14 Earthquake Spectrum Used For the Analysis

Plaxis allows the use of earthquake records in smc (strong motion CD-ROM) format as input data for earth quake loading.

3.5.1 Basic Equation for Dynamic Behaviour.

The basic equation for the time dependent movement of a volume under the influence of a dynamic load is;

$$M\ddot{u} + C\dot{u} + Ku = F \qquad (3.20)$$

Here M is the mass matrix, ü is the acceleration, u is the displacement vector, C is the damping matrix, $\dot{u}$ is the velocity, K is the stiffness matrix and F is the load vector**.**

3.5.2 Model Parameters

Additional model parameters, may be used to define wave velocities and material damping. When entering the elastic parameters E and ν, the corresponding wave velocities v_p and v_s are automatically generated. The compression wave velocities v_p can be expressed as a function of E and the mass ρ, as

$$V_p = \sqrt{\frac{E_{oed}}{p}} \qquad (3.21)$$

Where E = $\frac{(1-\nu)E}{(1+\nu)(1-2\nu)}$, and ρ = (γ)/g

In which E = Modulus of Elasticity, ν = Poisson's ratio, γ = total unit weight of soil and g is the acceleration due to gravity, E_{oed} is the Oedometer modulus.

Similar expression for shear wave velocity, $V_s = \sqrt{\frac{G}{\rho}}$ (3.22)

Where, G = E/ (2(1-ν))

For material damping, Rayleigh damping is used. The relation between damping mass and stiffness is,

$$C = \alpha M + \beta K \quad (3.23)$$

Where α and β are the Rayleigh coefficients, M is the mass and K is the stiffness. Rayleigh coefficients can be determined from at least two damping ratios ξ_i and corresponding frequencies of vibration ω_i and the relationship between those parameters,

$$\alpha + \beta\omega_i^2 = 2\omega_i\xi_i \quad (3.24)$$

The waves which generates due to compression and shear between body waves and solid body boundary is called as Rayleigh wave. In the event of earth quake, the largest disturbance, which recorded on a seismogram are usually caused by the Rayleigh waves (Plaxis 2D, Dynamic manual). The theoretical value of the velocity of the Rayleigh wave, V_R has been computed by Knopoff (1952):

$$V_R = 0.54V_P \quad (3.25)$$

Were $V_P = \sqrt{\frac{(1-\upsilon)E}{(1+\nu)(1-2\nu)\rho}}$ and $\rho = \frac{\gamma}{g}$

V_P is the velocity of the compression wave and g is the acceleration due to gravity (9.8m/s^2)

The user interface consists of three sub-programs (input, calculations and output data processing).

3.5.3. Input Pre-Processing

3.5.3. 1 Preparation of model

The cross section of the model is prepared in the Plaxis Input window. The model includes soil strata and structural elements.

3.5.3.2 Inputting of Material and Soil properties

After the model is drawn in the Input window, next step is the assigning of material and soil properties to the different structural elements and soil strata. In this project, Mohr-Coulomb model is used to stimulate the behaviour of soil and other continua.

3.5.3.3 Application of Loads

Next step is the application of loads and boundary conditions. The load applied in this project is an external live load of 50kN/m^2. As mentioned, Plaxis allows the use of earth quake records in SMC-format as input data for earth quake loading. The SMC files use centimeters as unit length. In the present study the plaxis unit is set as in meters. Hence for scaling the displacement, a displacement of 0.01m is provided at the bottom of the berthing structure in the x direction (u_x = 0.01m).

3.5.3.4 Mesh Generation

After the loads have been defined, the next step is the generation of mesh. The basic element type used here is the 15-noded triangular element.

3.5.3.5 Initial conditions

Once the mesh has been generated, the initial stress state and the initial configuration is specified.

3.5.3.6 Water conditions

In this step, the phreatic level and water conditions are defined. A phreatic level represents a series of points where the water pressure is just zero.

3.5.4 Starting calculations

After completing the Input-preprocessing, the next phase is the Calculations phase. In this calculation phase, staged construction is carried out. The initial stages are all similar to that of static analysis. After all the stages of static analysis are carried out, an additional stage is inputted. This calculation type for this stage is set as dynamic calculation and the time interval for analysis is set as 10 s.

In this stage, the response spectrum of the earthquake which is acting on the structure needs to be inputted. For this, the earthquake details need to be inputted into the Plaxis program in SMC format (Strong Motions CD-Rom).

3.5.5 Output Data Post Processing

The output of each stage can be generated using this phase. The bending moment, shear force, axial force and displacement of the diaphragm wall is obtained from this.

3.6 PLAXIS 3D

The Plaxis 3D program is a special purpose three dimensional finite element computer program used to perform deformation and stability analyses for various types of foundations and excavations in soil and rock, and it can also be used for other types of geotechnical problems. The program uses a convenient graphical user interface that enables users to quickly generate a geometry model and finite element mesh based on a representative vertical cross-section of the situation at hand.

3.6.1 Elements

During the generation of the mesh, the geometry is divided in to 15-node wedge elements. These elements are composed of 6-node triangular faces in the work planes and 8-node quadrilateral faces in y-directions.

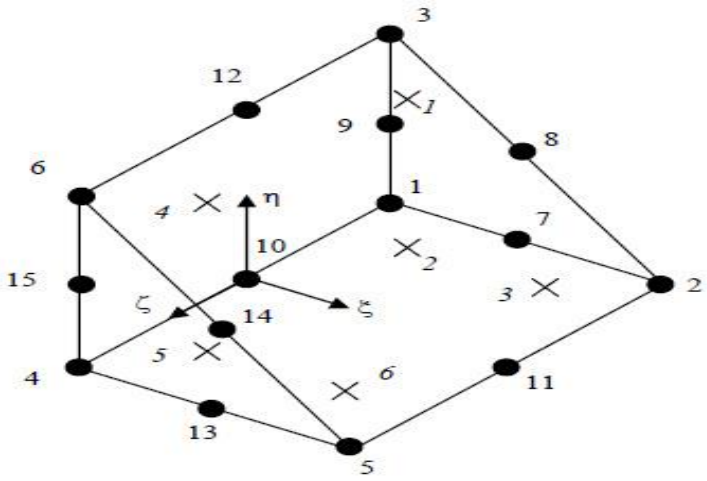

Fig. 3.15 Distribution of nodes (•) and stress points (×) in a 15- node wedge element

In addition to the volume elements, 2-node or 3-node line elements, 6-node or 8-node plate elements and 16-node interface elements may be generated to model structural behavior and soil- structure interaction analysis respectively. The wedge element used in Plaxis 3D program consist of 15-nodes and 6 stress points as shown in Fig. 3.15. Adjacent elements are connected with their common nodes.

3.6.2 Six-node Triangular Element

6-node triangular elements are created in the 2D mesh generation process and used in the horizontal planes of the 3-D model to form the faces of the 15-noded wedge element for soil as shown in Fig. 3.16. For triangular elements there are two local coordinates (ζ and η).

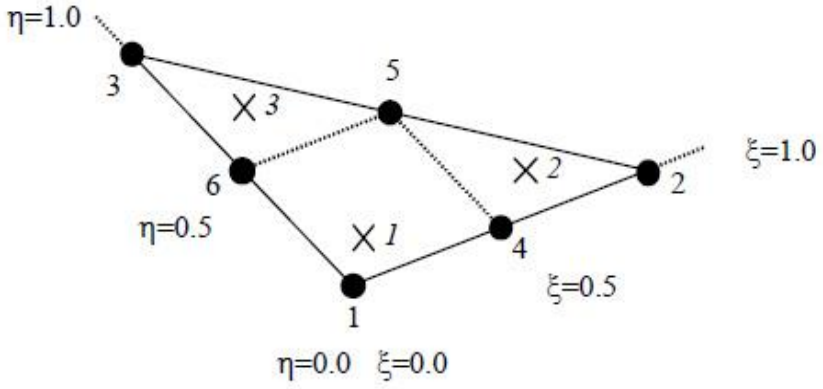

Fig. 3.16 The position of nodes (•) and integration points of a 6-node plate element.

3.6.3 Eight node Quadrilateral Element

The 8-noded quadrilateral elements (as shown in Fig. 3.17) are created in the 3D extension process and they are used at the faces of the 15-noded wedge elements in the y- direction. These elements are the basis for the wall elements, distribution loads on a vertical plane and for interface elements. Quadrilateral elements have local coordinates, ζ and η.

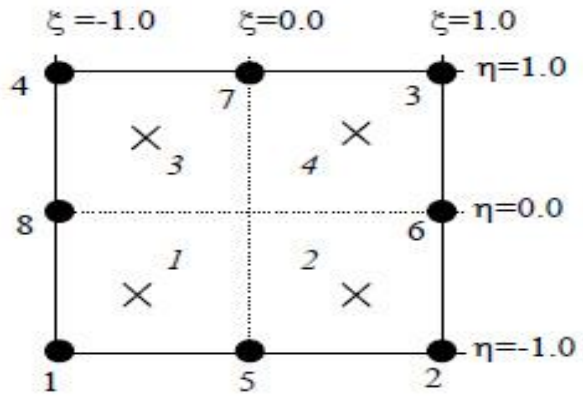

Fig. 3.17 Position of nodes (•) and integration points of an 8-node plate element.

The Plaxis program provides a convenient graphical user interface that enables users to quickly generate a geometry model and finite element mesh based on a representative vertical cross-section of the situation at hand. The user interface consists of four sub-programs (input, calculations, output and curves).

3.6.4 Input Pre-Processing

To carry out a finite element analysis using Plaxis 3D, the user has to create a finite element model and specify the material properties and boundary conditions. This is done in the Input program. To set up a three dimensional finite element model, the user must create a two-dimensional geometry model composed of points, lines and other components in the x-z plane. Later the model is extended into three dimension by means of work planes. The generation of an appropriate finite element mesh and the generation of properties and boundary conditions on an element level is automatically performed by the Plaxis 3D mesh generator based on the input of the geometry model. Users may also customize the finite element mesh in order to gain optimum performance. Fig. 3.18 shows Plaxis 3D input window.

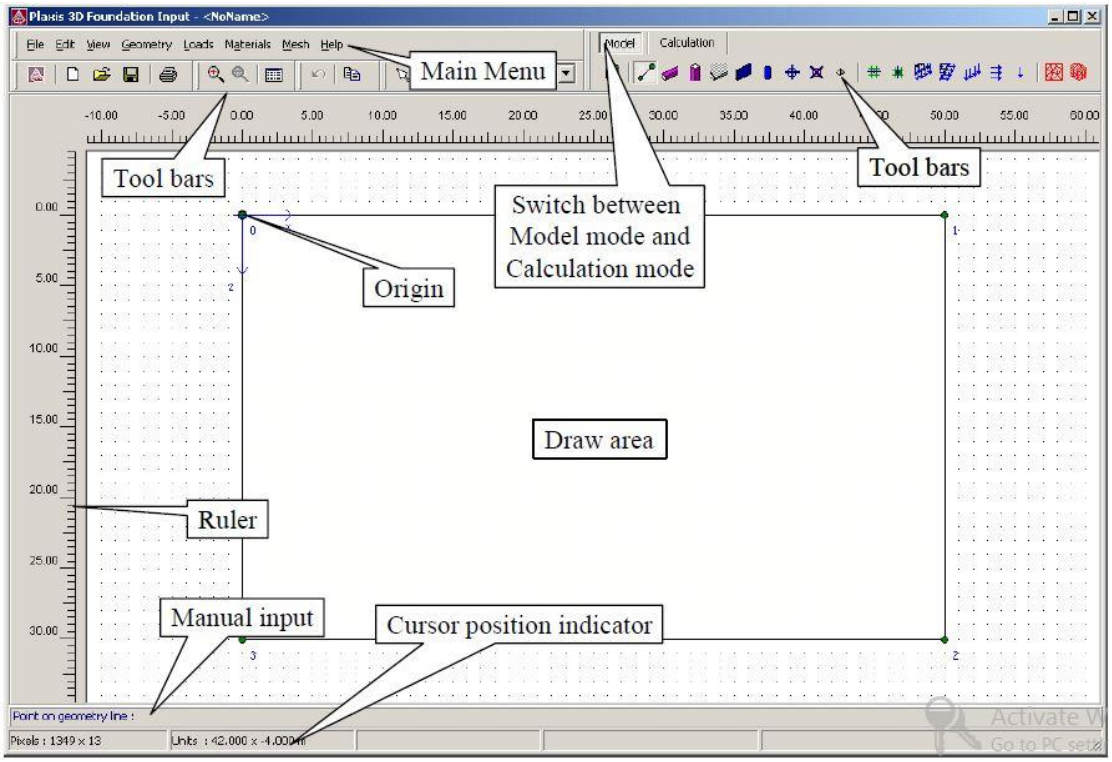

Fig. 3.18. Plaxis 3D input window

3.6.5 Geometry

The generation of a 3D finite element model begins with the creation of a geometry model. A geometry model is a composition of boreholes and horizontal work planes (x-z planes). The boreholes are used to define the local stratigraphy (vertical soil layer position), ground

surface level and pore pressure distribution. The work planes are used to define geometry lines, loads and structures.

It is recommended to start the creation of a geometry model by defining boreholes to identify the different soil layers. Multiple boreholes can be defined to create non horizontal soil layers. During the definition of boreholes, data sets of model parameters for the various soil layers can be created and assigned to the borehole. After all the boreholes have been defined, the user should create all necessary work planes. In a work plane, geometry points, lines and area clusters can be created. Points and lines are entered by the user, whereas clusters are generated by the program. In addition to these basic components, structural objects or special conditions can be assigned to the work planes to simulate beams, walls, floors, piles, soil-structure interaction or loadings.

Data sets of model parameters for structural behaviour can be created and assigned to the structural objects in the work planes. The full composition of work planes should not only be based on the initial situation, but also on situations that arise in the various calculation.

3.6.6 Work planes

Work planes are horizontal (x-z planes) at a certain vertical level (y-level) in which the geometry points and lines and, in particular, structures and loads can be defined. Moreover, work planes may be used to create different construction or excavation levels. However, work planes should not be used to create soil layers, since the latter is particularly taken care by the borehole facility. At the start of a new project, a single initial work plane is automatically created at the level y = 0. The level of this work plane may be changed by the user and the user may also create additional work planes. If the geometry model includes volume piles, it is recommended to first create the work planes corresponding to the pile top and bottom level, then create the volume piles and then create other work planes and structural objects.

3.6.7 Structural Elements

3.6.7.1 Horizontal beams

Horizontal beams are structural objects used to model slender (one dimensional) structures in the ground with a significant flexural rigidity (bending stiffness) and an axial stiffness. Horizontal beams coincide with the active work plane. Hence, before the creation of a horizontal beam, the appropriate work plane needs to be created in the work planes dialogue or selected from the active work plane combo box. Horizontal beams are composed of 3-

node line elements (beam elements) with six degrees of freedom per node. Three translational degrees of freedom (u_x, u_y and u_z) and three rotational degrees of freedom (ϕ_x, ϕ_y and ϕ_z). The element allows for beam deflections due to shearing as well as bending. In addition, the element can change length when an axial force is applied. When a beam element is connected to another beam element (horizontal or vertical beam) or a plate element (floor or wall), they share all degrees of freedom in the connecting node, which implies that the connection is rigid (moment connection).

3.6.7.2 Vertical Beams

Vertical beams are structural objects used to model slender (one-dimensional) structures in the ground with a significant flexural rigidity (bending stiffness) and an axial stiffness. Vertical beams are located between the active work plane and the next work plane below the current one. Hence, before the creation of a vertical beam, work planes need to be created corresponding with the top and the bottom of the beam. Vertical beams are composed of 3-node line elements (beam elements) with six degrees of freedom per node: Three translational degrees of freedom (u_x, u_y and u_z) and three rotational degrees of freedom (ϕ_x, ϕ_y and ϕ_z). The element allows for beam deflections due to shearing as well as bending. In addition, the element can change length when an axial force is applied. When a beam element is connected to another beam element (horizontal or vertical beam) or a plate element (floor or wall), they share all degrees of freedom in the connecting node, which implies that the connection is rigid (moment connection).

3.6.7.3 Floors

Floors are structural objects used to model thin horizontal (two-dimensional) structures in the ground with a significant flexural rigidity (bending stiffness). Floors coincide with the active work plane and extend over a full cluster. Before the creation of a floor, the corresponding contour (cluster) needs to be created using geometry lines. These geometry lines appear in all work planes. Hence, before the creation of the floor, the appropriate work plane needs to be selected from the Active work plane combo box.

Floors are composed of 6-node triangular plate elements with six degrees of freedom per node: three translational degrees of freedom (u_x, u_y and u_z) and three rotational degrees of freedom (ϕ_x, ϕ_y and ϕ_z). The element allows for plate deflections due to shearing as well as bending. In addition, the element can change length when an axial force is applied. When a plate element is connected to another plate element (floor or wall) or a beam element

(horizontal or vertical), they share all degrees of freedom in the connecting node(s), which implies that the connection is rigid (moment connection).

3.6.7.4 Walls

Walls are structural objects used to model thin vertical (two-dimensional) structures in the ground with a significant flexural rigidity (bending stiffness). Walls are located between the active work plane and the next work plane below the current one. Hence, before the creation of a wall, work planes need to be created corresponding with the top and the bottom of the wall. In addition, the work plane at the upper side of the wall needs to be selected from the Active work plane combo box. The wall can then be created on this work plane. If a wall is created on the lowest available work plane, a new work plane will automatically be introduced at a distance of 3 length units below this work plane.

Walls are composed of 8-node quadrilateral plate elements with six degrees of freedom per node: three translational degrees of freedom (u_x, u_y and u_z) and three rotational degrees of freedom (ϕ_x, ϕ_y and ϕ_z). Along degenerated soil elements, walls are composed of 6-node triangular plate elements, compatible with the triangular side of the degenerated soil element. The element allows for plate deflections due to shearing as well as bending. In addition, the element can change length when an axial force is applied. When a plate element is connected to another plate element (floor or wall) or a beam element (horizontal or vertical), they share all degrees of freedom in the connecting nodes, which implies that the connection is rigid (moment connection).

3.6.7.5 Interface Elements

Interfaces are composed of 16-node interface elements as shown in Fig. 3.19. Interface elements consist of eight pairs of nodes, compatible with the 8-noded quadrilateral side of a soil element. Along degenerated soil elements, interface elements are composed of 6-node pairs, compatible with the triangular side of the degenerated soil element. At wall ends (both in horizontal direction and in vertical direction) interface element node pairs are 'degenerated' to single node. There are no interface elements beyond the wall. Also when walls are connected to floors or horizontal beams, interface element node pairs are locally degenerated to single nodes to avoid a disconnection between the wall and the floor or beam.

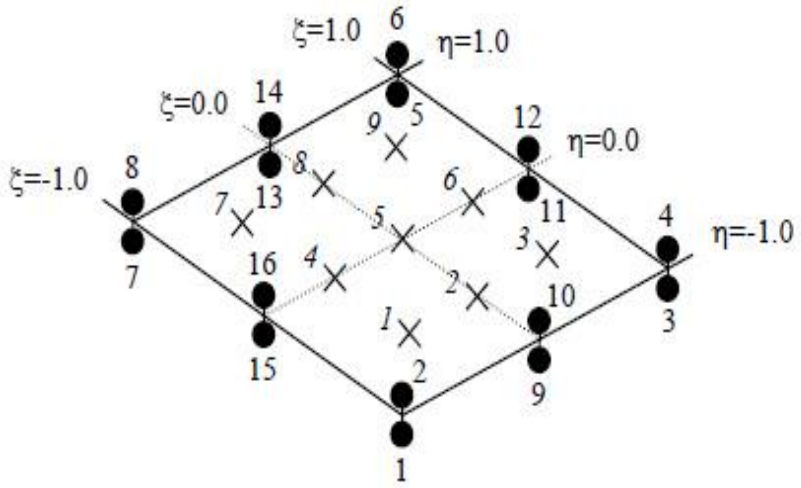

Fig. 3.19 The position of nodes (•) and integration points of a 16-node inter face element

3.6.8 Loads And Boundary Conditions

The loads sub-menu contains the options to introduce distributed loads , line loads or point loads and prescribed displacements in the geometry model. Loads and prescribed displacements can be applied at the model boundaries as well as inside the model.

3.6.9 Material Properties

In PLAXIS 3D, soil properties and material properties of structures are stored in material data sets. There are eight different types of material sets: data sets for soil and interfaces, embedded piles, volume piles, horizontal beams, vertical beams, Walls, Floors, Springs and Ground anchors. All data sets are stored in a material data base.

3.6.9.1 Material Model

Plaxis 3D supports various models to simulate the behaviour of soil and other continnua. The elastic-plastic Mohr-Coulomb model is considered for soil modelling and plate element is considered for wall modelling in the present study.

3.6.10 Calculations

After the generation of a finite element model, the actual finite element calculations can be executed. Therefore it is necessary to define which types of calculations are to be performed and which types of loadings or construction stages are to be activated during the calculations. This is done in the calculations program.

3.6.11 Output Data Processing

The main output quantities of a finite element calculation are the displacements at the nodes and the stresses at the stress points. In addition, when a finite element model involves structural elements, structural forces are calculated in these elements. The moments and forces which are induced in these elements and the displacements of these elements are obtained in this stage.

3.7 STUDY AREA

For the purpose of analysis, diaphragm wall provided in the deep draft multipurpose berth of NMPT is considered.

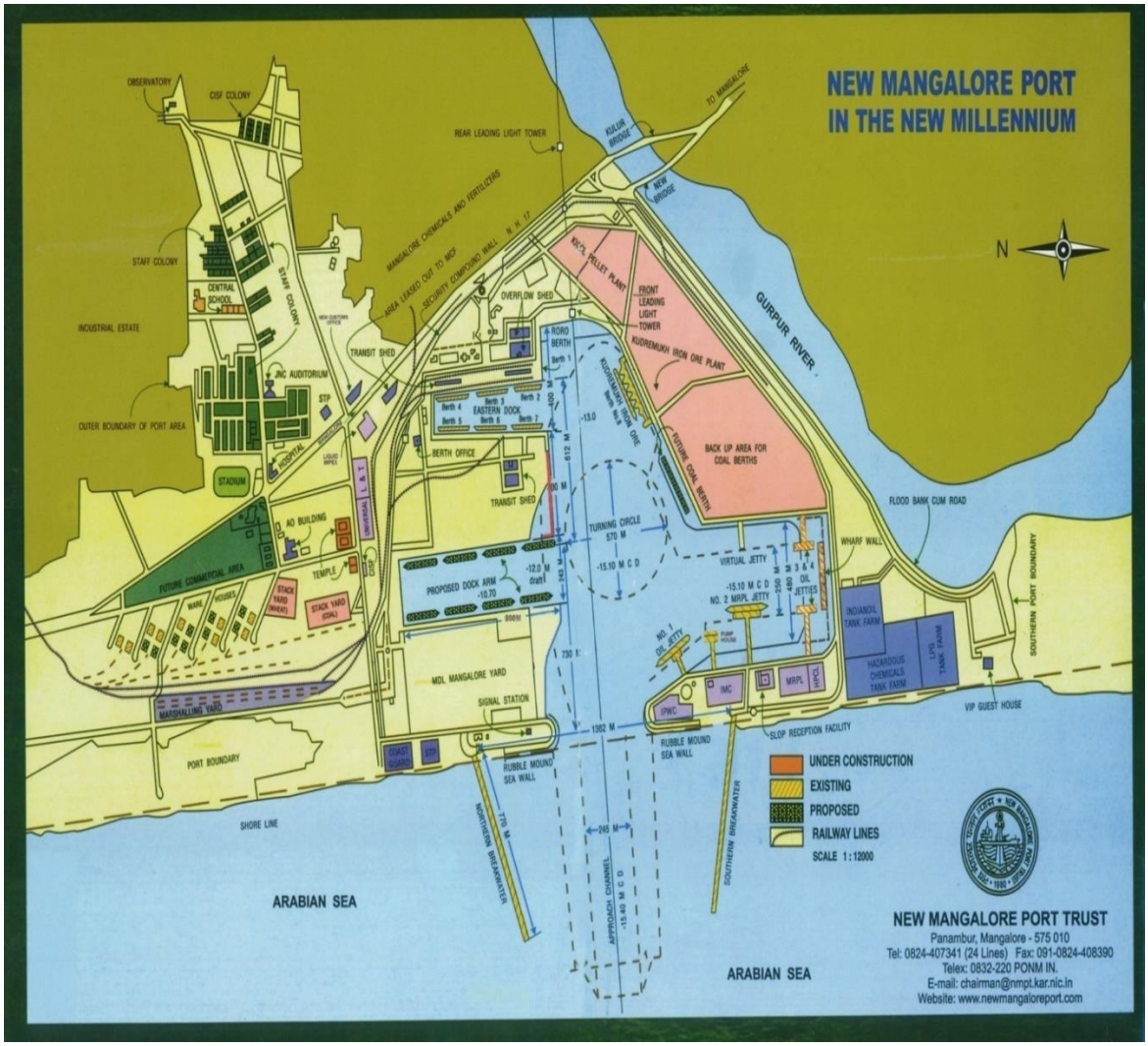

Fig. 3.20 Location Plan of New Mangalore Port Trust

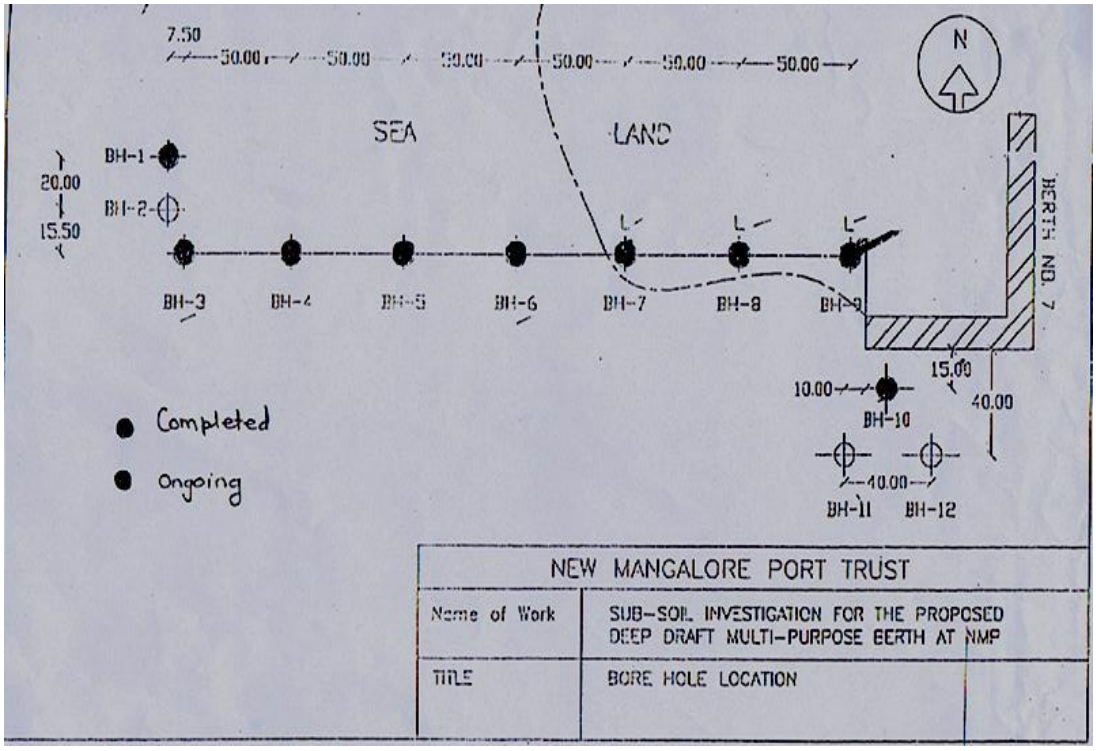

Fig. 3.21 Bore hole Location details of the deep draft berth of NMPT

The location plan of the berth is shown in Fig. 3.20. The deep draft multipurpose berth is situated in the New Mangalore Port. It is located opposite to the Kudremukh iron ore berth 8. The borehole location plan of the deep draft berth at NMPT is shown in Fig. 3.21. In the analysis of the berth the critical cases of the boreholes near to the sea and land are considered. Since the boreholes 6 and 7 are located near to the land and sea, these 2 boreholes are considered for the analysis. The bore log details of the boreholes are given in Fig. 3.22.

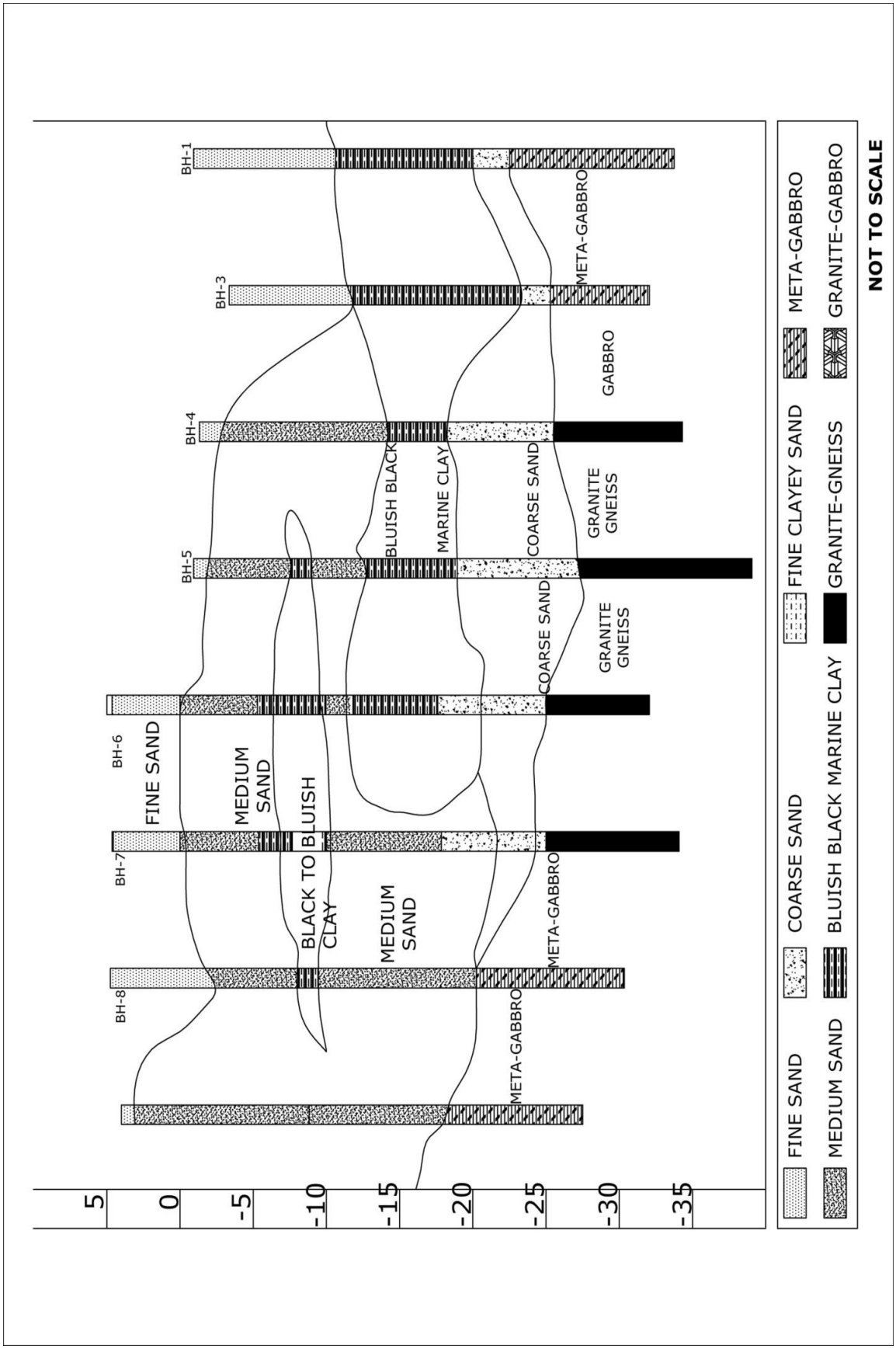

Fig. 3.22 Soil profiles of boreholes

3.7.1 Cross Section of Deep Draft Berth

The cross section of deep draft berth is shown in Fig 3.26. The tie rod anchor is inclined at an angle of 45°. Hard rock is found at a depth of -30 m. The length of the model is 66 m and height of the model is 29.5 m. The chart datum is at 0.0 m. The width of the berthing structure is 33 m. The berth is supported by a diaphragm wall and 4 rows of 1000mm diameter piles. The piles are terminated at a depth of -30 m. The dredge depth is -10m near the diaphragm wall and -17 m near the first pile as shown in Fig 3.26. In addition, anchor rods are also provided at every 2.5 m.

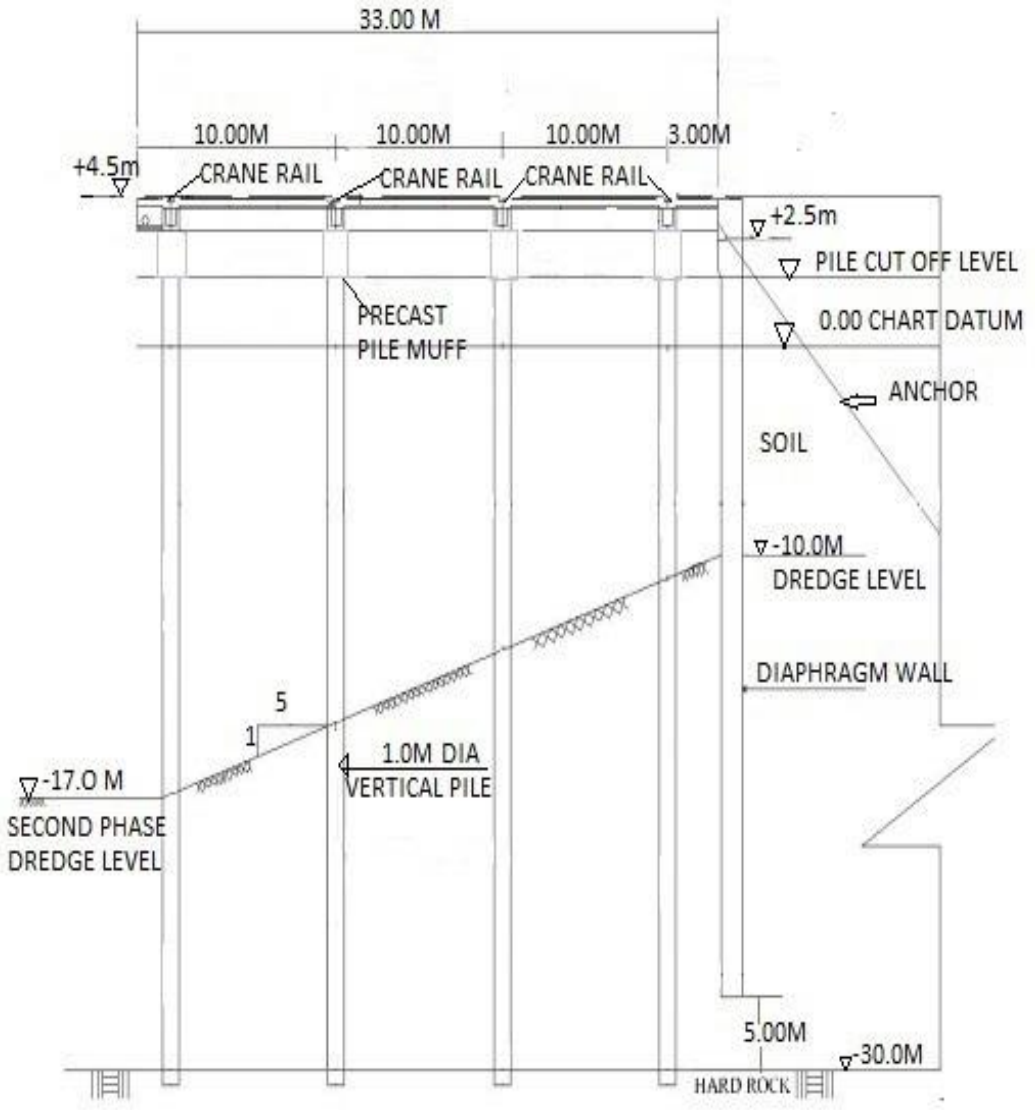

Fig. 3.23 Cross-section of deep draft berth

Table 3.1 Different soil layers in the borehole 6 & 7

Type of Soil (Bore hole 6)	Depth (m)	Type of Soil (Bore hole 7)	Depth (m)
Fine sand	+4.5 to 0	Fine sand	4.5 to 0
Medium sand	0 to - 6	Medium sand	0 to - 6
Black to bluish clay	- 6 to – 10	Black to bluish clay	- 6 to - 10
Medium sand	-10 to – 12	Medium sand	-10 to - 18.5
Black to bluish clay	-12 to – 18	Coarse sand	-18.5 to - 25
Coarse sand	-18 to – 25		

3.7.2 Material parameters.

Young's modulus of concrete is calculated by using the equation given in Bureau of Indian Standards - 456 -2000.

For M40 grade concrete, the Young's modulus $E=5000\sqrt{fck}$

$$E=5000\sqrt{40} =31.62\times 10^{6} kN/m^2$$

3.7.3 Embedded Pile

Dia of pile (D) = 1200mm

Cross sectional area of pile (A) = $(\pi\times D^2)/4 = 1.13m^2$

Density (γ) = 25 KN/m^3

Axial Modulus (EA) = 31.62×10^{6}x1.13 = $35.73x10^6$ kN

Modulus of rigidity (G) = $E/2(1+\upsilon) =31.62\times 10^{6}/2(1+0.15) = 13.75\times10^6$ kN/m^2

3.7.4 Diaphragm Wall

Thickness (t) = 1100mm

Density (γ) = 25 kN/m^3

Axial Modulus (EA) = 31.62×10^6 x 1.1x1=34.782×10^6 kN

Modulus of rigidity (G) = $E/2(1+\upsilon) = 31.62\times10^6/2(1+0.15) = 13.75\times10^6$ kN/m^2

3.7.5 Beams

Depth (d) = 1200 mm

Bredth (b) = 1200 mm

Cross sectional area (A) = $1.2\times1.2 = 1.44$ m^2

Density (γ) = 25 kN/m^3

Moment of Inertia $I_3 = 1.2\times1.2^3/12 = 0.173\ m^4$

$I_2 = 1.2\times1.2^3/12 = 0.173\ m^4$

$I_{23} = 0$

Axial Modulus (EA) = 1.77×10^7 kN

3.7.6 Anchor rod

Dia of anchor = 0.14 m

Cross sectional area (A) = $(\pi\times D^2)/4 = (\pi\times0.14^2)/4 = 0.0154 m^2$

Pre-stressing force in the anchor = 225 Tonnes

Modulus of Elasticity (E) = $2.08\times10^6/0.0154 = 1.351\times10^8$ kN/m^2

The input parameters are of structural and soil properties are shown in Table 3.2 and 3.3.

Table 3.2 Input Parameters of Structural Elements

Material	Axial modulus(EA) (kN)	Flexural rigidity(EI) (kN-m^2)	Poisson's Ratio (μ)
Embedded pile	$35.73x10^6$	5.57×10^6	0.15
Diaphragm wall	34.782×10^6	1.7533×10^7	0.15
Beam	17.75×10^6	5.324×10^5	0.15
Anchor rod	2.08×10^6	_	0.29

Table 3.3 Input Parameters of Soil Properties

Material	Model	Young's modulus kN/m^2	Saturated density γ_{sat} kN/m^3	Poisson's ratio (υ)	c kN/m^2	Φ in degrees
Fine sand	Elastic	80000	18	0.3	0.5	30
Medium sand	Elastic	70000	18	0.3	0.45	30
Marine clay	Elastic	20000	18	0.49	17	0
Coarse sand	Elastic	60000	18	0.25	0.4	30

CHAPTER 4

2D ANALYSIS OF DIAPHRAGM WALL WITH STATIC AND DYNAMIC LOADING

4.1 STATIC ANALYSIS

The two dimensional finite element program Plaxis 2D is used for the analysis. Plane strain finite element approach is used for the analysis of the berthing structure. In this analysis equivalent sheet pile walls are modeled as beam column elements and soil strata is represented by 15-noded triangular elements of elasto-plastic Mohr-Coulomb model. The different nodes are connected by bilinear Mohr-Coulomb interface elements. The different parameters to be inputted into the software include the structural details of the different elements and also the properties of the different soil layers. All the details to be inputted are collected from NMPT.

4.1.1 Preparation of Model

The cross section of the model is prepared in the Plaxis Input window. The model includes soil strata and structural elements.

4.1.2 Inputting of Material and Soil Properties

After the model is drawn in the Input window, next step is the assigning of material and soil properties to the different structural elements and soil strata. In this project, Mohr-Coulomb model is used to simulate the behaviour of soil and other continua.

4.1.3 Application of Loads and Boundary Conditions

Next step is the application of loads and boundary conditions. The load applied in this project is an external live load of 50 kN/m^2 in addition to the standard fixities.

4.1.4 Mesh Generation

After the loads have been defined, the next step is the generation of mesh. The basic element type used here is the 15-noded triangular element.

Once the mesh has been generated, the initial stress state and the initial configuration is specified.

4.1.5 Water Conditions

In this step, the phreatic level is defined. A phreatic level represents a series of points where the water pressure is zero.

4.1.6 Initial Geometry Configuration

After defining the water conditions, the initial stresses are generated. After completing the Input-preprocessing, the next phase is the calculation phase. Since this is the static analysis, the calculations program is set as plastic calculation. In this phase, staged construction is carried out. The different elements are activated at different stages and are finally calculated.

4.1.7 Output data Post Processing

The output of each stage can be generated using this phase. The bending moment, shear force, axial force and displacement of the diaphragm wall are obtained from this.

4.2 LOADS AND BOUNDARY CONDITIONS

The loads sub-menu contains the options to introduce distributed loads, line loads or point loads and prescribed displacements in the geometry model. Loads and prescribed displacements can be applied at the model boundaries as well as inside the model.

For 2D analysis boundary conditions are as follows;

- ✓ Vertical model boundaries with their normal in x direction (i.e. parallel to the y-z plane) are fixed in x direction ($u_x = 0$) and free in y and z direction.
- ✓ Horizontal geometric lines for which the y-coordinates is equal to the lowest y coordinate in the model (The model bottom boundary) obtain a full fixity ($u_x = u_y = 0$).
- ✓ Horizontal beams, vertical beams, floors or walls that extend to the model boundary where at least one displacement direction is fixed to obtain a fixed rotation in the point at the boundary ($z = 0$)

4.2.1 Loads Acting on the Structure

A uniform surcharge of 50 kN/m^2 is acting on top of the soil and structure. Additionally a uniform load of 50 kN/m^2 is considered for the analysis because the berth was designed for that load. Since the water level on both the sides of the diaphragm wall is considered to be at the same height in this analysis (chart datum is at 0.0 m level), differential water pressure is zero. The passive and active earth pressure due to the soil present on both sides acts on the wall. The structural members such as slabs, beams, diaphragm wall and piles are assumed of having a density of 25 kN/m^3. Plaxis 3-D accounts for self-weight based on the geometric dimensions (length, depth and breadth) and densities of the structural elements.

4.3 2D ANALYSIS AND RESULTS

The following cases are considered in Plaxis 2D analysis:-

Case 1. Comparison of performance of diaphragm wall for 2 borehole locations

Case 2. Analysis of diaphragm wall in the absence of anchor

Case 3. Analysis of diaphragm wall for varying locations of anchor

Case 4: Analysis of effect of dredging on the diaphragm wall

4.3.1 Comparison of Performance of Diaphragm wall for Soil Strata Corresponding to Two Bore hole Locations

The analysis of the diaphragm wall is done for the soil data corresponding to 2 borehole locations. The behaviour of the diaphragm wall will be different for both the borehole locations. There will be variation in the forces and moments induced in the diaphragm wall in both the cases. This difference is analyzed in this case. The two borehole locations (6 and 7) are compared for the case without any anchor. The comparison of the displacements, shear forces and bending moments induced in the diaphragm wall in both the locations are discussed.

The variation of displacement of the diaphragm wall for both the borehole locations is as shown in Fig. 4.1. It is clear from the graph that the maximum displacement occurs for the soil profile in borehole 6. The difference in the soil layer is mainly presence of additional marine clay in borehole 6. So we can say that the displacement is more in marine clay as compared to medium sand. This may be because the clayey soil is more

cohesive and the resistance offered to displacement is less, hence allows more movement. The difference in extreme displacement for both the borehole locations is used to find out which is more critical and so further studies are carried out only for

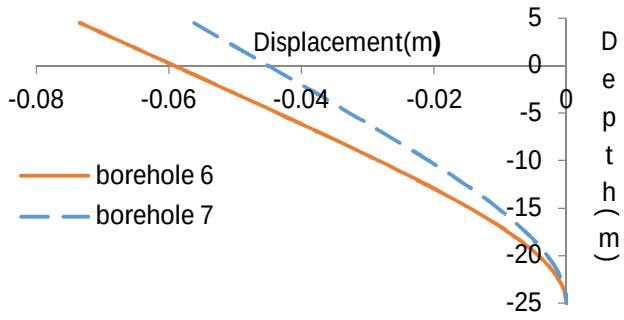

that borehole location.

Fig. 4.1 Comparison of displacement of diaphragm wall for soil profiles in two boreholes in static analysis, without anchor

The variation of shear force is as shown in Fig. 4.2. The shear force variation for both the borehole locations is same till a depth of -12 m. After -12 m, the difference in shear force occurs. The soil profile for borehole 6 is found as marine clay and for the borehole 7 is medium sand for the depth -12 m to -18 m. Because of the lesser passive resistance offered by the marine clay when compared with medium sand, shear force is increased in borehole 6 with respect to 7 for the depths -12 m to -18 m. The shear force variations, after -18 m shows similar trend and is maximum at -25 m for the both borehole locations.

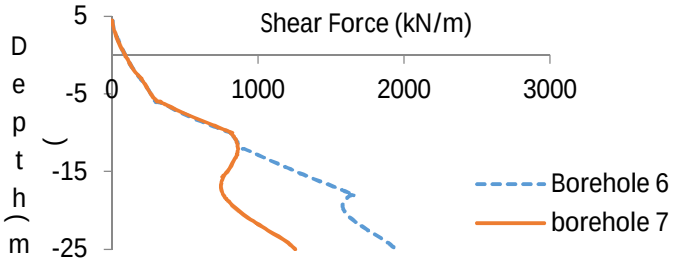

Fig. 4.2 Comparison of shear force with depth of diaphragm wall for soil profiles in two boreholes in static analysis, without anchor.

The variation of bending moment is dependent on the variation in shear force. Here also, the bending moment in both the cases is the same till a depth of -12 m, after which the variation begins. This variation of bending moment with depth of diaphragm wall

is shown in Fig. 4.3. The maximum bending moment is obtained at -25 m depth for the both cassis.

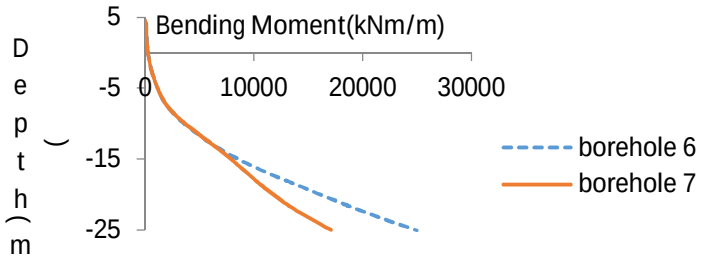

Fig. 4.3 Comparison of bending moment with depth of diaphragm wall for soil profiles in two boreholes in static analysis, without anchor.

From the study it is found that, the maximum displacement and bending moment occur for the soil profile of borehole no 6. Hence, soil profile of bore hole no 6 is considered for further investigation.

4.3.2. Analysis of Diaphragm wall in the Absence of Anchor rod.

The variation of displacement with depth for the diaphragm wall is shown in Fig. 4.4. The maximum displacement in this case is found to be -0.073 m at +4.5m level. The diaphragm wall in the absence of anchor behaves like a cantilever beam with the bottom end fixed. In a cantilever beam, the maximum displacement occurs at the free end which in this case is at the top of the wall. The displacement of the diaphragm wall is zero at the bottom

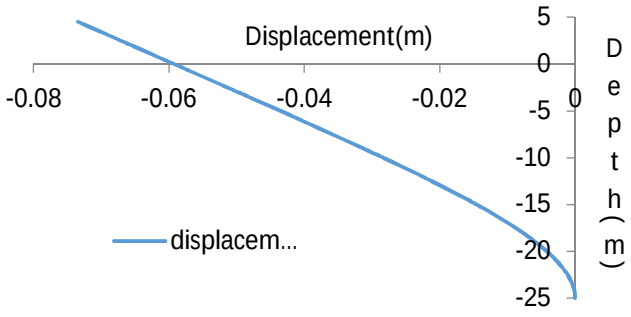

Fig. 4.4 Variation of displacement of diaphragm wall in static analysis without anchor

The variation of shear forces is as shown in Fig. 4.5. Since no external force acts at a depth of + 4.5 m, the value of shear force is zero at the top of the diaphragm wall. Till a depth of -10 m only force due to the active earth pressure acts on the diaphragm wall.

The passive force starts to act from -10 m. The maximum shear force is obtained at the bottom of the diaphragm wall. The considerable reduction in the shear force at a depth of -18 m is due to change in the soil layer from marine clay to coarse sand. The reduction In passive resistance causes increase in the shear force. At the interface of the two soil strata, the shear force value shows a considerable decrease. This is evident from Fig. 4.5. The maximum value of shear force obtained is at the bottom of the diaphragm wall and is equal to 1947.82 kN/m.

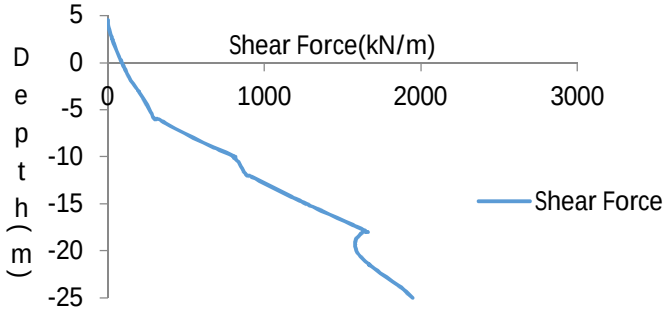

Fig. 4.5 Variation of shear forces with depth of diaphragm wall in static analysis without anchor

The variation of bending moment in the diaphragm wall is shown in Fig. 4.6. The maximum value is obtained at the bottom of the diaphragm wall. The bending moment value is dependent on the value of shear force. So the bending moment is zero at the

top. The maximum value of bending moment which is obtained at the bottom of the diaphragm wall is 24,936.03 kNm/m.

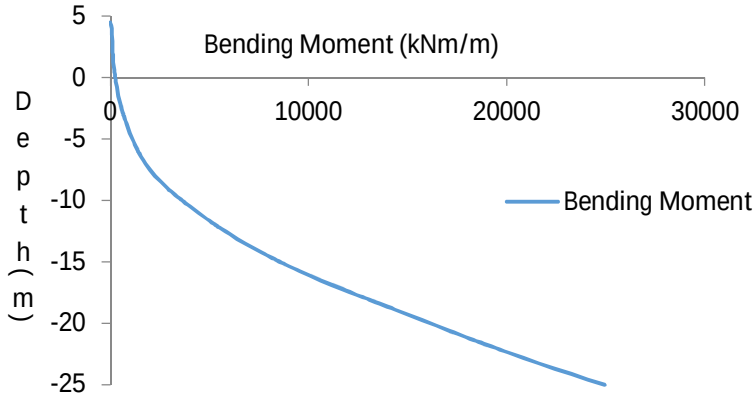

Fig. 4.6: Variation of bending moment with depth of diaphragm wall in static analysis without anchor.

4.3.3 Analysis of Diaphragm wall for Varying Locations of Anchor rod.

The anchor is placed at different locations and displacement, bending moment, and shear force of the diaphragm wall is studied.

The different anchor locations considered in the analysis are:

i. At the top of diaphragm wall, at +4.5 m

ii. At the water table, at 0.0 m

iii. At the different soil levels, at +2.5 m, -6.0 m and -10.0 m

The maximum displacement, shear force and bending moment of the diaphragm wall for the various anchor locations are shown in Table 4.1.

Anchored diaphragm wall acts like a propped cantilever. From Fig 4.7, it is clear that the maximum displacement of the diaphragm wall depends on the location of anchor. When the anchor is placed at +4.5 m, the maximum displacement of the wall of 0.00599 m is obtained at -9 m. In this case, the maximum deflection occurs in between the support and the position where the anchor is located. When the anchor is placed at a depth of +2.5 m, the maximum displacement obtained is 0.00492 m. The anchor position when shifted to 0 m, the length of the diaphragm wall in between the anchor and the bottom of the diaphragm wall is reduced as a result of which the maximum deflection in between these two points is reduced. But the portion of the diaphragm wall

above the anchor deflects in the opposite direction. The anchor position when at -6 m, the diaphragm wall deflection is almost same in both the directions. When the anchor position is shifted to -10 m, the displacement of diaphragm wall between the anchor and the support at the bottom is less than the displacement at the top of the diaphragm wall. From the graph, it is clear that the maximum displacement occurs for +4.5 m. The variation of shear force is shown in Fig. 4.8. The shear force is zero at the top and gradually increases as the depth is increased. When the anchor is placed at a particular position, the shear force at that point is decreased due the force taken by the anchor. Till a depth of -10 m the shear force increases gradually. After -10 m, the shear force value starts to decrease. This is due to the presence of passive earth pressure. After -18 m, the shear force again reduces due to the increase in the passive earth pressure.

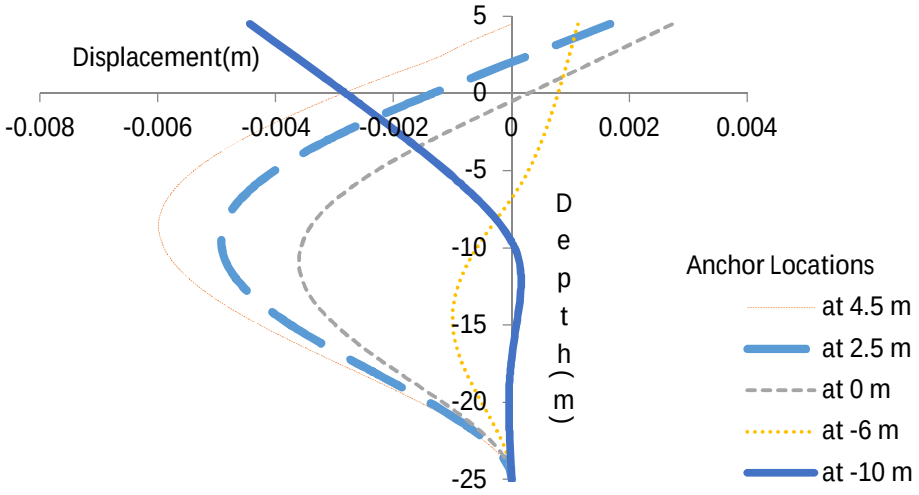

Fig. 4.7 Variation of displacement with depth of the diaphragm wall for different anchor locations (Static analysis)

The maximum value of positive shear force is obtained at -25 m depth, when the anchor is placed at +4.5 m. The maximum value of negative shear force is obtained at -25 m depth, when the anchor is placed at -10 m. The minimum positive shear force is obtained when the anchor is placed at -6 m.

The variation of bending moment is shown here in Fig. 4.9. The bending moment is zero at the top of the diaphragm wall, when there is no anchor fixed at top hence, the diaphragm wall behaves like a cantilever. At the position where the anchor is placed, the bending moment value increases in the positive direction. The maximum value of

positive bending moment and negative bending moment is obtained when the anchor is placed at +4.5 m.

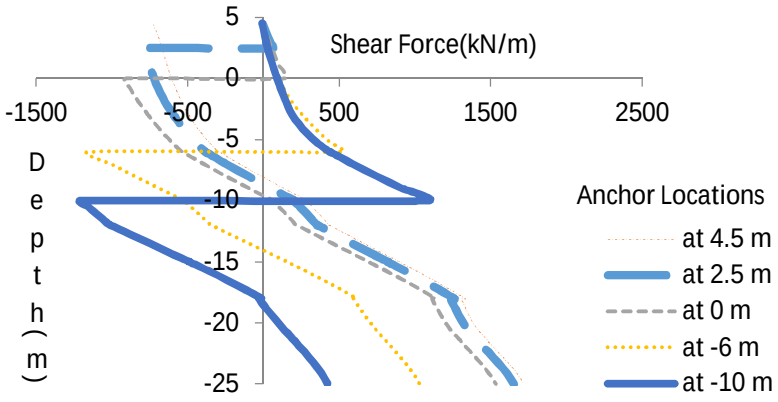

Fig. 4.8 Variation of shear force with depth for the diaphragm wall for different anchor locations (Static analysis)

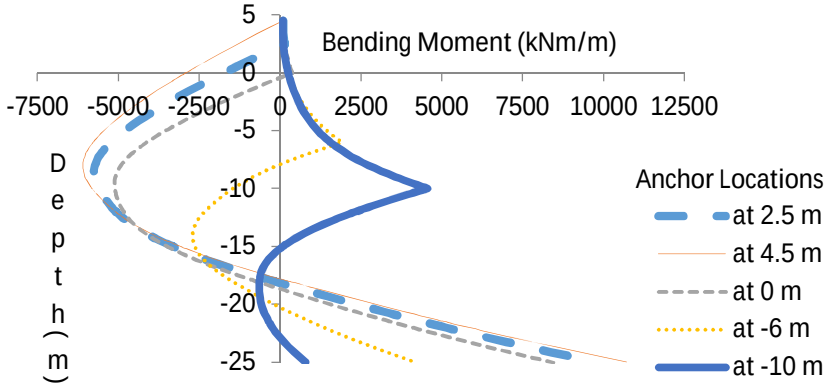

Fig. 4.9 Variation of bending moment with depth for the diaphragm wall for different anchor locations (Static analysis).

From the study it is observed that the maximum displacement is reduced by 17.86% (from 0.00599 m to 0.00492 m), 39.57% (from 0.00599 m to 0.00362 m), 81.13%(from 0.00599 m to 0.00113 m) & 25.87% (from 0.00599 m to 0.00444 m) for the anchor locations +2.5 m, 0.0 m,-6 m & -10 m respectively, with respect to anchor at +4.5 m. Similarly the maximum positive shear force is reduced by 4.09% (from 1720 kN/m to 1650 kN/m), 11.19% (from 1720 kN/m to 1530 kN/m), with respect to the anchor at +4.5 m. But the maximum negative shear force is increased 4.3% (from 1160 kN/m to 1210 kN/m) when the anchor shifted from -6 m to -10 m. The increase in shear force may due to the anchor located at dredge level (-10 m) and the reduction in passive resistance of soil below dredge level.

Similarly the bending moment is reduced by 8.49% (from 10710 kNm/m to 9800 kNm/m), 21.19% (from 10710 kNm/m to 8440 kNm/m), 60.78% (from 10710 kNm/m to 4200 kNm/m) & 57.42% (from 10710 kNm/m to 4560 kNm/m) for the anchor locations +2.5 m, 0.0 m, -6.0 m and -10.0 m respectively, with respect to the anchor at +4.5 m.

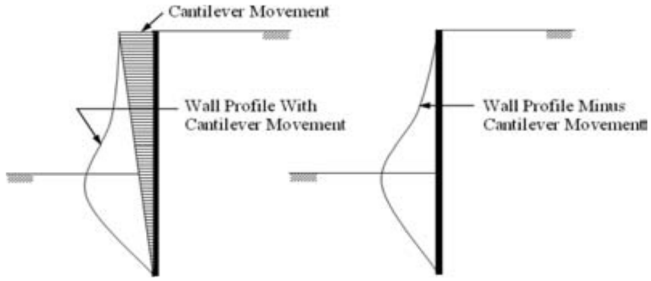

Fig. 4.10 Effect of cantilever stage movement on system displacement (Clough et al. 1989)

Table 4.1 Maximum values of displacement, shear force and bending moment for varying locations of anchor (Static analysis).

Anchor Location (m)	Max. Displacement & its location		Max. Shear force & its location		Max. Bending Moment & its location			
	Displacement (m)	Location (m)	S.F (kN/m)	Location (m)	B.M (+ve) (kNm/m)	Location (m)	B.M (-ve) (kNm/m)	Location (m)
+4.5	-0.00599	-9	1720	-25	6010	-8	10710	-25
+2.5	-0.00492	-10	1650	-25	6030	-9	9800	-25
0	-0.00362	-10	1530	-25	5125	-8	8440	-25
-6	-0.00113	+4.5	-1160	-6	2645	-15	4200	-25
-10	-0.00444	+4.5	-1210	-10	640	-18	4560	-10

Clough et al. (1989) suggested that the wall deforms in a cantilever mode before the installation of the first support and the total displacement may be the summation of cantilever displacement and bulging displacement. Fig. 4.10 shows typical diagrams of a cantilever stage movement on system displacement.

The present study shows some similar behavior in wall displacement as suggested by Clough. Fig. 4.7 shows considerable reduction in bulging displacement when the

anchor located at -6 m level with respect to +4.5 m, +2.5 m and 0 m level. When the anchor is at -10 m the bulging displacement considerably reduced.

From the study it is found that the bulging displacement can be controlled by shifting the anchor locations from top of the wall to dredge level.

The minimum displacement, shear force and bending moment is obtained at -10 m,-25 m and -25 m respectively, when the anchor is placed at -6 m. So the best suitable position for placing the anchor according to static analysis is at -6 m.

The maximum displacement, shear force and bending moment are reduced by 91.79% (from 0.073 m to 0.00599 m),11.69% (from 1947.82 kN/m to 1720 kN/m) & 57% (from 24936 kNm/m to 10710 kNm/m) respectively, when anchor is introduced in the diaphragm wall comparing with diaphragm wall without anchor

4.3.4 Analysis of Effect of Dredging on the Diaphragm wall

Dredging is the process of removal of column of soil from the sea side of a retaining structure. The dredging analysis is carried to study the effect of deep excavation and its effects on an earth retaining structure. During dredging, additional lateral forces are caused by the landside earth pressure. The removal of soil on sea side causes the diaphragm wall to deflect more. Therefore the analysis of diaphragm wall during dredging is conducted using Plaxis 2D software.

In order to study the effect of dredging on the berthing structure, the following two cases are studied and the results are compared.

a. Berthing structure not subjected to dredging

b. Berthing structure subjected to dredging as in the actual case.

The significance of the study in the case of without dredging is to investigate the post installation effects in wall caused due initial stress generation in soil before excavation. In the case of with dredging, the study analyses the performance of wall after the excavation of soil up to dredge level. The comparison of these two cases project the dredging effects on wall.

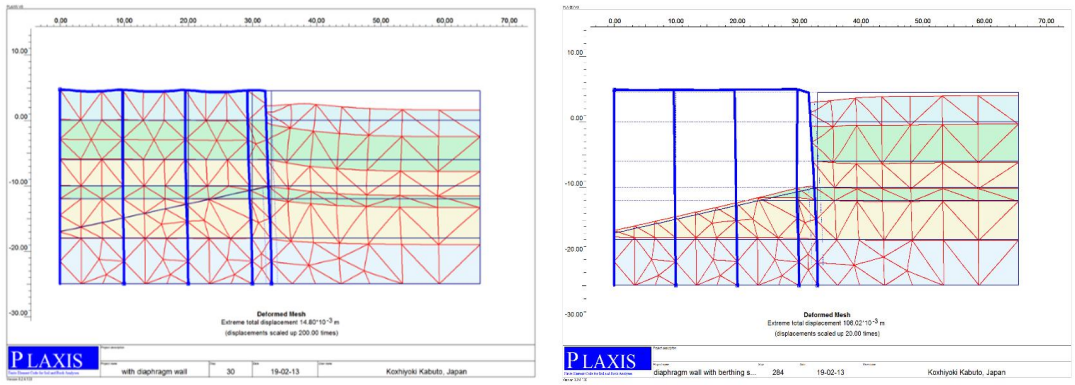

(a) (b)

Fig. 4.11(a) Plaxis model of berthing structure without dredging and (b) with dredging

Fig. 4.11 (a) shows the Plaxis 2D model for without dredging case. In this case, soil exist on both side of the diaphragm wall. Fig. 4.11 (b) shows the Plaxis 2D model for with dredging case. Dredging is carried on one side of the wall up to -10m (dredge level) and on the other side, full column of soil exist, in the case of with dredging.

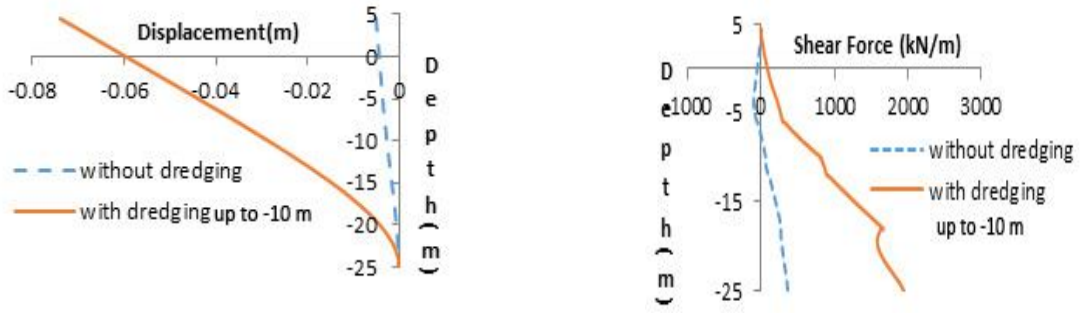

(a) Displacement (b) Shear force

Fig. 4.12 Variation of displacement & shear force with depth of diaphragm wall for analyzing effect of dredging in static analysis, without anchor.

The variation of displacement for without dredging condition, Fig. 4.12(a) shows linear variation till the depth of -8 m and gradually decreases thereafter. This may be due soil pressure variation along the depth of soil layer. The maximum displacement of the wall for without dredging case is 0.00493 m and for the dredging case is 0.0734 m at +4.5m level.

The variation of shear force is shown in Fig. 4.12 (b). Initially the passive pressure is more than the active pressure and hence the shear force decreases and then increases after a certain depth due to increase in the active pressure. For dredged condition, the

shear force increases steadily till a depth of -10 m, then passive pressure acts on wall at below dredge level. At –18 m, the shear force value shows a considerable decrease indicating that the passive pressure at this point is very high. The maximum shear force for without dredging case is 349.27 kN/m/m and for with dredging case is 1940 kN/m/m at -25 m level.

Fig. 4.13 shows the variation of bending moment with depth. For without dredge condition, the bending moment initially decreases due to decrease in the shear force. Due to increase in the active pressure, the bending moment also increases after a certain depth. The maximum bending moment of 2930 kNm/m is obtained for without dredging case and for with dredging case it is 24860 kNm/m at -25 m level.

The results obtained in the dredging analysis shows that the displacement, shear force and bending moment are increased by 93.2% (from 0.00493 m to 0.0734 m), 81.99% (from 349.27 kN/m to 1940kN/m) & 88.21% (from 2930kNm/m to 24860 kNm/m) respectively, when compared to without dredging case.

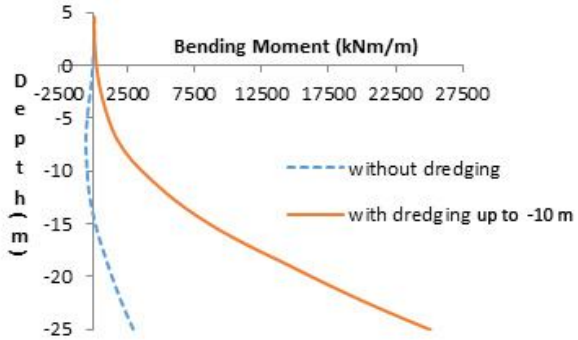

Fig. 4.13 Variation of bending moment with depth of diaphragm wall for analysing effect of dredging in static analysis, no anchor present.

The investigation highlites, there will be some initial displacements, shear forces and bending moments occuring after the wall erection eventhough soil exist on both sides. The soil is more compressible compared to rigid wall. The compressible soil may causes some stresses due to the retaining rigid wall,after the completion of the wall erection. Hence the initial stress generation in the soil after the wall installation may be the reason for the initial displacement, shear force and bending moment occured in the wall. Generaly these effcts are not considered in the conventional methods. Hence the

study reccomends that the effect of dredging analysis is so important in the case of diaphragm wall design.

4.4 DYNAMIC ANALYSIS

The input structural and soil parameters (Table 3.1, 3.2 and 3.3, chapter 3) are similar to that used during static analysis. The earthquake response spectrum (Fig. 3.14, chapter 3) used in this analysis is the acceleration-time details of the Imperial Valley earthquake, California (1987). The peak acceleration considered in this case is -307.053 cm/s^2 at 2.15 s.

The following conditions were considered for dynamic analysis:-

Case 1. Comparison of performance of diaphragm wall for 2 borehole locations

Case 2. Analysis of diaphragm wall in the absence of anchor

Case 3. Analysis of diaphragm wall for varying locations of anchor

Case 4. Analysis of effect of dredging on the diaphragm wall

4.4.1 Comparison of Performance of Diaphragm wall for Soil Strata Corresponding to two Borehole Locations

Fig. 4.14 shows the displacement of the diaphragm wall in the case of dynamic analysis for the soil profile of two borehole locations when no anchor is provided to the diaphragm wall. Here also the maximum displacement of the diaphragm wall occurs for soil profile of borehole 6 as in the static analysis. The displacement pattern in the case of dynamic analysis is similar to that of static analysis. The diaphragm wall is supported only at the bottom and so it acts like a cantilever with bottom fixed at depth of -25 m. For the case of soil profile of borehole 6, the maximum displacement of the diaphragm wall obtained at the top is - 0.0749 m and that for soil profile of borehole 7 is - 0.0578 m.

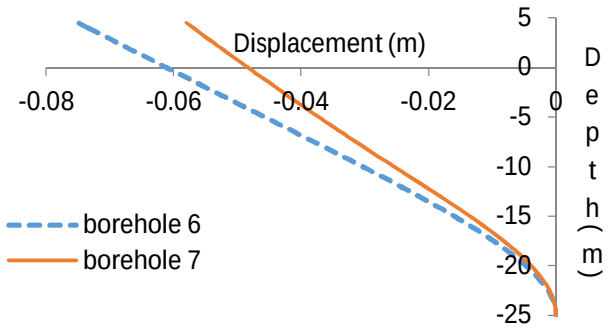

Fig. 4.14 Comparison of displacement of diaphragm wall for soil profiles in two boreholes in dynamic analysis, without anchor.

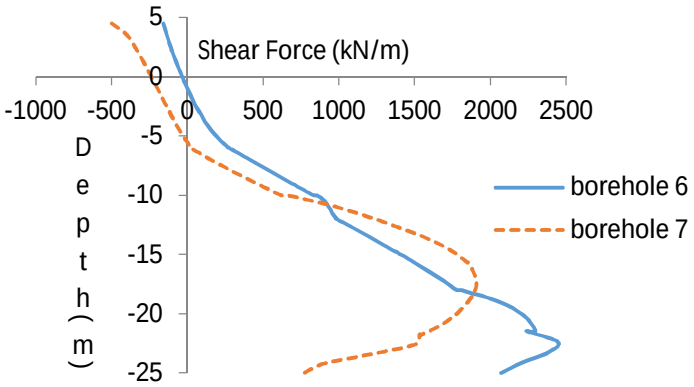

Fig. 4.15 Comparison of shear force with depth of diaphragm wall for soil profiles in two boreholes in dynamic analysis, without anchor.

The variation of shear force is as shown in Fig. 4.15. It is clear from the figure that the maximum value of shear force occurs for soil profile of borehole 6. The shear force variation is similar for both the borehole profiles till a depth of -10 m. After this depth, the deviation starts. In the case of borehole 7, the shear force value increases gradually till a depth of -17 m. In the case of borehole 6, the value of shear force increases till a depth of -22 m, where the maximum value of shear force is obtained. This may be because of the difference in soil layers. The maximum value of shear forces obtained are 1903 kN/m (at -17 m) and 2445 kN/m (at -22 m) for the soil profile of boreholes 7 & 6 respectively.

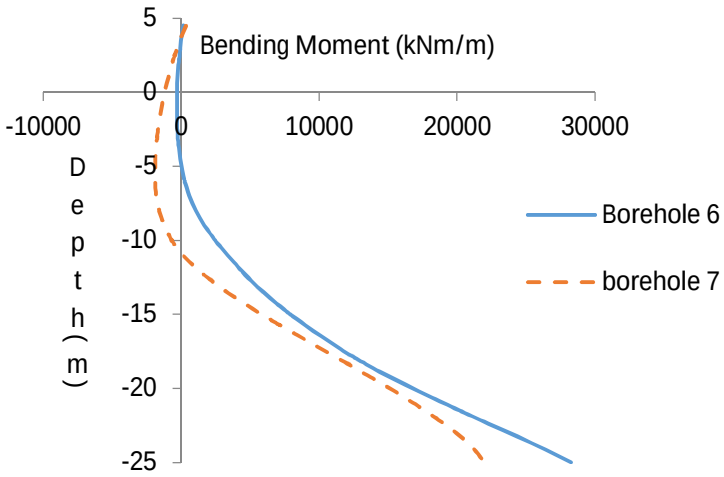

Fig. 4.16 Comparison of bending moment with depth of diaphragm wall for soil profiles in two boreholes in dynamic analysis, without anchor.

Since the bending moment induced in a structure is directly dependent on the shear force acting on the structure, it is obvious that the bending moment will be maximum for the borehole profile 6. It is depicted in Fig. 4.16. Since the shear force variation is not much, the bending moment variation is a smooth curve in the figure.

For the case, when the soil profile present in borehole 6, the maximum displacement, shear force and bending moment of the diaphragm wall obtained are - 0.0749 m @ +4.5 m, 2071 kN @ -25 m, & 28260 kNm/m @ -25 m, and in the case of soil present in borehole 7 are - 0.0578 m @ +4.5 m, 1903 kNm/m @-17 m, 24450 kNm/m @ -22 m. The displacement, shear force and bending moment for borehole no 6 are higher than that of borehole 7, hence it is considered for further study.

4.4.2. Analysis of Diaphragm wall in the Absence of Anchor rod

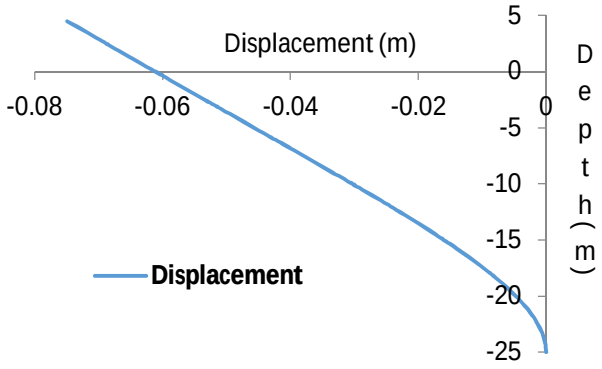

Fig. 4.17 Variation of displacement with depth of diaphragm wall during dynamic loading, without anchor.

The study shows that the displacement of diaphragm wall in the absence of anchor rod during seismic loading, is similar to that of static loading but, the values are different. The pattern of displacement is similar, zero displacement at the bottom of the diaphragm wall and maximum displacement at the top of the wall as it behaves like a cantilever beam. The variation pattern is shown in Fig. 4.17. The maximum displacement of the diaphragm wall obtained in this case is -0.0749 m @ +4.5 m level.

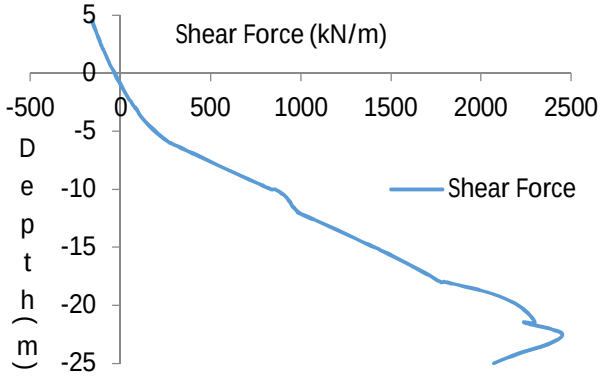

Fig. 4.18 Variation of shear force with depth of diaphragm wall during dynamic loading, without anchor.

Fig. 4.18 shows the variation of shear force along the depth of the diaphragm wall for the case without anchor. Unlike in the case of static loading, here the shear force at the top of the structure at an elevation of +4.5 m is not zero. This is due to the action of dynamic incremental active pressure. Since the direction of earthquake analysed in this case is opposite to the direction of the active earth pressure, the initial shear force is negative. Due to the presence of active and passive earth pressure the shear force value at the bottom of the structure is reduced. The maximum shear force obtained in this

case is 2445.57 kN/m at -22 m, where the layer changes from medium to course sand. There will be difference in wave velocities due to difference in soil stiffness. So shear force values have sudden increase and decrease in the case of soil layer changes from marine clay to coarse sand.

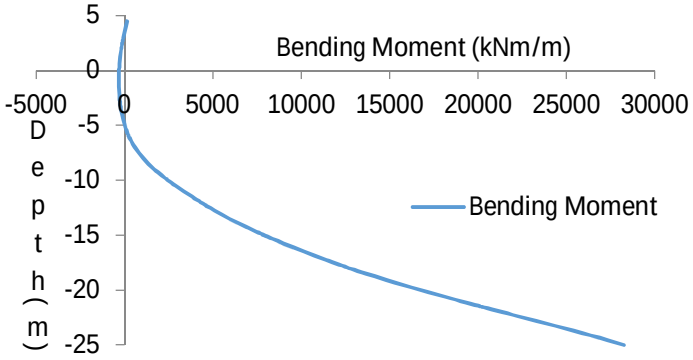

Fig. 4.19 Variation of bending moment with depth of diaphragm wall during dynamic analysis, without anchor.

The bending moment variation is shown in Fig.4.19. The bending moment at a particular position depends upon the value of shear force distribution up to that point. The value of maximum bending moment is 28263.68 kNm/m which is obtained at the bottom of the diaphragm wall.

4.4.3. Analysis of diaphragm wall for varying locations of anchor.

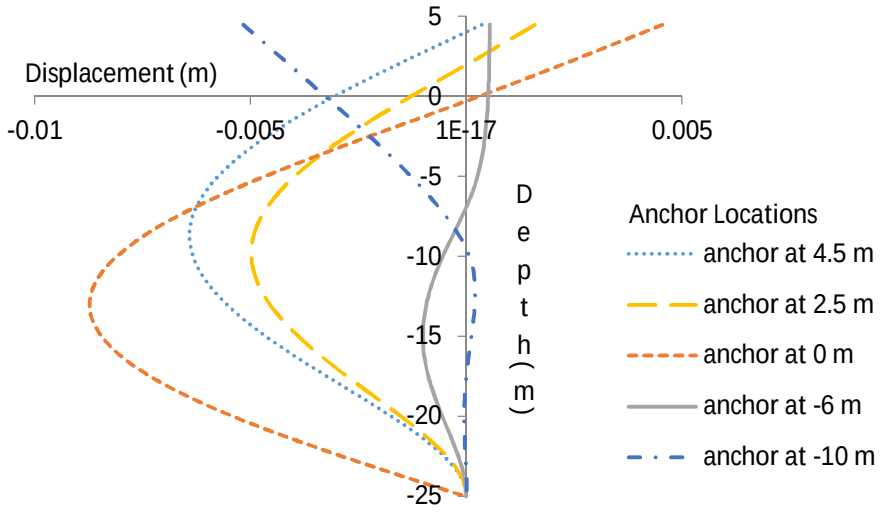

Fig. 4.20 Variation of displacement with depth of the diaphragm wall for different anchor locations (Dynamic analysis).

The variation of displacement of the diaphragm wall in the case of earthquake loading for various locations of anchor is shown in Fig 4.20. The displacement pattern of the diaphragm wall for the dynamic analysis is similar to the static analysis. The displacement at the position of the anchor is zero. The minimum displacement, shear force and bending moments are obtained when the anchor is placed at -6 m, the displacement being 0.001 m at -14 m depth.

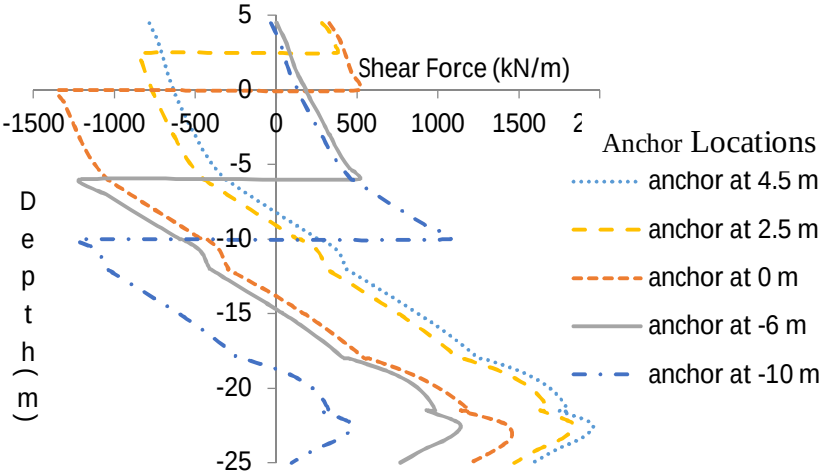

Fig. 4.21 Variation of shear force with depth of the diaphragm wall for different anchor locations (Dynamic analysis)

The variation of shear force in dynamic analysis is similar to the static analysis. It is shown in Fig 4.21. The shear force at the location where the anchor is placed decreases abruptly. Due to the presence of the horizontal earthquake force, the shear force is not zero at the top of the diaphragm wall. After a depth of -18 m, the shear force variation is different. The passive pressure starts to act from a depth of -10 m (dredge level). From a depth of -18 m, the soil layer is of coarse sand. The shear force due to dynamic loads acting in this layer is more and so initially there is an increase in the shear force value. But after a depth of around -23 m, the passive force becomes more and hence the net shear force starts to decrease. For all the cases, at the point where the anchor is placed, the shear force is changing its sign. The maximum value of shear force is obtained when the anchor is placed at +4.5 m, the value being 1950 kN/m at -22 m depth.

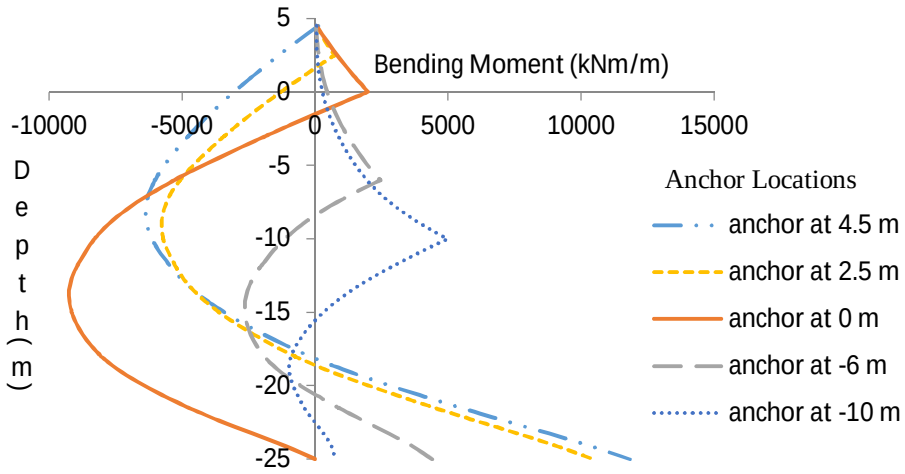

Fig. 4.22 Variation of bending moment with depth for the diaphragm wall for different anchor locations (Dynamic analysis).

The variation of bending moment up to a depth of -10 m is similar to that of static loading. The bending moment is zero at the top of the diaphragm wall. The maximum bending moment occurs when the anchor is placed at +4.5 m and the minimum value of bending moment is obtained when the location of anchor is at -6 m. The variation of bending moment is shown in Fig. 4.22.

From the study it is observed that that the maximum displacement is reduced by 22.24% (from 0.00642 m to 0.00499 m), 84.42% (from 0.00642 m to 0.0010 m) & 19.47% (from 0.00642 m to 0.00517 m) for the anchor locations +2.5 m, -6 m & -10 m respectively, with respect to anchor at +4.5 m. Similarly the maximum positive shear force is reduced by 5.6% (from 1950 kN/m to 1840 kN/m) and 25.6% (from 1950 kN/m to 1450 kN/m) for the anchor locations +2.5 m and 0.0 m with respect to the anchor at +4.5 m. But the maximum negative shear force is increased by 2.5% (from 1200 kN/m to 1230 kN/m) for the anchor location -10 m with respect to anchor at -6 m. The increase in shear force may be due to the anchor located at dredge level (-10 m). Similarly the bending moment is reduced by 11.49% (from 11830 kNm/m to 10470 kNm/m), 21.8% (from 11830 kNm/m to 9250 kNm/m), 62.89% (from 11830 kNm/m to 4390 kNm/m) & 57.9% (from 11830 kNm/m to 4980 kNm/m) for the anchor locations +2.5 m, 0.0 m,-6.0 m and -10 m respectively with respect to the anchor at +4.5 m.

The dynamic analysis of diaphragm wall with anchor shows considerable reduction in the maximum displacement, shear force and bending moment. It is observed that for

anchored diaphragm wall maximum displacement decreases by 91.42% (from 0.0749 m to 0.00642 m), maximum shear force by 20.26% (from 2445.57 kN/m to 1950 kN/m) and bending moment decrease by 58.1% (from 28263.68 kNm/m to 11830 kNm/m) when compared to wall without anchor.

Table 4.2. Maximum values of displacement, shear force and bending moment for varying locations of anchor for dynamic analysis.

Anchor Location (m)	Max. Displacement		Max. Shear force & its location		Max. Bending Moment & its location			
	Displacement (m)	Location (m)	S.F (kN/m)	Location (m)	B.M (+ve) (kNm/m)	Location (m)	B.M (-ve) (kNm/m)	Location (m)
+4.5	-0.00642	-9	1950	-22	11830	--25	6393	-8
+2.5	-0.00499	-10	1840	-22	10470	-25	5782	-9
0	-0.0087	-13.5	1450	-23	1991	0	9250	-14.5
-6	-0.00010	-14.0	-1200	-6	2645	-15	4390	-25
-10	-0.00517	+4.5	-1230	-10	1000.2	-18	4980	-10

4.4.4: Analysis of effect of dredging on the diaphragm wall.

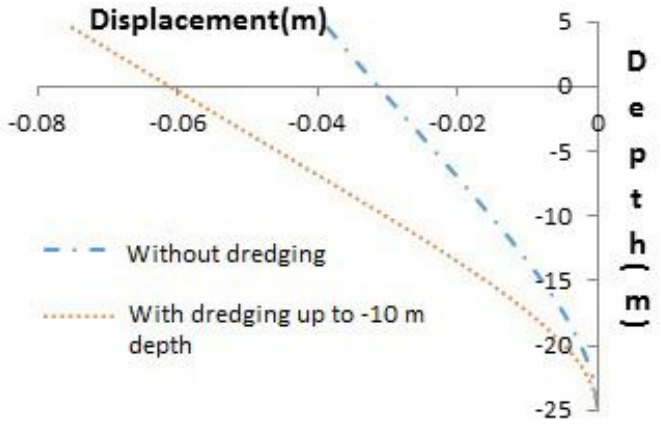

Fig. 4.23 Variation of displacement of diaphragm wall for analysing effect of dredging in dynamic analysis, no anchor present.

The dredging effects in dynamic analysis shows similar trend as in the static case. The displacement of diaphragm wall under earthquake loading for comparison of effect of dredging is as shown in Fig. 4.23. The maximum value of displacements of 0.0379 m and 0.0749 m is obtained at +4.5 m (top level of diaphragm wall) for the cases without and with dredging. The displacement of the diaphragm wall is increased by 49.4% in the case of dredging.

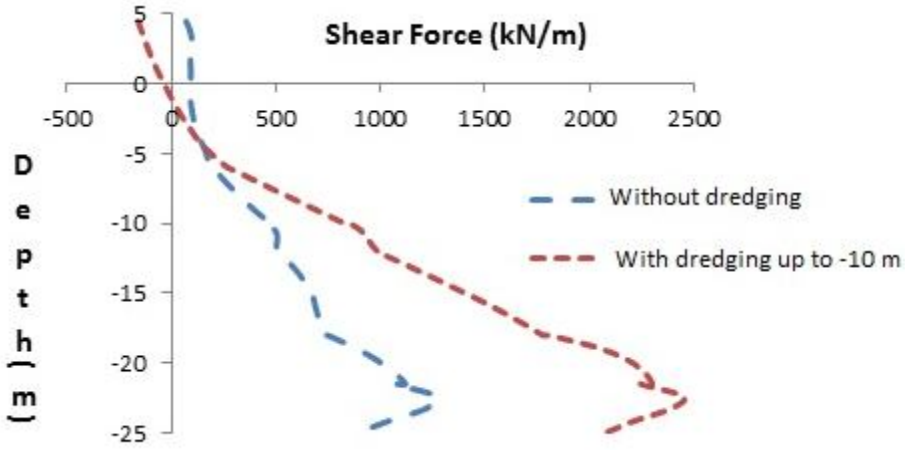

Fig. 4.24 Variation of shear force of diaphragm wall for analysing effect of dredging in dynamic analysis, without anchor.

The variation of shear force in the diaphragm wall during earthquake is shown in Fig. 4.24. During the action of earthquake, dynamic force will be acting on the structure due to which the shear force will not be zero at the top of the diaphragm wall. The maximum value of shear force of 1271.93 kN/m and 2545.47 kN/m is obtained at -22 m depth for the cases without and with dredging. The maximum shear force on the diaphragm wall is increased by 47.9% in the case of dredging, when compared to without dredging case. The bending moment variation along the depth of the diaphragm wall for studying the effect of dredging is as shown in Fig. 4.25. The value of bending moment is maximum at the bottom of the diaphragm wall for both the cases. The maximum value of bending moment of 13951 kNm/m and 28263.68 kNm/m is obtained at -25 m depth for the cases without and with dredging. The bending moment on the diaphragm wall is increased by 50.63% in the case of dredging with respect to without dredging.

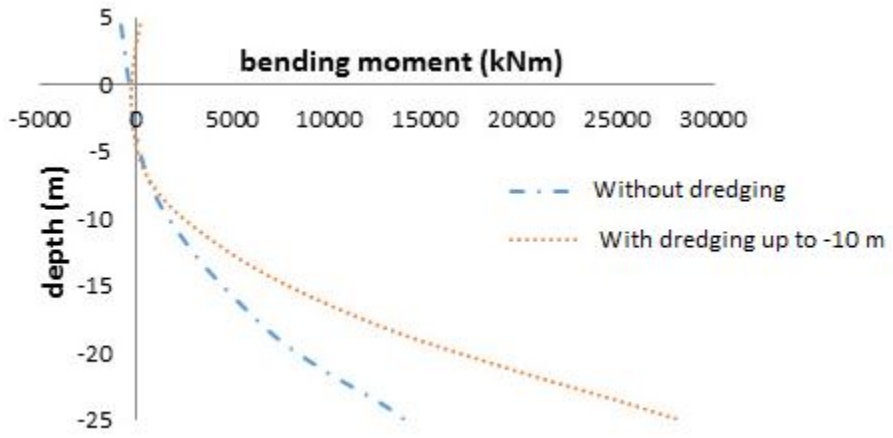

Fig. 4.25 Variation of bending moment of diaphragm wall for analysing effect of dredging in dynamic analysis, no anchor present.

Seismic shaking produces significant changes in the distribution of horizontal stresses and significant increment in the bending moment (Luigi and Fabio, 2007). The horizontal ground acceleration would simultaneously decrease the passive resistance of the wall (Neelakantan et al, 1992). In without dredging case the soil column exist on both side of diaphragm wall and dredging up to -10 m is carried out with dredging case. The study shows considerable increase in displacement, shear force and bending moment in the case of dredging. The reason may be due to the increase in horizontal stresses at active zone and reduction in passive resistance of the soil column in the passive zone.

4.5 COMPARISON OF STATIC AND DYNAMIC ANALYSIS.

Comparison is made to realise the effects on diaphragm wall subjected to static as well as dynamic loads. The analysis is carried out separately for static and dynamic loading conditions to obtain the maximum displacement, shear force and bending moment on diaphragm wall.

4.5.1 Comparison of Static and Dynamic Analysis of the Diaphragm wall, without Anchor

The displacement of diaphragm wall during static and dynamic analysis for the case of without anchor is as shown in Fig. 4.26. It is clear that the deviation in displacement

between the two analyses is less. The displacement caused in the dynamic analysis comparing with static analysis is not showing large variations in the present study for without anchor case.

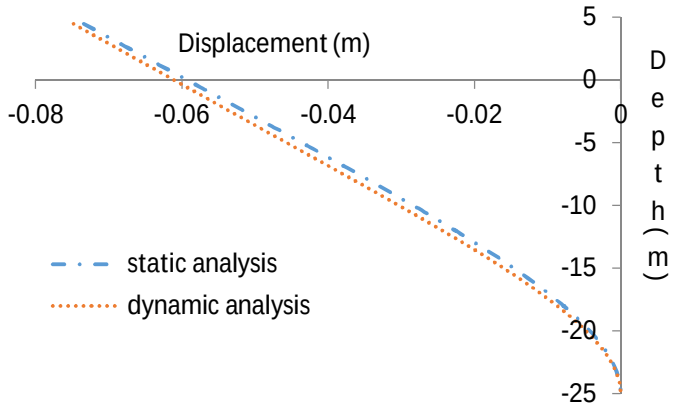

Fig. 4.26 Comparison of displacement of diaphragm wall for static and dynamic analysis.

The maximum displacement due to static loading is -0.073 m whereas in the case of dynamic loading it is -0.0749m. In absence of anchor there is no fixity for the wall above dredge level. Hence the displacement variation in static and dynamic analysis are found lesser. The displacement is increased by 2.54% in dynamic analysis when compared with static analysis.

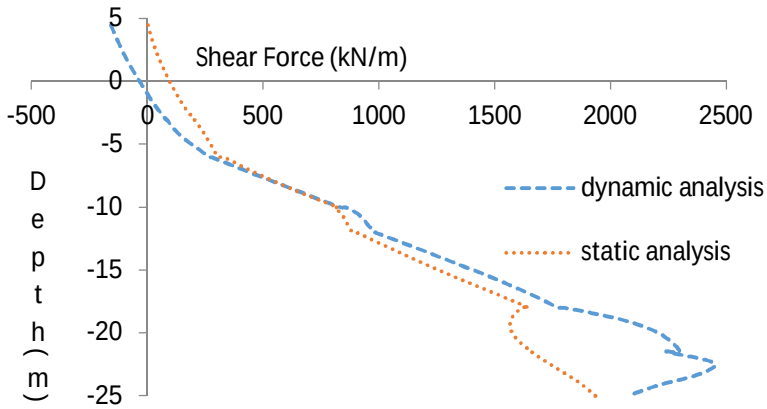

Fig. 4.27 Comparison of shear force with depth of diaphragm wall for static and dynamic analysis.

The variation of shear force in the case of static and dynamic analysis is similar till a depth of -18 m. The passive dynamic earth pressure is higher than the total dynamic active earth pressure. So from -18 m onwards, the net earth pressure tends to decrease. The variation in shear force is as shown in Fig. 4.27. The main difference in shear force

between static and dynamic cases can be seen at the top of the diaphragm wall, because of the effect of dynamic incremental active pressure and also after a depth of –18 m because of the effect of the variation in dynamic passive resistance of soil. The maximum shear force in the case of static analysis is 1947.82 kN/m at a depth of -25 m whereas in the case of dynamic analysis it is 2445.47 kN/m at a depth of -22 m. The minimum shear force in both the cases is at the top of the diaphragm wall. For the static analysis it is zero and for the dynamic analysis it is -157.77 kN/m. The main difference in the pattern of shear force for static and dynamic analysis is due to the dynamic passive resistance variation in the medium sand and coarse sand layers (Ingale, et al, 2015).

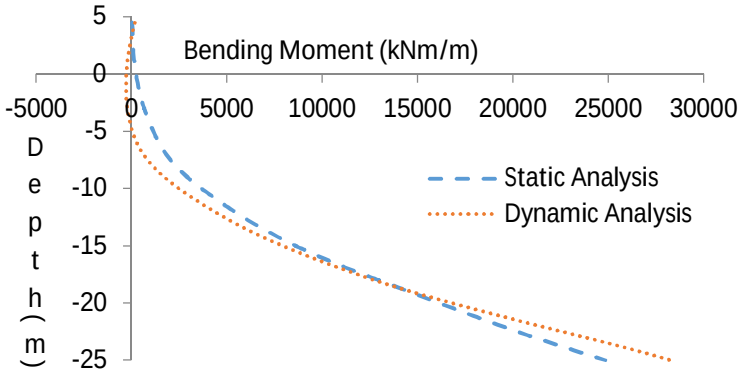

Fig. 4.28 Comparison of bending moment with depth of diaphragm wall for static and dynamic analysis.

Since the variation of shear force is almost similar in both the cases, the bending moment variation is similar. The maximum bending moment in the case of static analysis is 24936.03 kNm/m located at -25 m whereas in the case of dynamic analysis it is 28263.68 kNm/m at a depth of -25 m. This is because the earthquake considered in this analysis is of low magnitude. The variation of bending moment is as shown in Fig. 4.28.

The results obtained for the dynamic analysis in the absence of anchor (Table 4.3) show increase in maximum displacement, shear force and bending moment by 2.5% (from 0.0734 m to 0.0749 m), 20.34% (from 1947.92 kN/m to 2445.47 kN/m) & 11.77% (from 24936.03 kNm/m to 28263.68 kNm/m) with respect to static analysis.

Table 4.3 Comparison of maximum values of displacement, shear force and bending moment in static and dynamic analysis without anchor.

	Static analysis	Dynamic analysis
Max. displacement (m)	-0.0734 occurs at +4.5 m	-0.0749 occurs at +4.5 m
Max. shear force (kN/m)	1947.82 occurs at -25 m	2445.47 occurs at -22 m
Max. bending moment (kNm/m)	24936.03 occurs at -25 m	28263.68 occurs at -25 m

4.5.2 Comparison of static and dynamic analysis of the diaphragm wall, with anchor

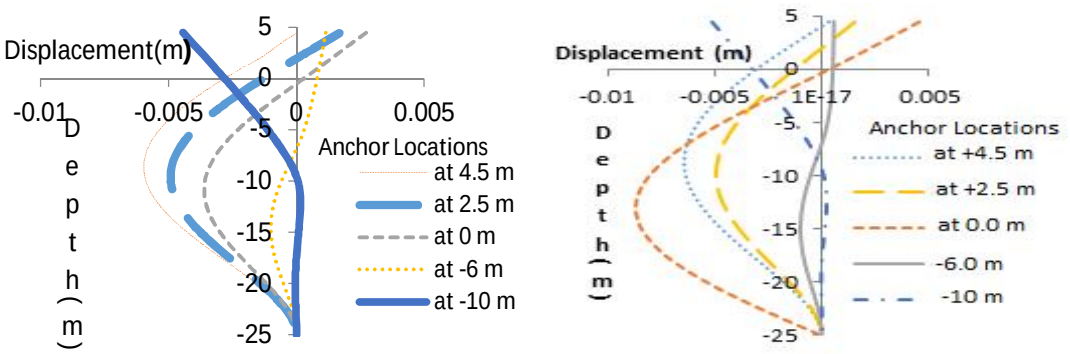

(a) Static analysis (b) Dynamic analysis

Fig. 4.29 Variation of displacement with depth of the diaphragm wall for different anchor locations.

Fig. 4.29, 4.30 and 4.31 show variation of displacement, bending moment and shear force for the cases static and dynamic analysis with depth. The trend of the variation in displacement, shear force, and bending moment for static and dynamic analysis are similar but in magnitude, the dynamic analysis shows higher percentage variation than static. The results obtained in the dynamic analysis (Table 4.4) show that, the maximum values of displacement, shear force and bending moment are increased by 7.2% (from 0.00599 m to 0.0064 m), 10% (from 1720 kN to 1950 kN) & 13.5% (from 10710 kNm/m to 11830 kNm/m) with respect to static analysis.

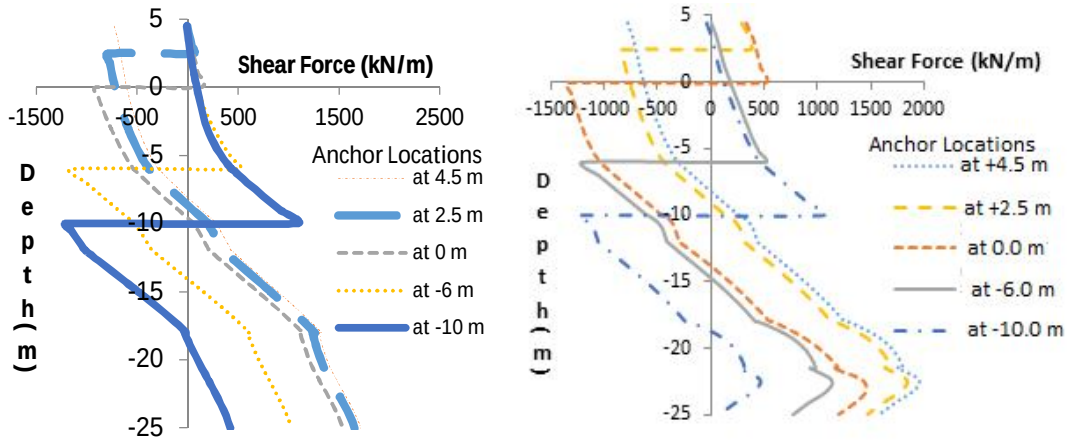

(a) Static analysis (b) Dynamic analysis

Fig. 4.30 Variation of shear force with depth for the diaphragm wall for different anchor.

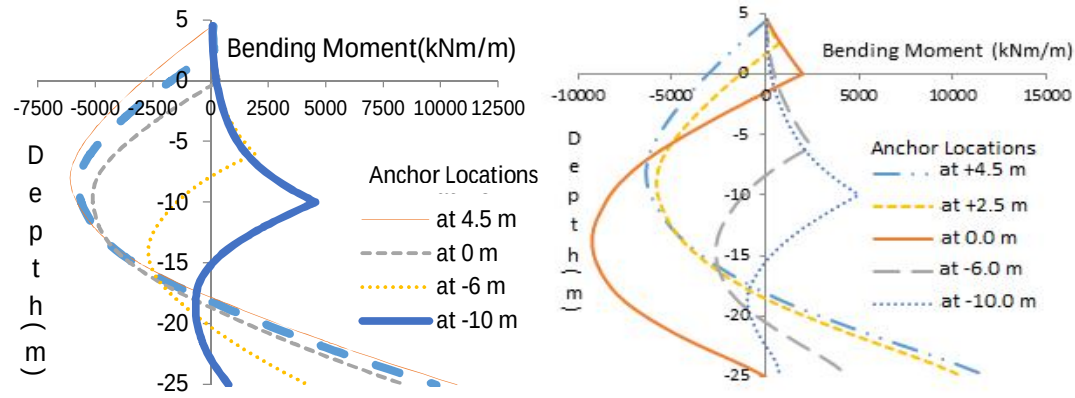

(a) Static analysis (b) Dynamic analysis

Fig. 4.31 Variation of bending moment with depth of the diaphragm wall for different anchor

In the earth quake cases, the wall may experience significant bending stresses due to inertia effects of the wall, in addition to the stresses caused by the changes in total lateral earth pressures for an anchored wall (Thomas J. Siller and Matthew O. Dolly, 1992).The combined effect of inertial force of the wall and increased seismic earth pressure of the backfills may be the cause for the increase in displacement, shear forces and bending moment in dynamic analysis when compared to static analysis. Hence the dynamic analysis is essential for anchored wall.

Table4. 4 Comparison of maximum values of displacement, shear force and bending moment in static and dynamic analysis with anchor

Static analysis			Dynamic analysis		
	Anchor position (m)	Location of Max. value (m)		Anchor position (m)	Location of Max. value (m)
Max. displacement 0.00599 m	+4.5	-9	Max. displacement 0.0064 m	0	-13.5
Max. shear force 1720kN/m	+4.5	-25	Max. shear force 1950kN/m	+4.5	-22.375
Max. bending moment 10710kNm/m	+4.5	-25	Max. bending moment 11830kNm/m	+4.5	-25

4.6 SUMMARY

2D static and dynamic analysis are focussed on obtaining the maximum displacement, shear force and bending moment of a diaphragm wall with and without anchor. The analysis without anchor shows cantilever type behavior of the diaphragm wall where the maximum displacement is observed at top of the wall and the maximum shear force and bending moment is at the bottom fixed end. Similar behaviour of wall is observed in dynamic analysis, but the displacement, shear force and bending moment values are increased. The analysis of diaphragm wall with anchor shows variations in displacement, shear force and bending moment with varying anchor locations. The comparison of 2D static and dynamic analysis of diaphragm wall with anchor shows considerable reduction in displacement, shear fore and bending moment comparing with the diaphragm wall without anchor. Attempt has been made to obtain the dredging effect on diaphragm wall in static and dynamic load conditions.

Based on the present 2D analysis of diaphragm wall, the following conclusions are drawn:

- From the study it is observed that the maximum displacement is reduced by 17.86% (from 0.00599 m to 0.00492 m), 39.57% (from 0.00599 m to 0.00362 m), 81.13%(from 0.00599 m to 0.00113 m) & 25.87% (from 0.00599 m to

0.00444 m) for the anchor locations +2.5 m, 0.0 m,-6 m & 10 m respectively, with respect to anchor at +4.5 m in static analysis.

- The static analysis shows reduction in maximum positive shear forces by 4.09% (from 1720 kN/m to 1650 kN/m), 11.19% (from 1720 kN/m to 1530 kN/m) for the anchor location +2.5 m and 0.0 m respectively, with respect to the maximum shear force corresponding to anchor at +4.5 m. But the maximum negative shear force is increased by 4.3% (from 1160 kN/m to 1210 kN/m) when the anchor is shifted from -6 m to -10 m. The increase in shear force may be due to the anchor located at dredge level (-10 m) and reduction in passive resistance below dredge level.
- The bending moment is reduced by 8.49% (from 10710 kNm/m to 9800 kNm/m), 21.19% (from 10710 kNm/m to 8440 kNm/m), 60.78% (from 10710 kNm/m to 4200 kNm/m) & 57.42% (from 10710 kNm/m to 4560 kNm/m) for the anchor locations +2.5 m, 0.0 m, -6.0 m and -10.0 m respectively, with respect to the anchor at +4.5 m.
- The maximum displacement ,shear force and bending moment are reduced by 91.79% (from 0.073 m to 0.00599 m),11.69% (from 1947.82 Kn/m to 1720 kN/m) & 57% (from 24936 kNm to 10710 kNm) respectively, when anchor is introduced in the diaphragm wall comparing with diaphragm wall without anchor in static analysis.
- The dynamic analysis for without anchor case shows higher values for the maximum displacement, shear force and bending moment by 2.5% (from 0.0734m to 0.0749m), 20.85% (from 1935.14kN to 2445.47kN) & 12.05% (from 24856.9 kNm/m to 28263.68 kNm/m) with respect to static analysis.
- The dynamic analysis for the case with anchor show that, the maximum displacement, shear force and bending moment are increased by 7.2% (from 0.00599 m to 0.0064 m), 10% (from 1720kN/m to 1950kN/m) & 13.5% (from 10710kNm/m to 11830 kNm/m) with respect to static analysis.
- The results obtained for the dynamic analysis in the case without anchor, show increase in maximum displacement, shear force and bending moment by 2.5% (from 0.0734 m to 0.0749 m), 20.85% (from 1935.14kN/m to 2445.47kN/m) &

12.05% (from 24856.9 kNm/m to 28263.68 kNm/m) with respect to static analysis.

- The static and dynamic analysis show that the minimum displacement, shear force and bending moment are obtained at -10 m,-25 m and -25 m respectively, when the anchor is placed at -6 m. So the best suitable position for placing the anchor according to static analysis is at -6 m. But practical difficulty of anchor installation is the challenge.
- The dredging have considerable effect in performance of the diaphragm wall. From the analysis it is found that there will be considerable increase in displacement, shear force and bending moment as 93.2% (0.00493 m to 0.07344m),81.99% (349.27 kN/m to 1940 kN/m) & 88.21% (2930 kNm/m to 24860 kNm/m) respectively.
- The dynamic analysis of with dredging case shows considerable increase in displacement, shear force and bending moment by 49.4%, 47.9% and 50.63% respectively, when compared to the case of without dredging case.

CHAPTER 5

3D ANALYSIS OF DIAPHRAGM WALL FOR STATIC LOADING

5.1 GENERAL

In the present investigation the berthing structure is analyzed by using finite element software Plaxis 3D. The berthing structure is analyzed for the static loading considering the dead loads and live loads acting on the structure. In this study, the entire berthing structure is analyzed, but the forces and moments which are induced only in the diaphragm wall are considered and the variation of the same with the depth of wall are plotted.

Plaxis supports various models to simulate the behavior of soil. In this analysis equivalent sheet pile walls are modeled as 5-noded beam column elements and soil strata is represented by 15-noded triangular elements of elasto-plastic Mohr-Coulomb model. Procedure followed in static analysis

•Input pre-processing

•Preparation of model

•Calculations

•Output data processing

The cross section of the model is prepared in the Plaxis 3D Input window. The model includes soil strata and structural elements. The diaphragm wall is modeled as a single panel. The length of the panel is taken as 5m. The diaphragm wall is provided with anchors at a spacing of 2.5m. Diaphragm wall panel modeled in Plaxis 3D is shown in Fig. 5.1 & 5.2.

5.1.1 Inputting of Material and Soil Properties

After the model is drawn in the Input window, next step is assigning of material and soil properties to the different structural elements and soil strata. Boreholes are used to define the soil stratigraphy and ground surface level. In this project, Mohr- Coulomb model is used to simulate the behaviour of soil and other continuum. The input parameters of structural elements are shown in Table 3.1. The various soil parameters are shown in Table 3.2.

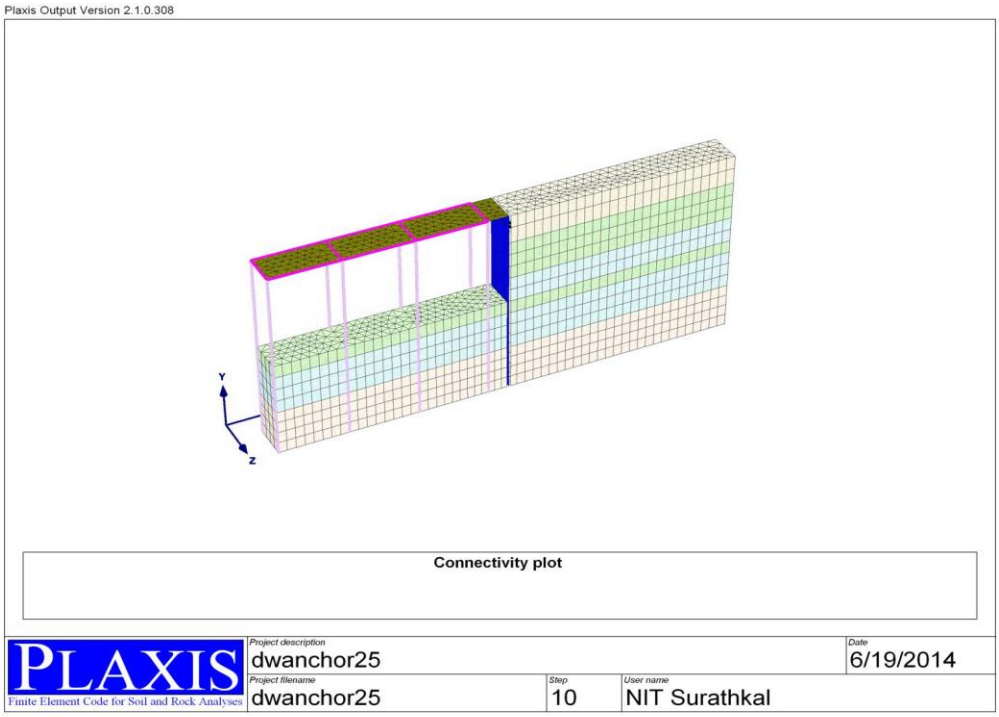

Fig. 5.1 Model of berthing structure in PLAXIS 3D

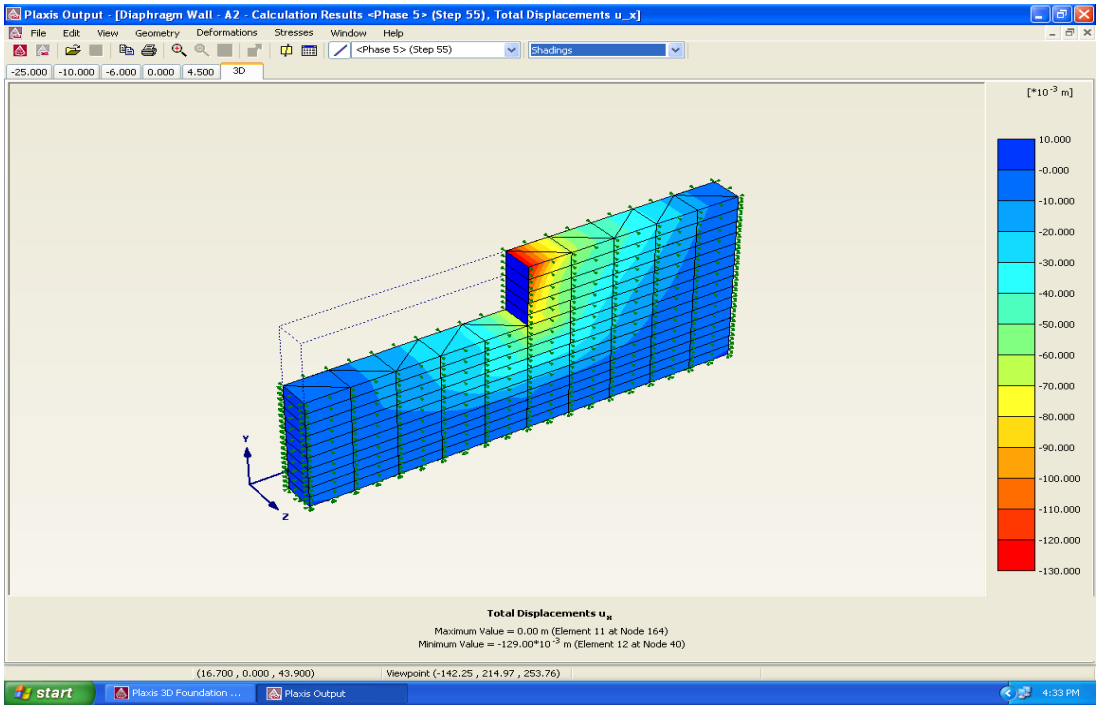

Fig. 5.2 Model of diaphragm wall in Plaxis 3D

Plaxis 2D analysis (Chapter 4) shows that the maximum, displacement shear force and bending moment are observed for the soil profile of borehole no 6. Hence, the soil profile of bore hole 6 is considered for the study in Plaxis 3D.

5.1.2 Application of Loads and Boundary Conditions

The boundary conditions are imposed using standard fixities option. Plaxis 3D automatically imposes a general set of standard fixities to the boundaries of the geometry model. These conditions are generated according to the following boundary conditions.

- ✓ Vertical model boundaries with their normal in x direction (i.e. parallel to the y-z plane) are fixed in x direction ($u_x = 0$) and free in y and z direction.
- ✓ Vertical model boundaries with their normal in y direction (i.e. parallel to the x-z plane) are fixed in y direction ($u_y = 0$) and free in x and z direction.
- ✓ The model bottom boundary is fixed in all directions ($u_x = u_y = u_z = 0$).
- ✓ The ground surface of the model is free in all directions.
- ✓ At vertical model boundaries with a normal in x-direction; $\emptyset_y = \emptyset_z = 0$ ($\emptyset_x$= free)
- ✓ At vertical model boundaries with a normal in z-direction; $\emptyset_x = \emptyset_y = 0$ ($\emptyset_z = free$).
- ✓ At vertical model edges and at the bottom boundary; $\emptyset_x = \emptyset_y = \emptyset_z = 0$

5.1.3 Mesh generation

After the loads have been defined, the next step is the generation of mesh. The basic element type used here is the 15-noded triangular element. In Plaxis 3D, first 2D meshes are generated and when the 2D mesh is satisfactory, a full 3D mesh can be generated using 3D mesh generation option. If the soil layer thickness varies, the element distribution in vertical direction may also vary. As a result of different numbers of element layers in vertical direction, 15-noded wedge elements may be degenerated to 13-noded pyramid elements (single degeneration) or to 10-noded tetrahedral elements (double degeneration) at the point where the number of elements in vertical direction changes. A typical 2D mesh is shown in Fig. 5.3.

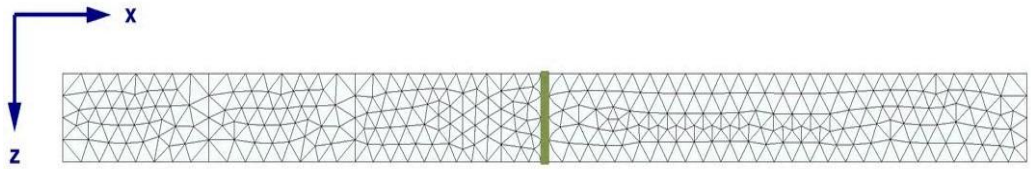

Fig. 5.3 Finite element mesh for diaphragm wall with back fill in 2D

5.2 STATIC ANALYSIS

The static analysis is carried out for the following cases:-

Case 1. Analysis of diaphragm wall in the without anchor

Case 2. Analysis of diaphragm wall for varying locations of anchor

Case 3. Analysis of diaphragm wall with anchor for staged construction

5.2.1 Analysis of diaphragm wall in the absence of anchor rod

The variation of displacement of the diaphragm wall with depth is shown in Fig. 5.4. The performance of the diaphragm wall is analyzed for the case without anchor to compare the results of with anchor. The maximum displacement in without anchor case is found to be 0.0693 m at +4.5 m level. The displacement of the diaphragm wall is found zero at the bottom. The diaphragm wall in the absence of anchor behaves like a cantilever with the bottom end fixed. Hence the displacements show maximum at top and zero at bottom

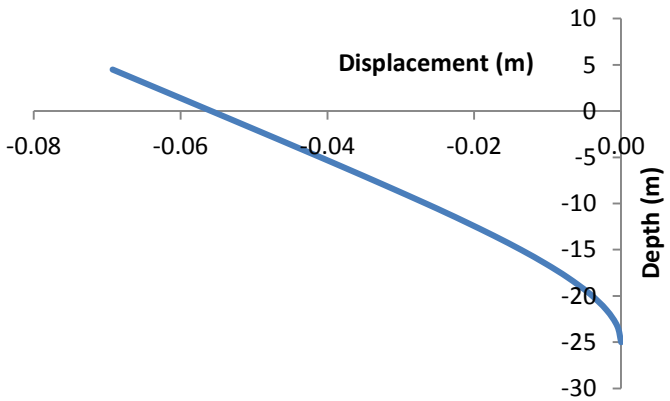

Fig. 5.4 Variation of displacement of diaphragm wall with depth in static analysis for the case without anchor

The variation of shear force is as shown in Fig. 5.5. Since no external force acts at top level, the value of shear force is zero at the top of the diaphragm wall. Till the depth of -10 m the

active earth pressure acts on the diaphragm wall. The passive force starts to act from -10 m. The maximum shear force is obtained at the bottom of the diaphragm wall. The reduction in the shear force at a depth of -18 m is due to change in the soil layer from marine clay to coarse sand. The passive earth pressure in marine clay is very low when compared to coarse sand due to the change in φ value. The maximum value of shear force obtained is at the bottom of the diaphragm wall and is equal to +1743 kN/m.

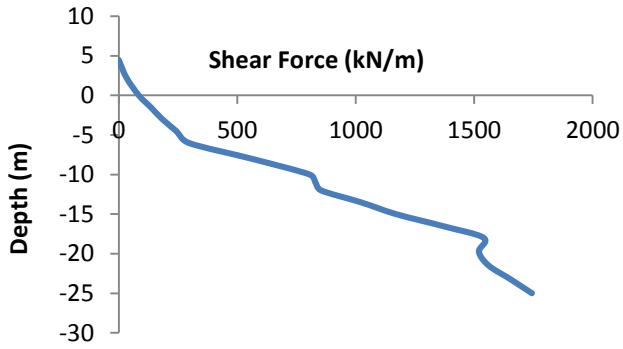

Fig. 5.5 Variation of shear forces in diaphragm wall with depth in static analysis, without anchor

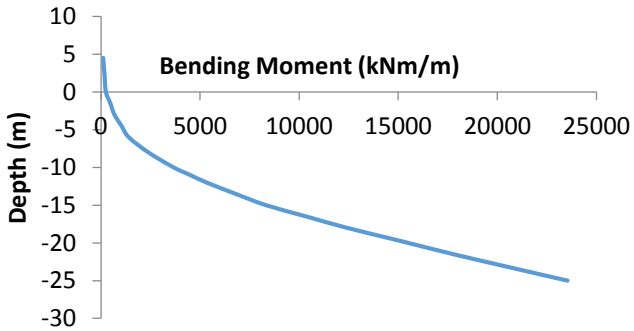

Fig. 5.6 Variation of bending moment in diaphragm wall with depth in static analysis without anchor

The variation of bending moment in the diaphragm wall is shown in Fig. 5.6. The bending moment varies gradually up to -8 m. The bending moment at -8 m depth is 2390 kNm. After -8 m depth, a sharp increase in bending moment is observed up -18 m. The bending moment at -18 m depth is 12413 kNm/m. This variation may be due to the reduction in

passive resistance in marine clay. The bending moment is zero at the top. The maximum value of bending moment which is obtained at the bottom of the diaphragm wall is 23,553 kNm/m.

5.2.2 Analysis of diaphragm wall for varying locations of anchor using Plaxis 3D

The anchor rod is placed at different locations and its effect on the displacement of the diaphragm wall is studied to find the most suitable location. The different locations considered in the analysis are,

i. At the surface of the structure, at +4.5 m

ii. At the water table, at 0.0 m

iii. At the different soil levels, at +2.5 m, -6.0 m and -10.0 m

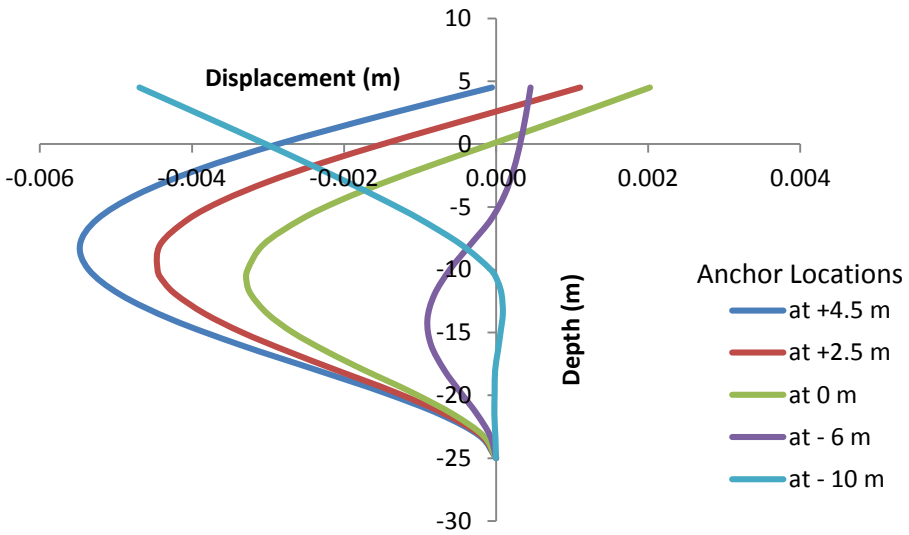

Fig. 5.7 Variation of displacement with depth of the diaphragm wall for different anchor locations (Static analysis, 3D)

Fig. 5.7 shows the variation of displacement with depth of the diaphragm wall for different anchor locations. Anchored diaphragm wall acts like a propped cantilever. When the anchor is placed at +4.5 m, the maximum displacement of the wall of -0.0057 m is obtained at location -8 m. In this case, the maximum deflection occurs in between the anchor location and dredge level. When the anchor is placed at location of +2.5 m, the maximum displacement obtained is -0.00446 m at -10 m, which is less than the previous case. The anchor position when shifted to 0 m, the length of the diaphragm wall in between the anchor

and the bottom of the diaphragm wall is reduced, as a result of which the maximum deflection in between these two points is reduced. But the portion of the diaphragm wall above the anchor deflects in the opposite direction. When anchor is located at -6 m, the diaphragm wall deflection is almost same in both the directions. When the anchor position is shifted to -10 m, the diaphragm wall above the dredge level deflects in negative direction. From the graph, it is clear that the maximum displacement occurs for the anchor location at +4.5 m.

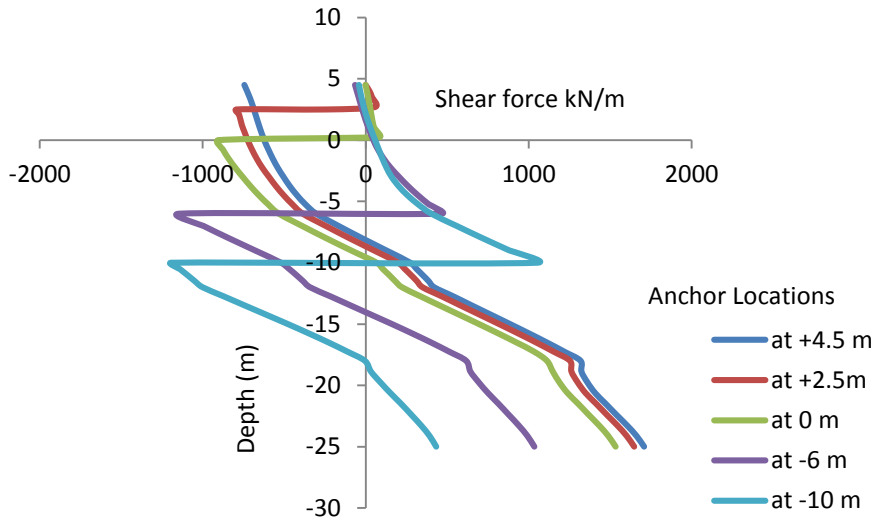

Fig. 5.8 Variation of shear force with depth of the diaphragm wall for different anchor locations (Static analysis, 3D)

The variation of shear force is shown in Fig. 5.8. The shear force is zero at the top and gradually increases as the depth increases. When the anchor is placed at a particular position, the shear force at that point is decreased due to the force taken by the anchor. Till a depth of -10 m the shear force increases gradually. After -10 m, the shear force value starts to decrease. This is due to the presence of passive earth pressure. After -17 m, the shear force again reduces due to the increase in the passive earth pressure. The maximum value of positive shear force of 1490 kN/m is obtained when the anchor is placed at +4.5 m. The maximum value of negative shear force of 1270 kN/m is obtained when the anchor is placed at -10 m. The minimum shear force -1120 kN/m is obtained when the anchor is placed at -6 m.

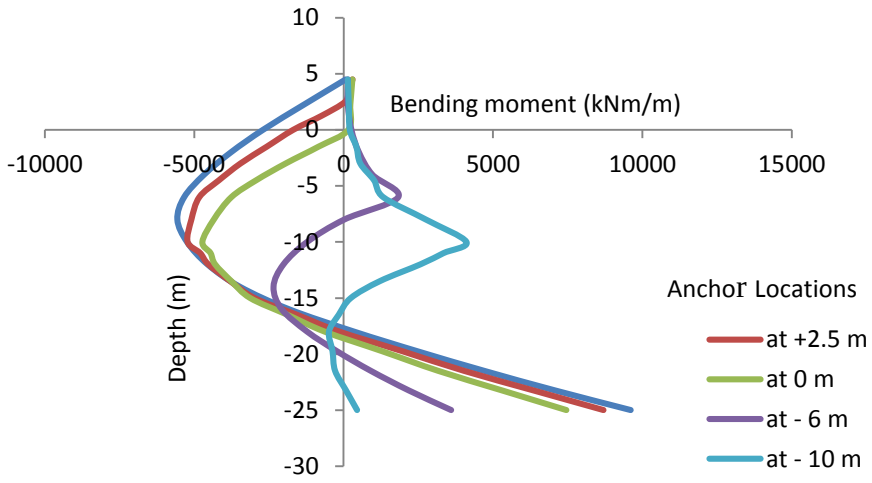

Fig. 5.9 Variation of bending moment with depth for the diaphragm wall for different anchor locations (Static analysis,3D)

The variation of bending moment is shown in Fig. 5.9. The bending moment is initially zero at the top of the diaphragm wall for the normal case when there is no anchor present. At the position where the anchor is placed, the bending moment value increases in the positive direction due to load being taken up by anchor. The maximum value of bending moment is obtained when the anchor is placed at +4.5 m, because the diaphragm wall behaves like a cantilever beam subjected to point load at free end and the bending moment is maximum at the fixed end. When the anchor is placed at -6m the bending moment reduces significantly because the anchor force is applied approximately at the center of diaphragm wall and it results in less moment at the fixed end of the diaphragm wall. But the shear force is increased with respect to the shear force at anchor location 0.0 m. The maximum displacement, shear force and bending moment values are tabulated as Table 5.1. From the study, it is seen that the maximum displacement decreases for anchor locations +2.5m, 0 m , -6 m & -10 m, by 21.75% (from 0.0057 m to 0.00446 m), 42.46% (from 0.0057 m to 0.00328 m), 83.86% (from 0.0057 m to 0.00092 m) & 17.71% (from 0.0057 m to 0.00469 m) respectively, with respect to anchor at +4.5 m. Similarly the maximum positive shear force is reduced by 4.6% (from 1490 kN/m to 1420 kN/m), 12.09% (from 1490 kN/m to 1310 kN/m), with respect to the anchor at +4.5 m. But the maximum negative shear force is increased by 13.3% (from 1120 kN/m to 1270 kN/m) when the anchor shifted from -6 m to -10 m. Similarly the bending moment decreases by 9% (from 9560 kNm/m to 8700 kNm/m), 22.0% (from 9560 kNm/m to 7460 kNm/m), 62.34% (from 9560 kNm/m to

3600 kNm/m) & 53% (from 9560 kNm/m to 4490kNm/m) with respect to the bending moment (9560 kNm/m) at +4.5 m anchor level.

Table 5.1. Values of maximum displacement, shear force and bending moment for varying locations of anchor obtained from Plaxis 3D.

Anchor Location	Max. Displacement & its location		Max. Shear force & location				Max. Bending Moment & its location			
	Displacement (m)	Location (m)	S.F (+ve) (kN/m)	Location (m)	S.F (-ve) (kN/m)	Location (m)	B.M (+ve) (kNm/m)	Location (m)	B.M (-ve) (kNm/m)	Location (m)
+4.5 m	-0.0057	-8	1490	-25	744	+4.5	9560	-25	5565	-8
+2.5 m	-0.00446	-10	1420	-25	1420	+2.5	8700	-25	5217	-10
0 m	-0.00328	-12	1310	-25	903	0.00	7460	-25	4732	-10
-6 m	-0.00092	-15.5	1035	-6	1120	-6	3600	-25	2345	-14
-10 m	-0.00469	+4.5	435	-10	1270	-10	4490	-10	491	-18

5.2.3 Comparison of the Results Corresponding to Plaxis 2D and 3D in the case of Varying Anchor Location.

The maximum values of displacement, bending moment and shear force obtained in Plaxis 2D (results mentioned in chapter 4) are compared with Plaxis 3D for various anchor locations and tabulated as Table 5.2

Table 5.2 shows the comparison between the maximum displacement, bending moment and shear force obtained in Plaxis 2D and 3D for the case of varying anchor locations. From the Table 5.2, it is observed that the maximum displacement of -0.00599 m is obtained in Plaxis 2D and -0.0057 m in Plaxis 3D for anchor location +4.5 m. The maximum bending moment and shear force obtained in Plaxis 2D analysis are 10710 kNm/m & 1720 kN/m and for Plaxis 3D, 9560 kNm/m & 1490 kN/m respectively. From the Table 5.2, it is seen that the minimum displacement of -0.00113 m is obtained in Plaxis 2D and -0.00092 m in Plaxis 3D for anchor location -6m. The maximum bending moment and shear force corresponding to -6 m location in Plaxis 2D and 3D are 4200 kNm/m & -1160 kN/m and 3560 kNm/m & -1120 kN/m respectively.

Table 5.2 Comparison of the maximum values of displacement, shear force and bending moment obtained by Plaxis 2D & 3D

Anchor location		Plaxis 2D	Location (m)	Plaxis 3D	Location (m)	% Variation w.r.t Plaxis 2D
+4.5 m	Displacement (m)	- 0.00599	-9	- 0.0057	-8	4.8%
	Shear force kN/m	1720	-25	1490	-25	**15.43%**
	Bending moment kNm/m	10710	-25	9560	-25	12.03 %
+ 2.5 m	Displacement (m)	- 0.00492	-10	- 0.00446	-10	10.31%
	Shear force kN/m	1650	-25	1420	-25	16.19%
	Bending moment kNm/m	9800	-25	8700	-25	12.64 %
0 m	Displacement (m)	-0.00362	-10	-0.00328	-12	10.36%
	Shear force kN/m	1530	-25	1310	-25	16.79%
	Bending moment kNm/m	8440	-25	7460	-25	13.14 %
- 6 m	Displacement (m)	-0.00113	+4.5	-0.00092	-15.5	**22.82%**
	Shear force kN/m	-1160	-6	-1120	-6	3.4%
	Bending moment kNm/m	4200	-25	3560	-25	**17.98 %**
- 10 m	Displacement (m)	-0.00444	+4.5	-0.00469	+4.5	5.63%
	Shear force kN/m	-1210	-10	-1270	-10	4.72%
	Bending moment kNm/m	4560	-10	4490	-10	1.56 %

The comparison shows that the maximum values of displacement, shear force & bending moment obtained in Plaxis 2D are higher by 22.82%, 15.43% & 17.98%, when compared with the results of Plaxis 3D as shown in Table 5.2. The basic element type used in the present study in Plaxis 2D is 15-noded triangular elements to model soil layer and for Plaxis 3D is 15-noded wedge elements. The variation in the results between Plaxis 2D and 3D may be due to the difference in basic element type used for the analysis and the mesh fines.

5.2.4 Analysis of Diaphragm wall with Anchor for Staged Construction

Construction stage analysis is important because of the non-linear behavior of soil and its dependency with loading path. The behaviour of wall is different for the cases: a) dredging up to final dredge level at a time, b) dredging in stages up to final dredge level. The construction of berthing structure consists of different stages. The simulation of the construction of diaphragm wall type berthing structure is a complex problem. It involves many stages such as installation of wall, excavation of soil, installation of anchor, applying the surcharge load etc. In Plaxis these construction stages are modelled using staged construction technique (phases). The construction phase in which the diaphragm wall performance is critical (maximum displacement, bending moment and shear force) is considered and the variation of displacement, shear force and bending moment are plotted for the critical phase .

Construction stage analysis is carried for the anchor locations +4.5 m,+2.5 m, 0 m, -6 m, and -10 m and maximum displacement, shear force and bending moment are obtained for critical phases. The diaphragm wall of deep draft berth of NMPT is considered for the analysis.

5.2.4.1 Sample analysis to obtain the critical phase for displacement for the anchor location +2.5m

The construction sequence of diaphragm wall considered for the analysis is described as below:

Initial phase: Initial stress generation

Phase 1: Installation of diaphragm wall

Phase 2: Activation of surcharge load of 50 kN/m^2 behind the wall

Phase 3: Excavation of soil from +4.5 m to +2.5 m

Phase 4: Installation and pre-stressing of anchor to 225 tonnes.

Phase 5 : Excavation of soil from +2.5 m to 0 m.

Phase 6 : Excavation of soil from +0 m to -6 m.

Phase 7 : Excavation of soil from -6 m to -10 m.

Phase 8 : Installation of piles

Phase 9 : Installation of slabs and beams

Phase 10 : Activation of live load of 50 kN/m^2

Analysis is carried to identify the critical phase for displacement for the anchor location +2.5 m. The phase 1 and 2 are the installation of wall and activation of surcharge load. In these phases there are no considerable displacement observed in the analysis. But in phase 3 to phase 7, considerable displacements are observed, hence the values are plotted with depth as shown in Fig. 5.10 to identify the critical phase. The displacement pattern after phase 7 is almost similar and it is not shown. From Fig. 5 .10, it can be seen that the displacement is maximum for phase 3 (before installation of anchor), which is excavation from + 4.5 m to +2.5 m. In this phase wall behaves like a vertical cantilever beam. Hence, maximum displacement of the wall is observed compared to other phases, which are after the anchor installation. The variation of displacement is almost linear till the depth up to +2.5 m then varies.

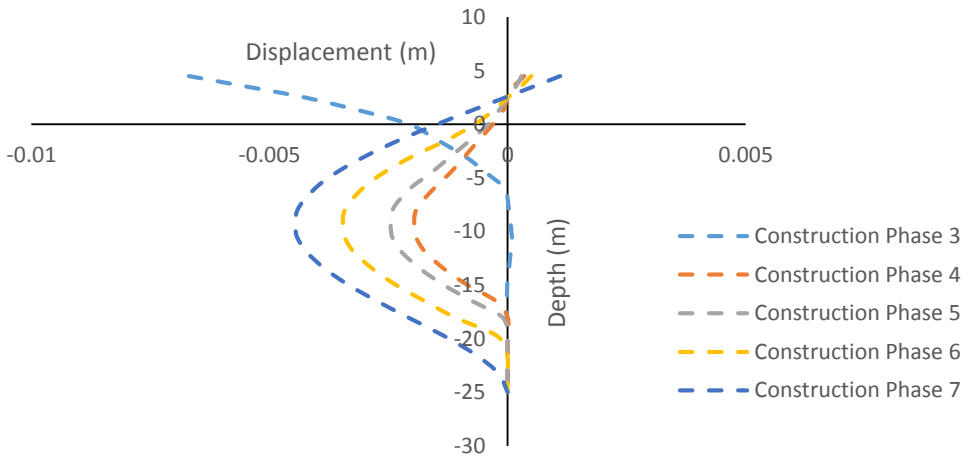

Fig. 5.10 Variation of displacement with depth of diaphragm wall for different construction stages for anchor at +2.5 m

The maximum displacement is observed at the top of wall and zero at the bottom of the wall. In phase 4, after the installation of anchor, the diaphragm wall moves back to positive direction and the displacement at anchor location +2.5 m is zero, and the variation of displacement is parabolic. In phase 5, 6 & 7 the displacement increased, but less than the displacement observed in phase 3. Hence phase 3 is the critical phase for displacement for the anchor location at +2.5 m.

Similar analysis are carried for anchor locations +4.5 m, 0 m, -6 m and -10 m and the critical phases and maximum displacement, shear force and bending moment are tabulated as shown in Table 5.2.

5.2.4.2 Construction stage analysis of diaphragm wall for varying locations of anchor using Plaxis 3D

Table 5.3. Construction sequences as phases for various anchor locations

Construction Sequences	Anchor Locations				
	+4.5 m	+2.5 m	0.0 m	-6 m	-10 m
Initial phase: Initial stress generation	✓	✓	✓	✓	✓
Phase 1: Installation of diaphragm wall	Phase 1	Phase 1	Phase 1	Phase 1	Phase 1
Phase 2: Activation of surcharge load of 50 kN/m^2 behind the wall	Phase 2	Phase 2	Phase 2	Phase 2	Phase 2
Phase 3: Excavation of soil from +4.5 m to +2.5 m	Phase 3	Phase 3	Phase 3	Phase 3	Phase 3
Phase 4: Installation and pre-stressing of anchor rod to 225 tonnes.	Phase 4	Phase 4	Phase 5	Phase 6	Phase 7
Phase 5 : Excavation of soil from +2.5 m to 0 m.	Phase 5	Phase 5	Phase 4	Phase 4	Phase 4
Phase 6 : Excavation of soil from +0 m to -6 m.	Phase 6	Phase 6	Phase 6	Phase 5	Phase 5
Phase 7 : Excavation of soil from +6 m to -10 m.	Phase 7	Phase 7	Phase 7	Phase 7	Phase 6
Phase 8 : Installation of piles	Phase 8	Phase 8	Phase 8	Phase 8	Phase 8
Phase 9 : Installation of slabs and beams	Phase 9	Phase 9	Phase 9	Phase 9	Phase 9
Phase 10 : Activation of live load of 50 kN/m^2	Phase 10	Phase 10	Phase 10	Phase 10	Phase 10

To analyze the construction stages, the construction phases have to be finalized for various anchor locations to provide as an input parameter in Plaxis 3D. Table 5.3 shows the construction sequences and phases considered for the present analysis. Construction phases includes Phase 1 to Phase 10. According to the anchor location the phase may have some variation and it can be observed in Table 5.3. Construction stage analysis is carried for the anchor locations +4.5 m,+2.5 m, 0 m, -6 m, and -10 m and displacement, shear force and bending moment are obtained for critical phases. For the anchor locations +4.5 m and +2.5 m, all the phases (Phase 1 to Phase 10) are continuous and anchor installation is at phase 4. But for the anchor location 0.0 m, the phase 4 is the excavation from +2.5 m to 0.0 m and the anchor installation is at phase 5. Similarly, for the anchor location -6 m, phase 4 is the excavation from +2.5 m to 0.0 m and phase 5 is the excavation from 0.0 m to -6 m, but the anchor installation is at phase 6 . Considering the anchor location at -10 m, phase 7 is the anchor installation phase. The anchor installation phase is coming after the excavation up to the anchor level. Hence before anchor installation, the diaphragm wall behaves like a cantilever and after the anchor installation, it behaves like a propped cantilever. According to these changes in structural behavior in the phases, variations in the displacement, shear force and bending moment are observed

Table 5.4. Maximum values of displacement, shear force and bending moment for varying locations of anchor obtained from Plaxis 3D for critical phase.

Anchor Locations	+4.5 m	+2.5 m	0 m	-6 m	-10 m
Max. Displacement (mm)	-9.5 @ +4.5 m Phase 3	-9.5 @ +4.5 m Phase 3	- 22.6 @ +4.5 m Phase 4	-53.3 @ +4.5 m Phase 5	- 69.22 @ +4.5 m Phase 6
Max. Shear Force (kN/m)	-1740 @ -25 m Phase 7	-1480 @ -25 m Phase 7	-1460 @ -25 m Phase 6	-1450 @ -25 m Phase 5	-1770 @ -25 m Phase 6
Max. Bending Moment (kN-m/m)	9900 @ -25 m Phase 7	10040 @ -25 m Phase 7	11990 @ -25 m Phase 6	18100 @ -25 m Phase 5	23710 @ -25 m Phase 6

Critical phases for anchor locations, +4.5 m, +2.5 m, 0 m,-6 m and -10 m are shown in Table 5.4. Critical phase displacement, shear force and bending moment with respect to depth are plotted for the different anchor location as shown in Fig. 5.11, 5.12 & 5.13.

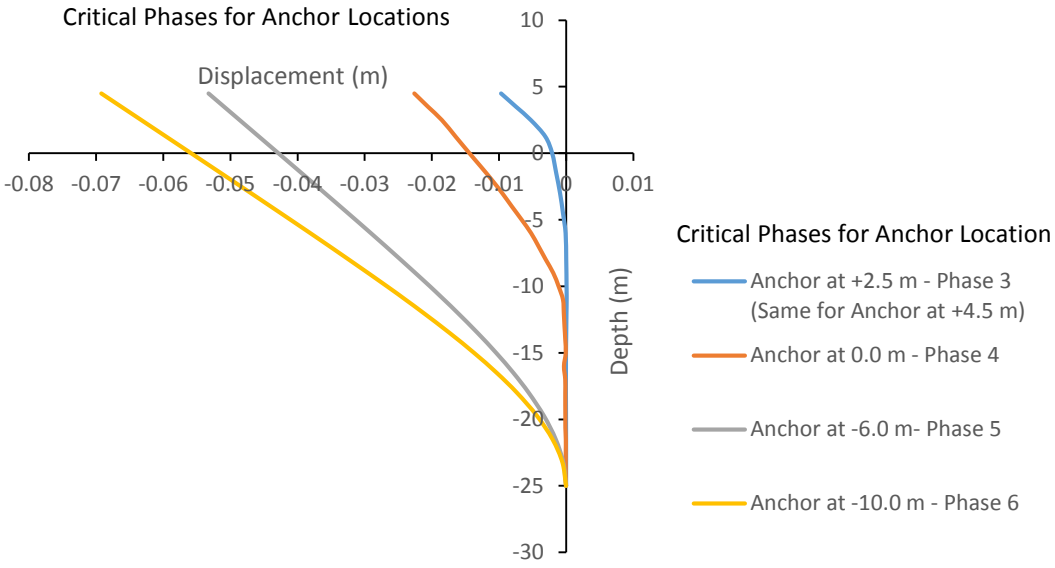

Fig. 5.11 Variation of displacement with depth for the diaphragm wall for different anchor locations for critical phase.

From the analysis it is found that the phase 3 is critical for displacement for the anchor locations +4.5 m and +2.5 m and the phases 4, 5 and 6 are critical for the anchor locations 0.0 m, -6 m and -10 m respectively. In all cases the maximum displacement is observed, before the anchor installation. Hence diaphragm wall acts like a cantilever before installation of anchor. From Fig 5.11, it is clear that the maximum displacement of the wall occurs at the free end, at +4.5 m. The variation of displacement is almost linear till -10 m then it is parabola. These variations are due to the change in soil pressure exerted by the back fill of the wall. From the graph, it is clear that the maximum displacement occurs when the anchor is at -10 m.

Similarly the phase7 is found critical phase for shear force for the anchor locations +4.5 m and +2.5 m and the phases 6, 5 and 6 are for the anchor locations 0.0 m, -6 m and -10 m respectively. The variation of shear force is shown in Fig. 5.12. The shear force is zero at the top and gradually increases as the depth increases. From Fig 5.12, it can be seen that the shear force decreases abruptly at the anchor point, because of the anchor pull against the soil active pressure.

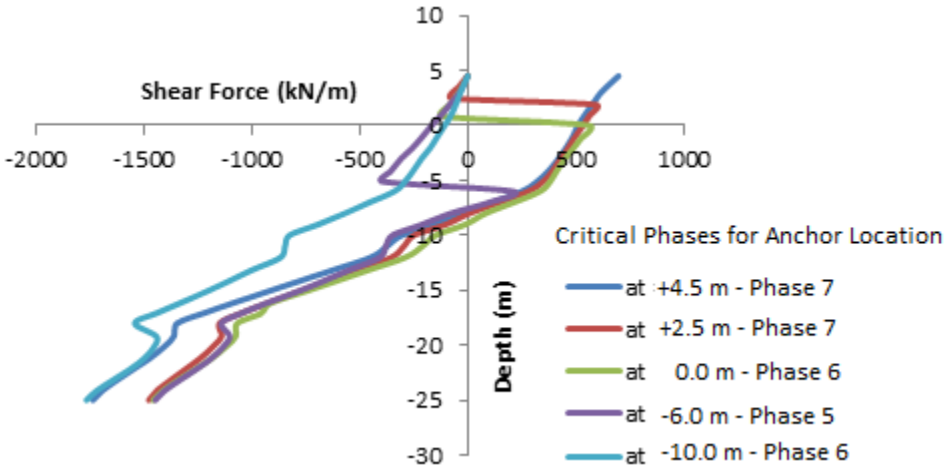

Fig. 5.12 Variation of shear force with depth for the diaphragm wall for different anchor rod locations for critical phase.

The shear force variation is different for all anchor locations between +4.5 m to -6m depth after which, the variation of shear force is almost similar and all the curves converge at -12m below the dredge level. The soil profile from -6 m to -10 m is marine clay below which lies medium sand layer up to -12 m. The next layer, from -12 m to -18 m once again consists of marine clay. The change in soil layer from medium sand to clay and anchor pull at anchor locations, may be the cause for the convergence of the curves at -12m. Below -8 m depth the shear force changes its sign due to the presence of passive earth pressure. The maximum value of negative shear force is obtained when the anchor is placed at -10 m.

For the case of bending moment, phase 7 (excavation up to dredge level,-10 m) is found critical for the anchor locations +4.5 m and +2.5 m and the phases 6, 5 & 6 are critical for the anchors at 0.0 m, -6 m and -10 m respectively. In phase 7, the excavation is carried up to the dredge level (-10 m). The variation of bending moment is shown in Fig. 5.13. The bending moment is initially zero at the top of the diaphragm wall for all the anchor locations because no horizontal forces are acting initially at top of the wall. At the anchor location, the bending moment values increases in the negative direction and gradually it is shifted to positive direction, which is caused due to the pre-stressing of anchor and also the behavior of wall like a propped cantilever.

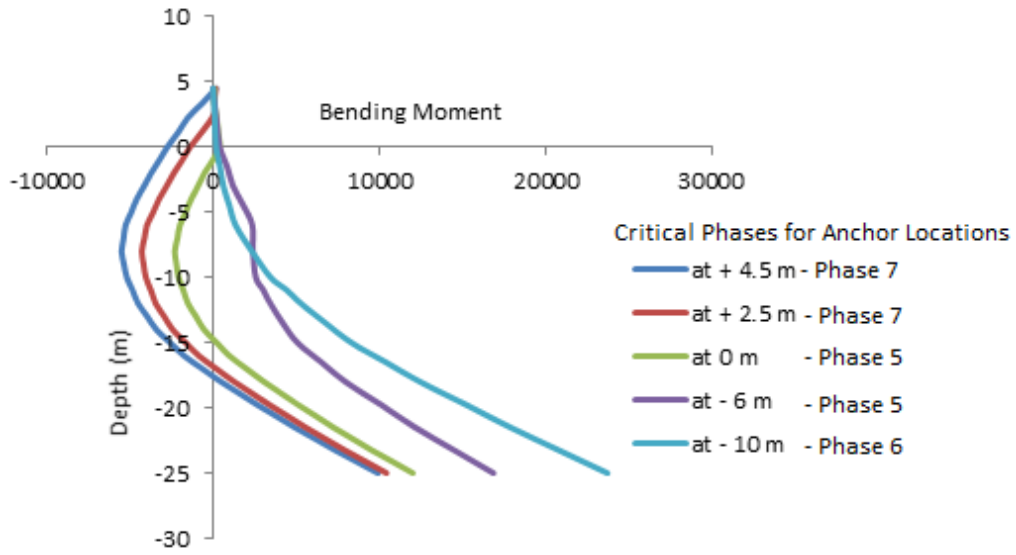

Fig. 5.13 Variation of bending moment with depth for the diaphragm wall for different anchor locations for critical phase.

But for anchor locations at -6.0 m and -10 m, the bending moment variations shows fully in positive direction as shown in Fig. 5.13. This may be due to the fact that critical phases are 5 & 6 which is before the installation of anchor. The maximum value of positive bending moment, 23710 kNm/m is obtained for the anchor location - 10 m at -25 m depth. From the study, it is observed that the maximum displacement is reduced by 86% (from 0.069 m to 0.0095 m), 85.12% (from 0.069 m to 0.0102 m), 67.35%(from 0.069 m to 0.0226 m) & 23% (from 0.069 m to 0.0533 m) for the anchor locations +4.5 m, +2.5 m, 0.00 m & -6 m respectively, with respect to the maximum displacement corresponding to anchor at -10 m (0.069 m). Similarly, the bending moment is reduced by 58.25% (from 23710 kNm/m to 9900 kNm/m), 57.65% (from 23710 kNm/m to 10040 kNm/m), 49.43% (from 23710 kNm/m to 11990 kNm/m) & 24% (from 23710 kNm/m to 18100 kNm/m) with respect to maximum bending moment corresponding to the anchor at -10 m. The results imply that anchor at dredge level is not advisable because of the higher value of displacement, and bending moment when compared to the other anchor positions.

From Fig. 5.11, 5.12 & 5.13, it is observed that the displacement and bending moment are minimum when the anchor is located at +4.5 m but the shear force is minimum when the anchor is at +2.5m. The displacement and bending moment values of diaphragm wall when the anchor is at + 2.5 m differ less when compared with the corresponding values for the anchor location at +4.5m. The installation of anchor at +4.5 m is not advisable because this level is the top of the soil surface. Hence, the anchor location at +2.5 m can be

recommended based on the construction stage analysis. The actual location of anchor in the real berthing structure at site is at +2.5 m.

5.2.4.3 Analysis of diaphragm wall for staged construction using Plaxis 2D.

Construction sequence analysis is also carried out by using Plaxis 2D and the results are compared with results obtained in Plaxis 3D. Construction sequences are same as that considered for 3D analysis. Analysis is carried out to identify the critical phase for maximum displacement, shear force and bending moment for the anchor locations +4.5 m, +2.5 m, 0.0 m, -6 m and -10 m and the results are tabulated as Table 5.5. Critical phase displacement, shear force and bending moment with respect to depth are plotted for the different anchor location as shown in Fig. 5.14, 5.15 & 5.16. The analysis shows that critical phases obtained in Plaxis 2D are as same as that observed in Plaxis 3D, but variations in values of maximum displacement, shear force and bending moment are noticed.

Table 5.5. Maximum values of displacement, shear force and bending moment for varying locations of anchor obtained from Plaxis 2D for critical phase.

Anchor Locations	+4.5 m	+2.5 m	0 m	-6 m	-10 m
Maximum Displacement (mm)	-9.6 @ +4.5 m Phase 3	- 9.6 @ 4.5m Phase 3	- 21.9 @ +4.5 m Phase 4	- 53.1 @ +4.5 m Phase 5	- 70.4 @ +4.5 m Phase 6
Maximum Shear Force (kN/m)	-1720 @ -25 m Phase 7	-1670 @ -25m Phase 7	-1620 @ -25 m Phase 6	-1570 @ -25 m Phase 5	-1760 @ -25 m Phase 6
Maximum Bending Moment (kN-m/m)	11020 @ -25 m Phase 7	11390 @ -25 m Phase 7	12680 @ -25 m Phase 6	17480 @ 25 m Phase 5	23380 @-25 m Phase 6

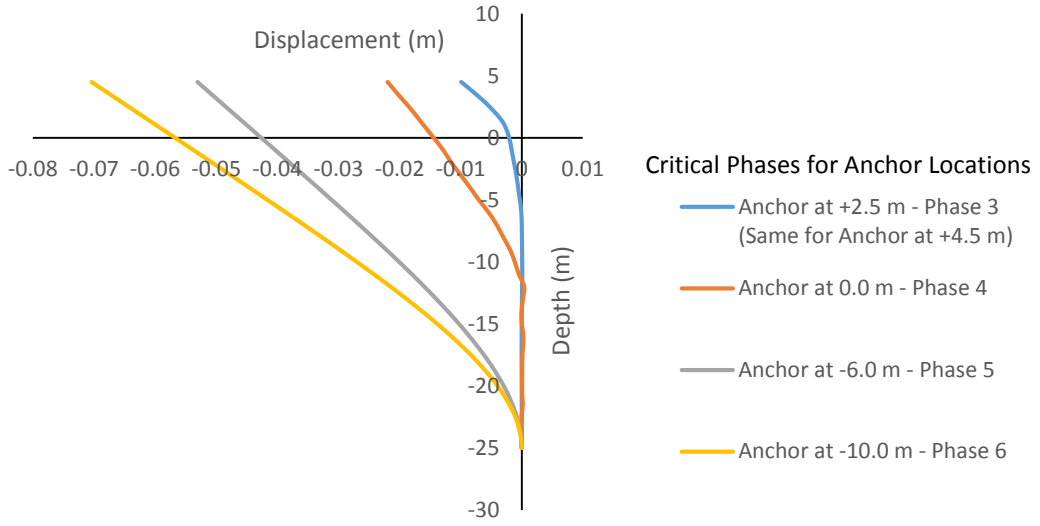

Fig 5.14 Variation of displacement with depth for the diaphragm wall for different anchor locations

The analysis shows that the phase 3 is the critical phase for displacement for anchor locations +4.5 m and +2.5 m and phase 4, 5 and 6 are critical for the anchor locations 0.0 m, -6 m and -10 m respectively. In all the above cases maximum displacement is observed before the anchor installation. The displacement variation pattern in Plaxis 2D is similar to that obtained in Plaxis 3D, but the values are different. From Fig. 5.14, it is seen that the diaphragm wall behaves like a cantilever with the maximum displacement at the free end. The variation of displacement is almost linear till -10 m then it is parabola. From Fig. 5.14, it is clear that the maximum displacement occurs when the anchor is at -10 m.

The variation of shear force is shown in Fig. 5.15. The shear force is zero at the top and gradually increases as the depth is increased. When the anchor is placed at a particular position, the shear force at that point is decreased due the force taken by the anchor. It can also be seen that the variation of shear force is almost similar for the anchor locations +4.5 m, +2.5 m, 0 m and -6 m up to -7 m depth, and there after the shear force changes sign from +ve to -ve. This is due to the presence of passive earth pressure. After -18 m, the shear force again increases due to the increase in the passive earth pressure. The maximum value of negative shear force is obtained when the anchor is placed at -10 m.

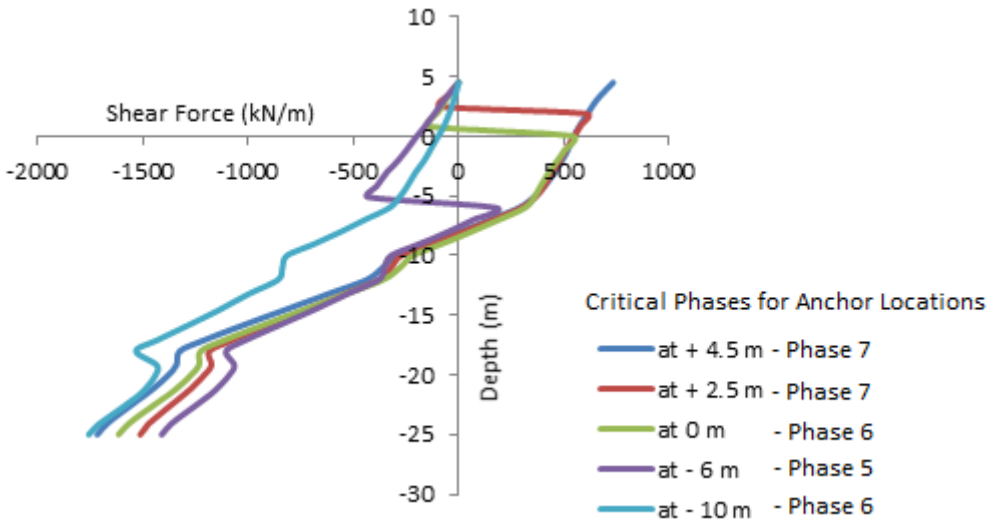

Fig. 5.15 Variation of shear force with depth for the diaphragm wall for different anchor rod locations

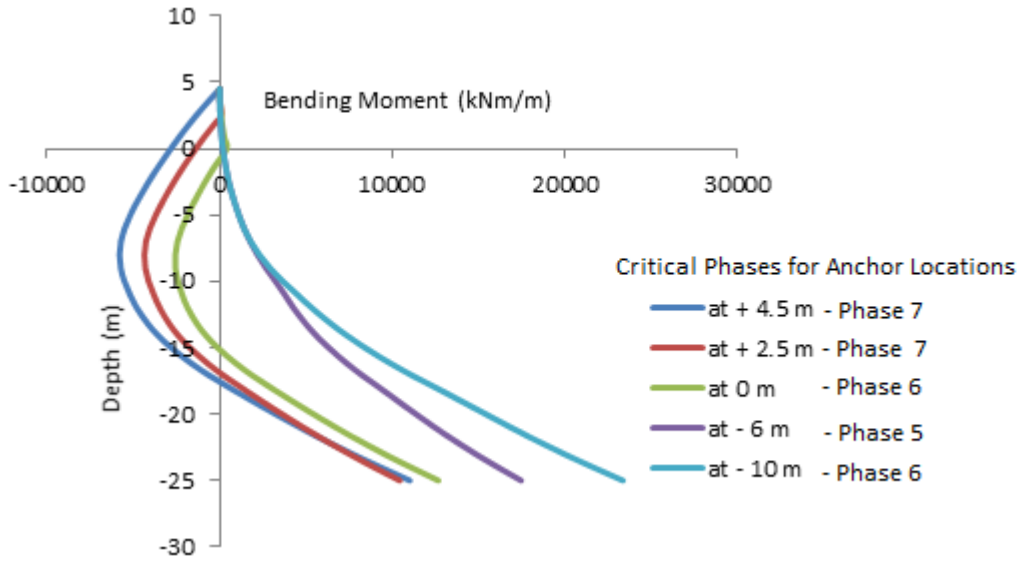

Fig. 5.16 Variation of bending moment with depth for the diaphragm wall for different anchor rod locations

The variation of bending moment is shown in Fig. 5.16. The bending moment is initially zero at the top of the diaphragm wall for the normal case. At the position where the anchor is placed, the bending moment value increases in the negative direction due to load being taken up by anchor. The bending moment increases in the positive direction after -10 m

depth. The maximum value of positive bending moment is obtained when the anchor is placed at - 10 m.

5.2.4.4 Comparison between Plaxis 2D and 3D results for construction stage analysis

The maximum values of displacement, bending moment and shear force obtained in the construction stage analysis in Plaxis 2D and 3D for various anchor locations are given in Table 5.6 and the results are compared. The comparisons show that maximum values of displacement, shear force and bending moment obtained in Plaxis 2D are higher by 5.09%, 12.84% and 11.31% respectively when compared with the results of Plaxis 3D

Table 5.6 Comparison of construction sequence analysis results using Plaxis 2D & 3D

Anchor location		Plaxis 2D	Location (m)	Plaxis 3D	Location (m)	% Variation w.r.t Plaxis 2D
+4.5 m	Displacement (m)	-0. 00957	+4.5	-0 .00948	+4.5	0.95%
	Shear force kN/m	-1880	-25	-1740	-25	7.44%
	Bending moment kNm/m	11020	-25	9900	-25	11.31 %
+ 2.5 m	Displacement (m)	- 0.00102	+4.5	- 0.00198	+4.5	5.09%
	Shear force kN/m	- 1670	-25	- 1480	-25	12.84%
	Bending moment kNm/m	11390	-25	10400	-25	9.52 %
0 m	Displacement (m)	-0.02263	+4.5	-0.02185	+4.5	3.57%
	Shear force kN/m	-1620	-25	-1460	-25	10.95%
	Bending moment kNm/m	12680	-25	11990	-25	5.75 %
- 6 m	Displacement (m)	-53.06	+4.5	-53.25	+4.5	0.36%
	Shear force kN/m	-1570	-25	-1450	-25	8.27%
	Bending moment kNm/m	17480	-25	18100	-25	3.55 %
- 10 m	Displacement (m)	-0.07038	+4.5	-0.06922	+4.5	1.67%
	Shear force kN/m	-1760	-25	-1770	-25	0.57%
	Bending moment kNm/m	23380	-25	23710	-25	1.41 %

The difference between the Plaxis 2D & 3D may be due to the difference in the element type considered and mesh fines of the model.

The Plaxis 2D analysis gives the maximum displacement of the anchored diaphragm wall without considering the construction stage as 0.00599 m, whereas with considering the construction stage as 0.0072m. Similarly, the maximum bending moment of the diaphragm wall without considering the construction stage is 10710 kNm/m, whereas with considering the construction stage is 23380 kNm/m. Similarly, Plaxis 3D analysis gives the maximum displacement of the diaphragm wall without considering the construction stage as 0.0057 m, whereas with considering the construction stage as 0.00692 m. Similarly, the maximum bending moment of the diaphragm wall without considering the construction stage is 9560 kNm/m, whereas considering the construction stage it is 23710 kNm/m. The study shows that some of the phases of construction cause higher displacement, shear force and bending moment in the construction stages which are not generally observed in the static analysis. This indicates the importance of construction stage analysis.

5.3 SUMMARY

Plaxis 3D static analysis is carried out to find displacement, shear force and bending moment for the diaphragm wall with and without anchor. The analysis is extended to find the behavior of diaphragm wall in construction phases. The study shows the importance of anchor and its location to control the displacement, shear force and bending moment on the structure. The study shows that some of the phases of construction experiences higher displacement, shear force and bending moment in the construction stages.

Based on the present investigation, the following conclusions can be drawn:

- ✓ From 3D analysis it is found that the presence of anchor has a significant impact on the stability of diaphragm wall. In the case when no anchor is provided, the maximum displacement of the diaphragm wall is -69.3 mm whereas when anchor is provided at an elevation of +2.5 m, the maximum displacement of the diaphragm wall is reduced to -4.46 mm which occurs at -10.0 m. The displacement is reduced by about 93.5% by placing the anchor at +2.5 m as in the actual field (NMPT deep draft berth).

- ✓ The maximum values of variation of displacement, shear force & bending moment obtained in Plaxis 2D are higher by 22.82% (from -0.00113 m to -0.00092 m), 15.43% (from 1720 kN/m to 1490 kN/m) & 17.58% (from 4200 kNm/m to 3560 kNm/m) when compared with Plaxis 3D results in static case.
- ✓ When the anchor position is shifted to -10 m, (at dredge level) the trend of deflection of diaphragm wall differs from other cases. When the anchor is at -10 m the diaphragm wall behaves like a vertical cantilever beam.
- ✓ The maximum positive bending moment for anchor locations +4.5 m, +2.5 m, 0 m, and -6 m is observed at a depth -25 m and for anchor location -10 m it is at -10 m depth. The change in location of maximum positive bending moment may be due the anchor located at dredge level -10 m.
- ✓ From the construction stage study in Plaxis 3D, it is observed that the maximum displacement is reduced by 86% (from 0.069 m to 0.0095 m), 85.12% (from 0.069 m to 0.0102 m), 67.35%(from 0.069 m to 0.0226 m) & 23% (from 0.069 m to 0.0533 m) for the anchor locations +4.5 m, +2.5 m, 0.00 m & -6 m respectively, with respect to the maximum displacement corresponding to anchor at -10 m.
- ✓ In Plaxis 3D analysis, the maximum displacement of anchored diaphragm wall without considering the construction stage is reduced by 91.763% (from 0.0692 m to 0.0057 m) and in Plaxis 2D, 91.4% (from 0.0703 m to 0.00599 m) when compared to the maximum displacement obtained by considering the construction stage for the case anchor at -10.0 m.
- ✓ In Plaxis 3D analysis the maximum shear force of anchored diaphragm wall without considering the construction stage is reduced by 14.36% (from -1740 kN/m to -1490 kN/m) and in Plaxis 2D, 8.51% (from -1880 kN/m to -1720 kN/ m) when compared to the maximum shear force obtained by considering the construction stage for the anchor location at +4.5 m.
- ✓ The maximum bending moment obtained in Plaxis 3D analysis for anchored diaphragm wall for the case without considering the construction stage is reduced by 59.6% (from 23710 kNm/m to 9560 kNm/m) and in Plaxis 2D, 54.41% (from 23380 kNm/m to 10710 kNm/m) when compared to the maximum bending moment obtained by considering the construction stage for the anchor location at +4.5 m.
- ✓ The construction stage analysis shows maximum value of displacement, shear force and bending moment obtained in Plaxis 2D are higher by 5.09%, 12.84% and

11.31% respectively when compared with Plaxis 3D analysis. But the 2D and 3D analysis agreed reasonably well for the construction stage analysis.

- ✓ The analysis shows that, the anchor at dredge level is not advisable because of the higher value of displacement, shear force. and bending moment. further from the construction point of view in the field it is not feasible.

CHAPTER 6

3D ANALYSIS OF DIAPHRAGM WALL WITH DIFFERENTCROSS SECTIONS

6.1 GENERAL

The static analysis are carried for a uniform thick diaphragm wall section using Plaxis 2D and 3D software and discussed in chapter 4 and 5. To study the effect of stiffness on the behavior of diaphragm wall, static analysis on non-uniform sections are considered in this chapter. It is one of the objectives of the present investigation. Seven different diaphragm wall sections having non uniform configurations are modelled and the results are compared with the actual section. The maximum displacement and bending moment of the wall for varying anchor locations are calculated and variations of the same with depth are plotted. The static analysis of the diaphragm wall in Plaxis 2D & 3D shows the shear force variations within 15%, but the displacement and bending moment variations observed are considerably higher as described in chapter 4 and 5. From literature it is found that major case studies related to stiffness of the anchored wall are focused on displacement as well as bending moment effect due to lateral load by the back fill. Also, it is found that the displacement and bending moment variations in anchored diaphragm wall are higher than the shear force variations. The present investigation of diaphragm wall in Plaxis 2D & 3D (Chapter 3 & 4) reasonably agreed with these observations. Hence in this chapter, study is focused on the analysis of maximum displacement and bending moment of an anchored diaphragm wall with varying stiffness. The soil and structural element data of the existing deep draft berth of New Mangalore Port is considered for modelling the different sections. Plaxis 3D finite element computer program is used to perform the model analyses in the present study under static loading.

6.2 BOUNDARY CONDITIONS

For 3D analysis boundary conditions are as follows;

- ✓ Vertical model boundaries with their normal in x direction (i.e. parallel to the y-z plane) are fixed in x direction ($u_x = 0$) and free in y and z direction. Vertical model boundaries

with their normal in y direction (i.e. parallel to the x-z plane) are fixed in y direction ($u_y = 0$) and free in x and z direction.

- ✓ The model bottom boundary is fixed in all directions ($u_x = u_y = u_z = 0$).
- ✓ The ground surface of the model is free in all directions.
- ✓ Vertical model boundaries with a normal in x-direction; $\emptyset_y = \emptyset_z = 0$ ($\emptyset_x$= *f*ree)
- ✓ Vertical model boundaries with a normal in z-direction;$\emptyset_x = \emptyset_y = 0$ ($\emptyset_z = free$).
- ✓ Vertical model edges and at the bottom boundary;$\emptyset_x = \emptyset_y = \emptyset_z = 0$

6.3 INPUTTING OF MATERIAL AND SOIL PROPERTIES

The input parameters of structural elements and soil parameters as shown in Table 3.1 and 3.3 of chapter 3 are considered for the analysis. Stiffness of the various sections are shown in Table 6.1.

Table 6.1 Stiffness of various cross-sections.

Different sections	Young's Modulus (concrete) (E) (kN/m^2	Young's Modulus (steel) (N/m^2)	Moment of Inertia (I)m^4	Stiffness(EI) ($kN\text{-}m^2$)
Section-1	31.62×10^6		0.09	2.846×10^6
Section-2	31.62×10^6		0.1829	5.78×10^6
Section-3	31.62×10^6		0.649	20.52×10^6
Section-4	31.62×10^6	210×10^9	0.0801	3.977×10^6
Section-5	31.62×10^6	210×10^9	0.0758	3.07464×10^6
Section-6	31.62×10^6		0.1445	4.569×10^6
Section-7	31.62×10^6		0.1147	3.626×10^6
Actual section	31.62×10^8		0.5545	17.533×10^6

6.4 DIFFERENT SECTIONS CONSIDERED FOR ANALYSIS AND RESULTS.

Section 1 is modelled as 0.6 m thick uniform RCC diaphragm wall. In section 2, 1.1m thick section is sandwiched between 0.6 m thick panels of RCC. Section 3 is designed as RCC T section has 0.6 m thick flange and 1.1m thick web. In section 4, rectangular hollow steel pile of 0.02 m thick and 1.1 m x 1.0 m size is used in between 0.6 m RCC panel where as in section 5, circular hollow steel pile of 0.02 m thick and 1.0 m diameter is used. The section 6 is

modelled as RCC hollow square pile with 0.2 m thick and 1.0 m x 1.0 m size between 0.6 m RCC panels.

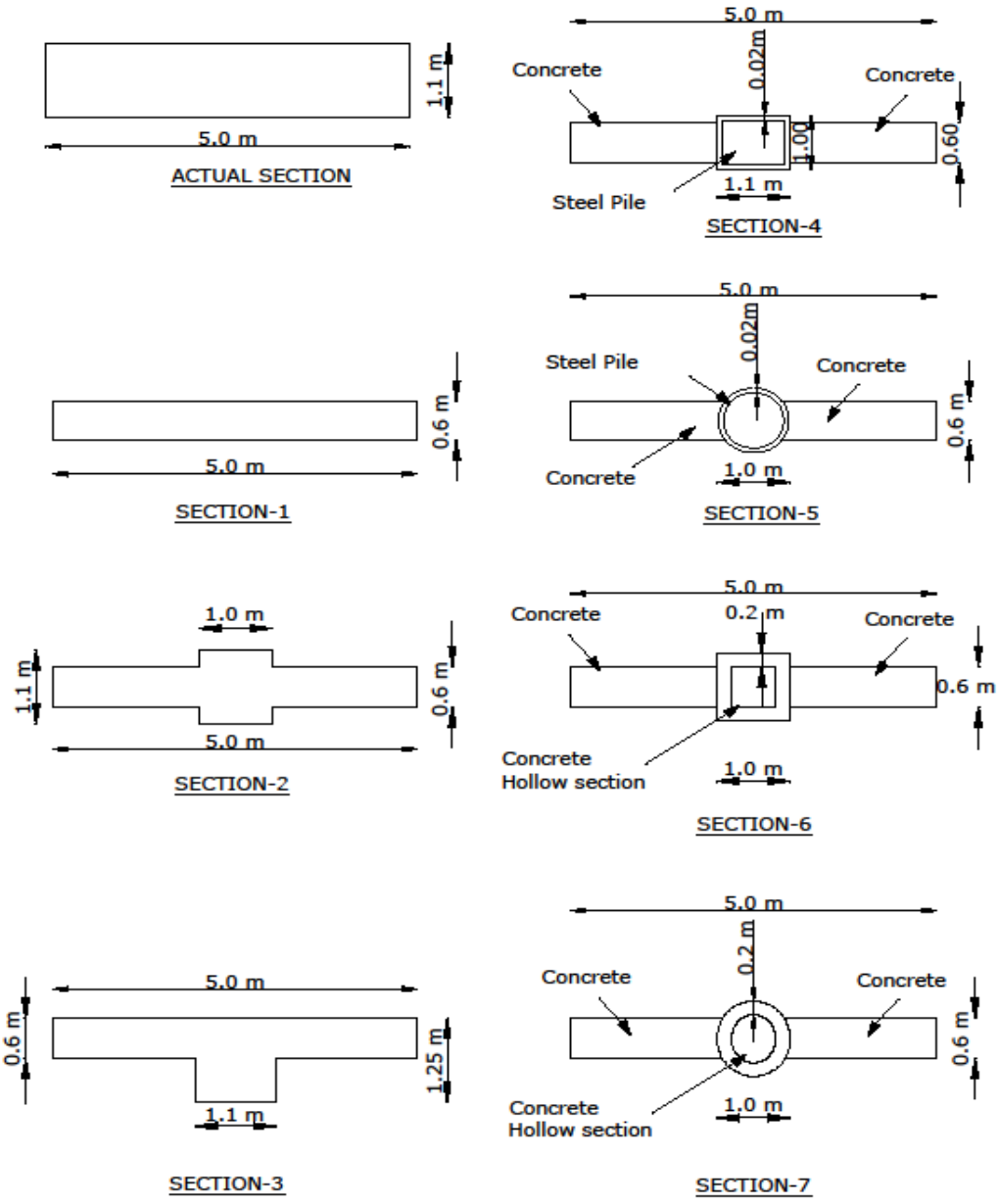

Fig. 6.1 Various diaphragm wall sections, considered for the analysis

The section 7 is modelled as RCC hollow circle pile with 0.2 m thick and 1.0 m dia. between 0.6 m RCC panels. The horizontal sections of wall panels which are considered for analysis are shown in Fig. 6.1.

6.4.1 Analysis of Actual Section (1.1m thick) with Anchor.

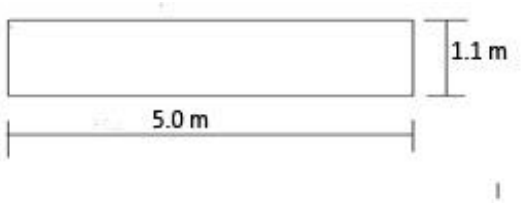

Fig. 6.2 Diaphragm wall actual section

The actual diaphragm wall is modelled as a 5 m wide and 1.1 m thick uniform concrete solid panel section as shown in Fig. 6.2. The variation of displacement with depth of diaphragm wall is shown in Fig. 6.3. From the figure it is clear that the maximum displacement of the diaphragm wall depends on the location of anchor. When the anchor is placed at +4.5 m, the maximum displacement of the wall of -0.0057 m is observed at location -8 m. In this case, the maximum displacement occurs in between the support at +4.5 m and dredge level, -10 m. When the anchor is placed at a level +2.5 m, the maximum displacement obtained is -0.00446 m at -10 m, which is less than the previous case. The anchor position when shifted to 0 m, the length of the diaphragm wall in between the anchor and the bottom of the diaphragm wall is reduced, as a result of which the maximum deflection in between these two points is reduced. But the portion of the diaphragm wall above the anchor deflects in the opposite direction. When the anchor position is at -6 m, the diaphragm wall deflection is almost same in both the directions. When the anchor position is shifted to -10 m, (at dredge level) the displacement of diaphragm wall between the anchor and the support at the bottom is considerably reduced, but above the dredge level it is considerably increased and maximum displacement occurred at +4.5 m level. The deviation may be due to the cantilever action of wall, when the anchor is located at dredge level. Maximum displacement occurs for the case of anchor located at +4.5 m.

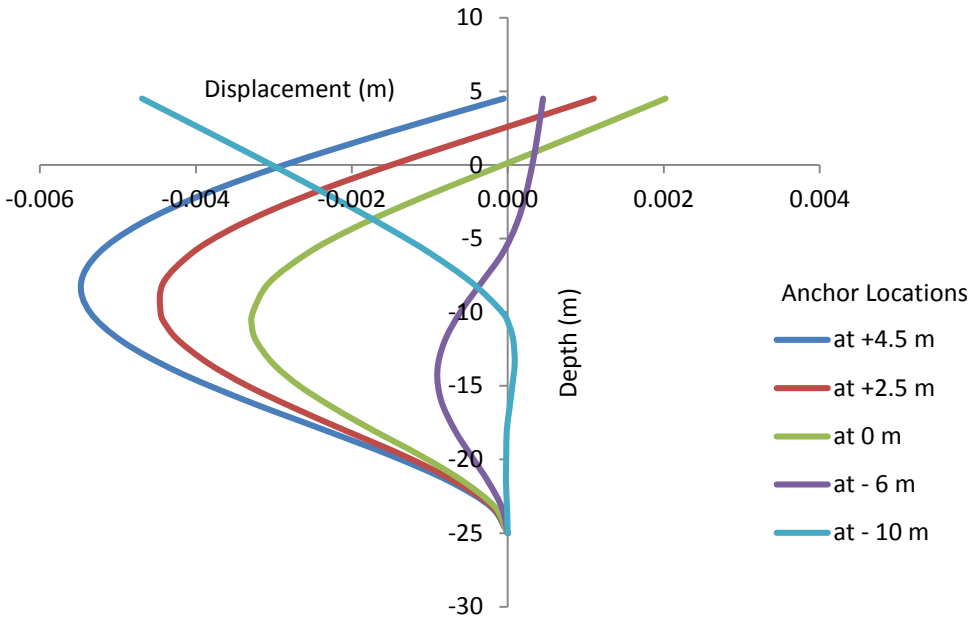

Fig. 6.3 Variation of displacement with depth of the diaphragm wall for different anchor locations for actual section.

The variation of bending moment with depth is shown in Fig. 6.4. The bending moment is initially zero at the top of the diaphragm wall. At the position where the anchor is placed, the shear force decreases because of the anchor pull, but the bending moment value increases in the positive direction due to load being taken by anchor. The maximum value of bending moment is obtained when the anchor is placed at +4.5 m. This is because, the diaphragm wall behaves like a propped cantilever beam subjected to anchor pull at free end and the bending moment is maximum at the fixed end. Also the reduction in passive resistance due to the presence of marine clay from -12 m to -18 m increases the bending moment at bottom fixed end. When the anchor is placed at -6 m the bending moment reduces significantly because the anchor force is applied approximately at the center of diaphragm wall and it results in less moment at the fixed end of the diaphragm wall. Maximum displacement and bending moment of actual section for different anchor locations are shown in Table 6.2.

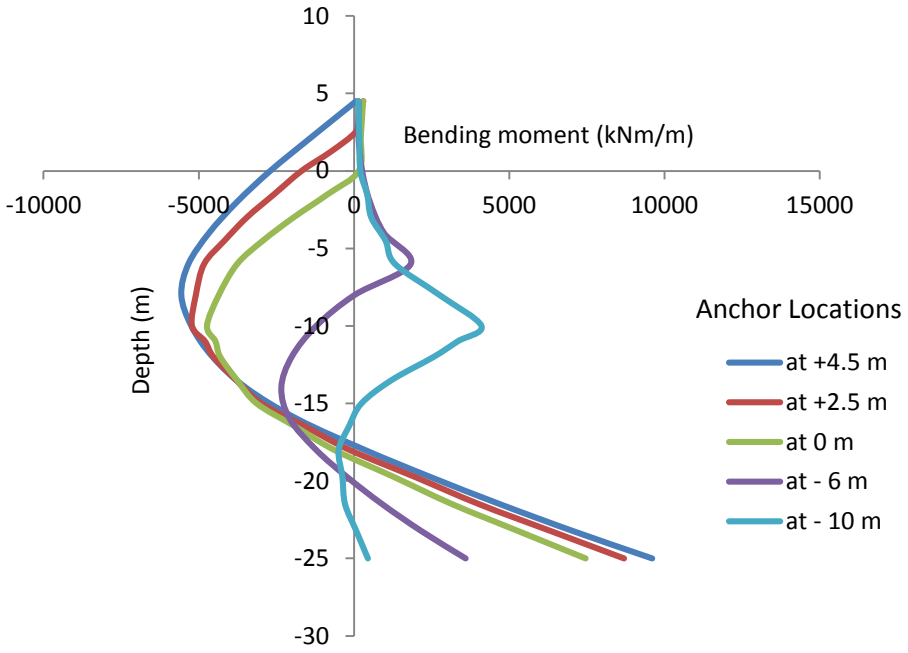

Fig. 6.4 Variation of bending moment with depth of the diaphragm wall for different anchor locations for actual section.

Table 6.2 Maximum Values of displacement and bending moment of actual section for varying locations of anchor (Static analysis)

Anchor Location (m)	Max. Displacement & its location		Max. Bending Moment & its location			
	Displacement (m)	Location (m)	B.M (+ve) (kNm/m)	Location (m)	B.M (-ve) (kNm/m)	Location (m)
+4.5	-0.0057	-8 m	9560	-25	5565	-8
+2.5	-0.00446	-10 m	8700	-25	5217	-10
0.0	-0.00328	-12 m	7460	-25	4732	-10
-6	-0.00092	-15 m	3600	-25	2345	-14
-10 m	-0.00469	+4.5	4490	-10 m	491	-18

6.4.2 Analysis of Section 1

Section 1 is modelled as 0.6 m thick uniform diaphragm wall with panel length 5 m. The section is analysed for different anchor location.

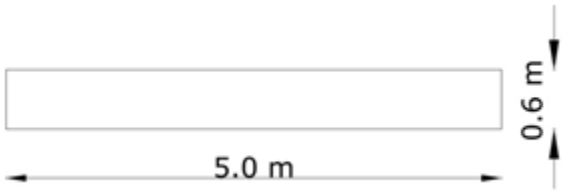

Fig. 6.5 Diaphragm wall section 1

Stiffness of this section (2.846×10^6 kNm^2) is 83.77% less than actual section (17.533×10^6 kNm^2) having thickness 1.1m. Deflection and bending moment of section 1 obtained are shown in Fig. 6.6 & 6.7. From Fig. 6.6 & 6.7, it is observed that even though the displacement has increased comparing with the displacement of actual section, the bending moment of the section 1 is considerably reduced. As stiffness decreases flexibility increases. In this case, the reduction in bending moment may be due to the reduction in stiffness. Maximum deflection and bending moment are obtained when anchor is at +4.5 m level. The maximum displacement of the section 1 is increased by70% (from 0.0057 m to 0.0097 m) and the maximum bending moment is reduced by 46% (from 9560 kNm/m to 5120 kNm/m) when compared with the actual section with respect to the anchor location at +4.5 m level. Both deflection and bending moment are found to be minimum when the anchor is at level -6 m. Maximum displacement and bending moment of section 1 for different anchor locations are shown in Table 6.3.

From the analysis it is observed that, even though the displacement has been increased by 70% (from 0.0057 m to 0.0097 m), there is considerable reduction in bending moment of 46% (from 9560 kNm/m to 5120 kNm/m) compared with the actual section. Maximum displacement and bending moment are obtained corresponding to anchor location +4.5 m. Both displacement and bending moment are found to be minimum for anchor location -6 m.

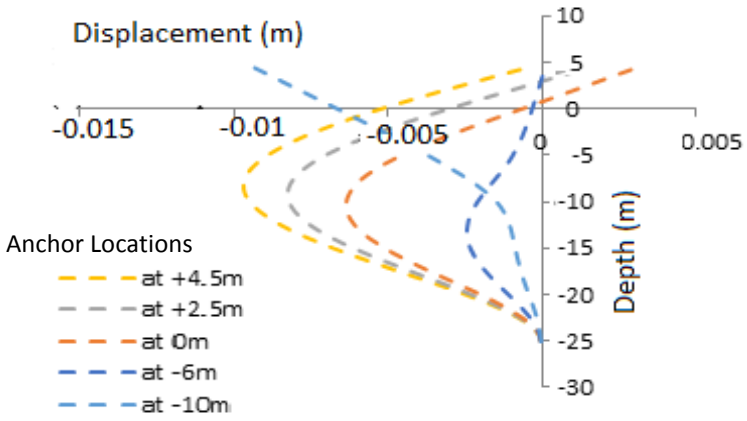

Fig. 6.6 Variation of displacement with depth for section 1

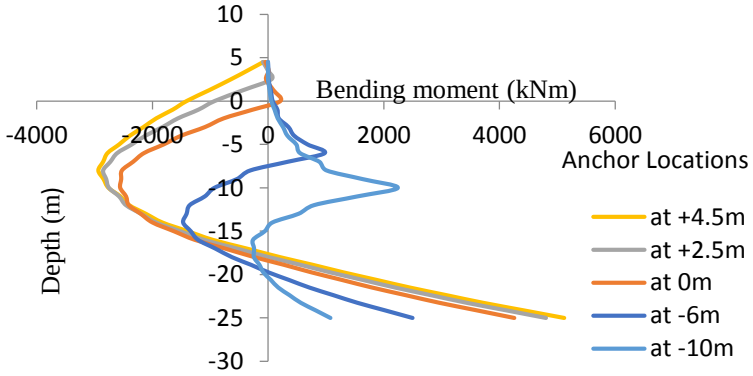

Fig. 6.7 Variation of bending moment with depth for section 1

Table 6.3 Maximum deflection and maximum bending moment of section 1 for different anchor locations.

Anchor location (m)	Max. Displacement & its location		Max. Bending Moment & its location			
	Displacement (m)	Location (m)	B.M (+ve) (kNm/m)	Location (m)	B.M (-ve) (kNm/m)	Location (m)
+4.5	-0.0097	-9	5120	-25	2935	-9
+2.5	-0.0086	-9.5	4800	-25	2850	-8
0.0	-0.00639	-12	4250	-25	2525	-10
-6.0	-0.00339	-15	2490	-25	1467	-14
-10.0	-0.00836	+4.5	2260	-10	245	-18

6.4.3 Analysis of Section 2

In order to check the behaviour of section when stiffness is varied, a compound section (section2) is designed as shown in Fig. 6.8. In this, 1.1m thick section (same as actual section) is sandwiched between 0.6 m panels

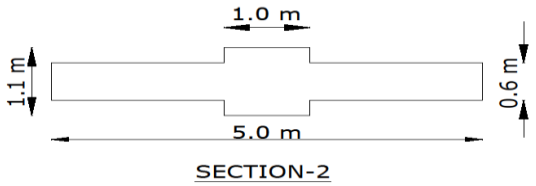

Fig. 6.8 Diaphragm wall section 2

The middle portion of the section has same thickness as that of actual diaphragm wall. While comparing the displacements and bending moments of actual section (Fig. 6.3 & 6.4) and section 2 (Fig. 6.9 & 6.10), the trend of the graph for both the cases are matching for various anchor locations. Since it is coupled with comparatively lesser stiff section (1.1 m thick to 0.6 m thick), it is expected to produce lesser bending moment as seen in the case of actual section. Since the stiffness of section 2 (5.78×10^6 kN-m^2) is approximately equal to $\frac{1}{3}$ of the stiffness of actual section (17.533×10^6 kN-m^2), the bending moment has to reduce as seen in the case of section1, because the reduction in stiffness has to reduce the bending moment. But it is observed that the maximum bending moment of 12730 kNm/m is found to act at 1.1 m thick section and which is more than that of actual section, which is 9560 kNm/m, even though the thickness and loading condition are same.

After detailed study it is found that bending moment acting at 0.6 m panel is reduced compared to section 1, as shown in Table 6.4 & 6.2. So it is obvious that whatever bending moment is reduced on 0.6 m thick section, a part of which has to be transferred to the adjacent thicker section, because the load applied is same for both section1 & 2. From the study it is found that

bending moment acting at 0.6 m panel (section 2) is reduced by 19.4% (from 5120 kNm/m to 4130 kNm/m) compared to section1, which is having 0.6 m thick uniform section. The reduction in bending moment on 0.6 m thick panel, and increase in bending moment in 1.1 thick panel of the same coupled section 2 may be due to the rearrangement by transferring moment from the thinner to the thicker panel (Potts, 1991). Hence the latter produces 24.9% (from 9560 kNm/m to 12730 kNm/m) higher bending moment.

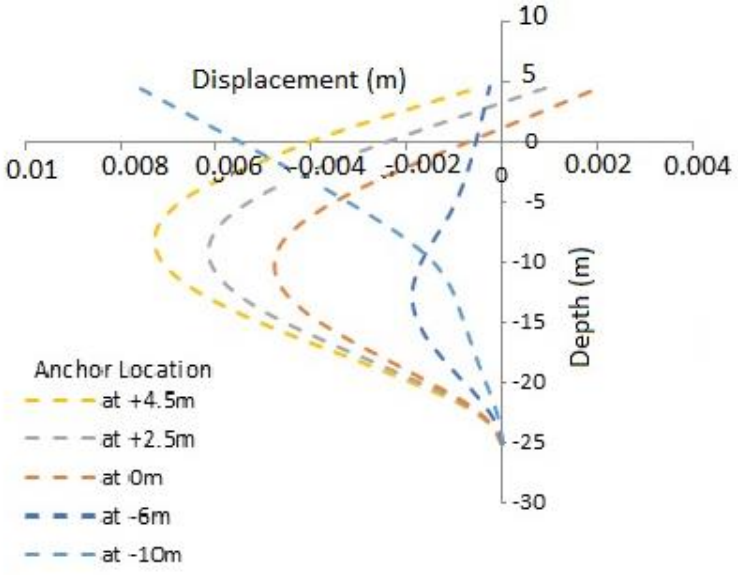

Fig. 6.9 Variation of displacement with depth for section 2

The displacement of section 2 is increased by 10.7 % (from 0.0057 to 0.0063 m) when compared with displacement of actual section. The increase in displacement may be due to the reduction in stiffness. Fig 6.9 & 6.10 shows displacement and bending moment for section 2. Maximum displacement and bending moment of section 2 for different anchor locations are shown in Table 6.4. The maximum displacement, 0.00763 m is observed at +4.5 m level for the anchor location -10 m and the displacement variations are found to be distinct from the displacement variations of other anchor locations as shown in Fig. 6.9. The displacement variations may be due to the position of anchor -10.0 m is at dredge level and it is greater than 1/(3) of the height of wall (29.5 m) and also the reduction in passive resistance due to the presence of marine clay below the anchor position.

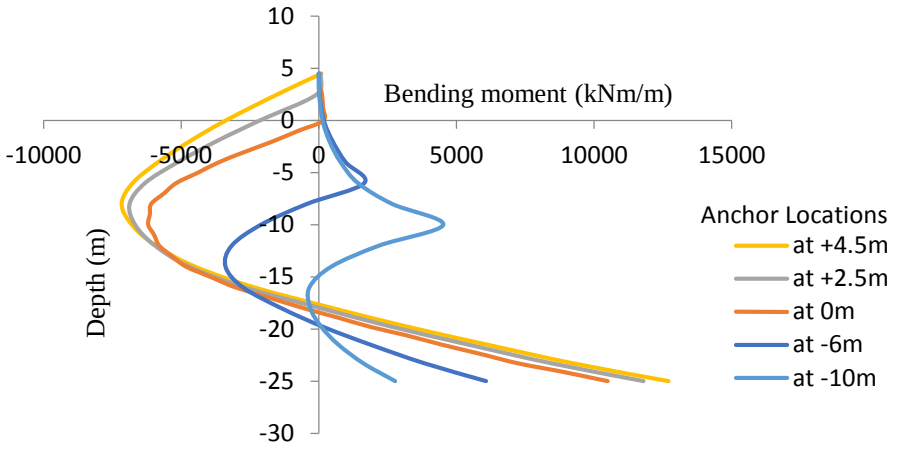

Fig. 6.10 Variation of bending moment with depth for section 2

Table 6.4 Maximum deflection and maximum bending moment of section 2 for different anchor locations.

Anchor location (m)	Max. Displacement & its location		Max. bending moment & its location (1.1m thick)		Max. bending moment & its location (0.6m thick)	
	Displacement (m)	Location (m)	B.M (kNm/m)	Location (m)	B.M (kNm/m)	Location (m)
+4.5	-0.00630	-8	12730	-25	4130	-25
+2.5	-0.00617	-10	11830	-25	3810	-25
0.0	-0.00476	-13	10450	-25	3260	-25
-6.0	-0.00218	-15	608	-25	1505	-25
-10	-0.00763	+4.5	4540	-10	1270	-10

6.4.4 Analysis of Section 3

In order to check the behavior of the wall with a web, T section is chosen as section 3 for further study**.** For the T section usually perimeter wall (flange) and buttress wall (web) are of same thickness, and same stiffness. But in this study thinner perimeter wall and thicker buttress wall are used to vary the stiffness to study the behavior of wall. The designed T section has 0.6 m thick perimeter wall and 1.1m thick buttress wall.

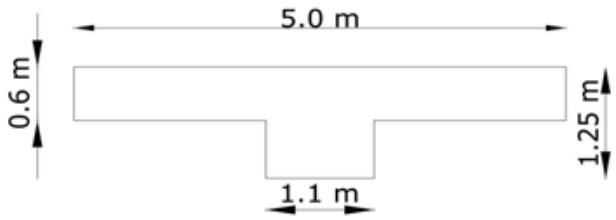

Fig. 6.11 Diaphragm wall section 3

Variations of displacement and bending moment for T section is shown in Fig. 6.12 & 6.13 respectively. These variations are similar to that observed in actual section. The displacement of the T section is reduced by 12.8% (from 0.0057 m to 0.00497 m), 43.5% (from 0.00446 to 0.00254 m), 38.4% (from 0.00328 m to 0.00202 m), 72.8% (from 0.00092 m to 0.00025 m) and 7.8% (from 0.00469 m to 0.00432 m) for the anchor locations +4.5 m, +2.5 m, 0 m, -6 m and -10 m respectively, with respect to the actual section. The bending moment of the T section is reduced by 83.8% (from 9560 kNm/m to 1660 kNm/m), 82.23% (from 8700 kNm/m to 1540 kNm/m), 81.64% (from 7460 kNm/m 1370 kNm/m), 75.5% (from 3600 kNm/m to 880.5 kNm/m) and 81.28% (from 4490 kNm/m to 840.52 kNm/m) for anchor location +4.5 m, +2.5 m, 0 m,-6 m and -10 m) respectively, with respect to actual section. The maximum displacement and bending moment are found to be 0.00492m (at -8 m) and 1660 kNm/m (at -25 m) respectively for the anchor location +4.5, and it is found to be the lowest while comparing with the other sections of present investigation. From Fig. 6.12 the displacement for the anchor locations -6.0 m and -10 m shows considerable deviations when compared with other anchor locations. Clough et al. (1989) suggested that the wall deforms in a cantilever mode before the installation of the first support and after the installation, the total displacement may be the summation of cantilever displacement and bulging displacement. For the anchor location -6.0 m and -10 m, the soil depth -6 m to -18 m show larger bulging displacement when compared with other anchor positions. The reason for bulging may be the presence of highly cohesive marine clay overlying a thick medium sand (Likitlersuang et al, 2013). Maximum displacement of -0.00432 m is observed at +4.5 m level for the anchor location -10 m and the displacement variations are found to be distinct from the displacement variations of other

anchor locations as shown in Fig. 6.12. The displacement variations may be due to the position of anchor at -10.0 m which is at dredge level, and greater than $\frac{1}{3}$ of the height of wall (29.5 m) and also due to the reduction in passive resistance because of the presence of marine clay below the anchor position.

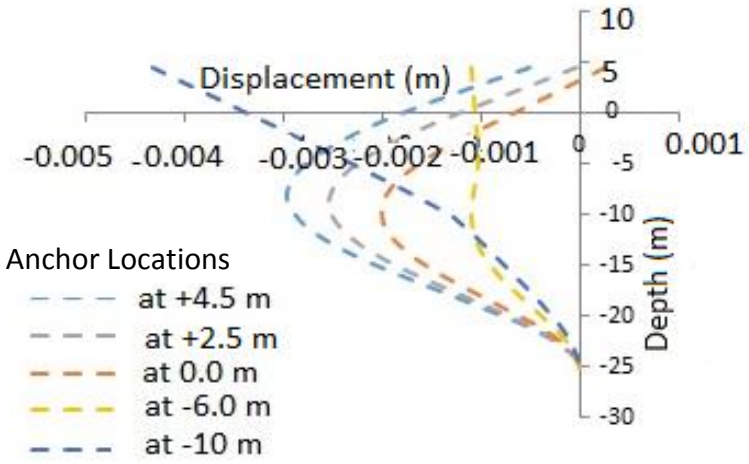

Fig. 6.12 Variation of deflection with depth for section 3

Hsieh et al (2011) found that for T shaped diaphragm wall, external side friction at buttress helps to reduce wall displacement. In the present study, the soil profile has fine, medium and coarse sand having effective friction angle 30° as shown in Table 3.3. The presence of sandy soil may produce additional side friction along the buttress of the T section. This may be one of the reasons behind the reduction in displacement for T section. The buttress provides anchorage by producing extra friction along its side. This will cause an overall reduction in soil mass movement towards the passive side. Section 1 is a solid concrete section having 5 m length and 0.6 m thickness which is similar as the perimeter wall of the T section. The comparison between the performance of section1 and T section shows considerable reduction in displacement and bending moment in T section. In the present study, the maximum displacement of section 1 is obtained as 0.0097 m and for T section is 0.00497 m for the anchor location +4.5 m.

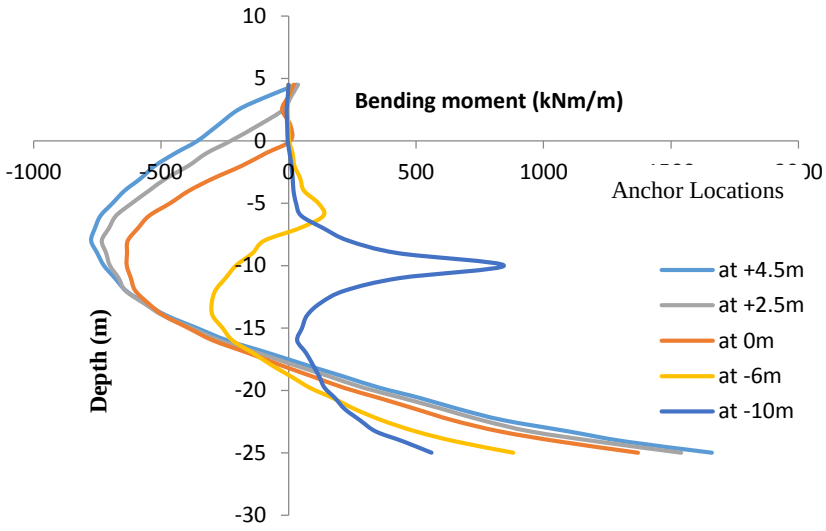

Fig. 6.13 Variation of bending moment with depth for section 3

These results show that, by introducing a web with perimeter wall, the maximum displacement of a wall is reduced by 48% (from 0.0097 m to 0.00497 m). Similarly the maximum bending moment is reduced by 67.57% (from 5120 kNm/m to 1660 kNm/m). These comparisons indicate that the buttress can be used to encounter the larger displacement and bending moment occurring in soil profile because it can mobilize frictional resistance between the wall and adjacent soil.

By considering all the anchor locations studied for T section, the maximum displacement and bending moment are found to be -0.00497 m and 1660 kNm/m acting at -10 m and -25 m respectively for the anchor location at +4.5 m. The maximum displacement is reduced by 12.8% (from 0.0057 m to 0.00497 m) and bending moment is reduced by 83.8% (from 9560 kNm/m to 1660 kNm/m) when compared with the actual section. Performance of T section can be further increased by giving more length to the buttress there by increasing the side friction. Value of deflection and bending moment for different anchor location is shown in Table 6.5.

Table 6.5 Maximum displacement and bending moment of section 3 for different anchor locations

Anchor location (m)	Max. Displacement & its location		Max. Bending Moment & its location			
	Displacement (m)	Location (m)	B.M (+ve) (kNm/m)	Location (m)	B.M (-ve) (kNm/m	Location (m)
+4.5	-0.00497	-9	1660	-25	774	-10
+2.5	-0.00254	-10	1540	-25	716	-9
0.0	-0.00202	-13	1370	-25	634	-9
-6.0	-0.00025	-15.5	880.51	-25	298	-14
-10	-0.00432	+4.5	840.52	-10	3	-2

6.4.5 Analysis of section 4 & section 5

Section 4 and 5 (as shown in Fig. 6.14) are designed almost similar except, in section 4, rectangular hollow steel pile is used in between 0.6 m RCC panel where as in section 5, circular hollow steel pile is used. Steel piles have higher flexibility than RCC panel, hence producing lesser bending moment. The results obtained for both the sections are almost similar. Since flexible piles produce more displacement, the displacement of the diaphragm wall for section 4 & 5 are increased compared to Section 1.

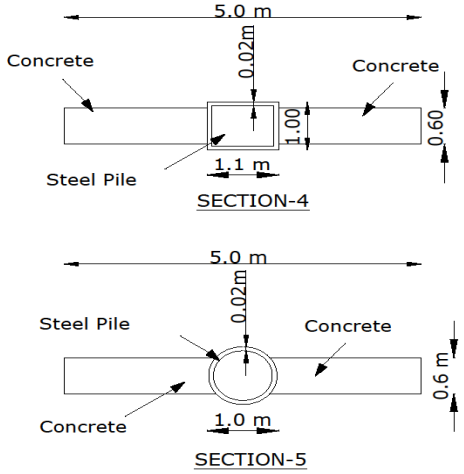

Fig. 6.14 Diaphragm wall section 4 and section 5

Maximum displacement in section 4 and 5 are found to be 0.0113 m and 0.01147 m respectively, for anchor location +4.5 m, whereas for actual section, it is 0.0057 m for anchor location +4.5m. The maximum displacement in section 4 is increased by 98.4% (from 0.0057 m to 0.01131 m) and for section 5 it is increased by 79.87% (from 0.0057 m to 0.01147 m) compared with the actual section. The displacement and bending moment for section 4 and 5 are shown in Fig 6.15 & 6.16 and 6.17 & 6.18 respectively. The comparison between the sections 1, having 0.6 m thick solid RCC uniform section and section 4 (0.6 m thick RCC and steel pile) shows that the displacement in section 4 is increased by 16.59% (from 0.0097 m to 0.01131 m) and for section 5 by18.29% (from 0.0097 m to 0.01147 m) with respect to section 1. These results show that by introducing a flexible steel pile in a solid concrete section the displacement increases. From Fig. 6.15 & 6.16 it is observed that for anchor location at -10 m the displacement variation is different from other anchor locations. In this case the anchor is installed at -10 m (dredge level), hence wall behave like a cantilever above the dredge level.

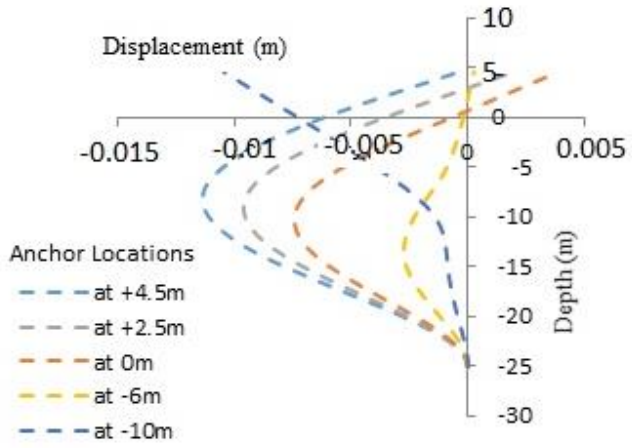

Fig. 6.15 Variation in displacement with depth for section 4

When the sections 4 & 5 are studied for bending moment, it is found that, in both the sections, maximum bending moment is acting on the 0.6 m thick RCC panel as shown in Table 6.6 and 6.7. From the study it is observed that, the maximum bending moment in section 4 is reduced by 35.5% (from 9560 kNm/m to 6161 kNm/m) in 0.6 m thick RCC panel and 71.65% (from 9560 kNm to 2710 kNm) in rectangular steel pile compared with the actual section.

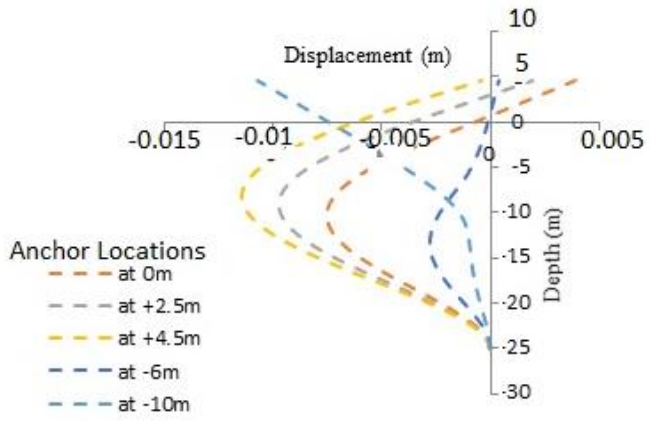

Fig. 6.16 Variation in displacement with depth for section 5

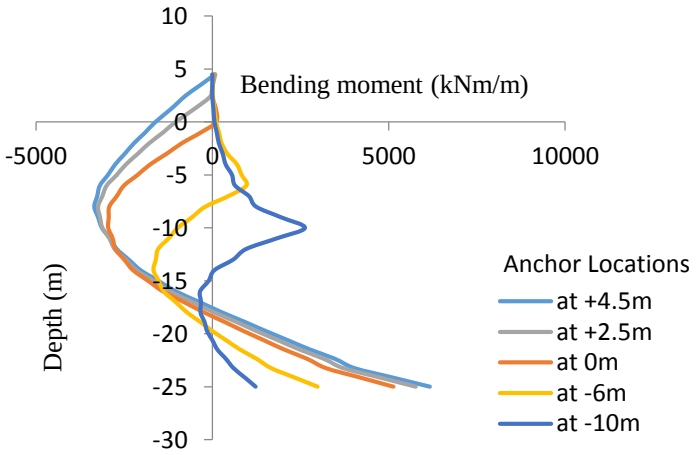

Fig. 6.17 Variation in bending moment with depth for section 4

Similarly, in section 5, maximum bending moment is reduced by 34.62% (from 9560 kNm/m to 6250 kNm/m) in RCC panel and 74.26% (from 9560 kNm to 2460 kNm) in circular steel pile comparing with actual section. The stiffness of the section 4 (3.977×106 kN-m2) and section 5 (3.0746×106 kN-m2) are 77% & 82.4% lesser than the stiffness of the actual section (17.533×106 kN-m2). The reduction in stiffness of section 4 and 5 results in lower bending moment in these sections.

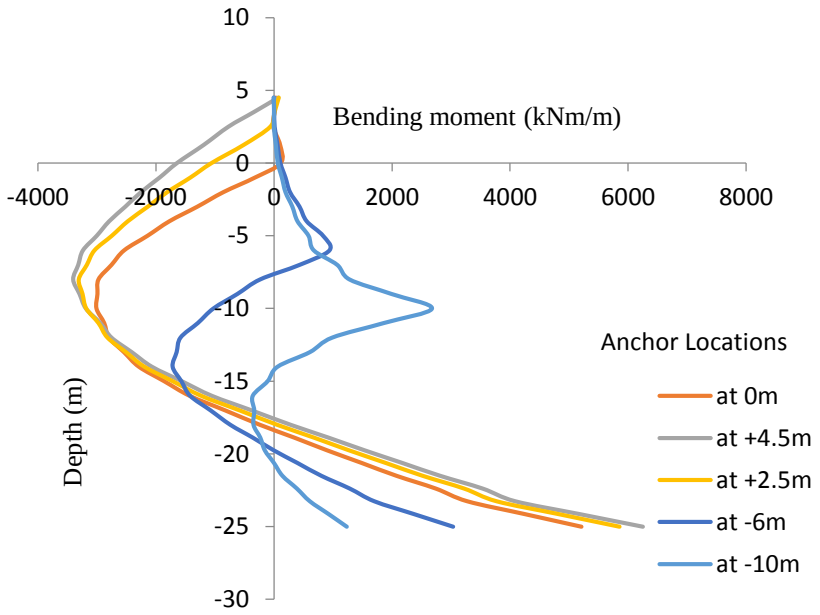

Fig. 6.18 Variation in bending moment with depth for section 5

The comparison between section 1(0.6 m thick RCC uniform section) and sections 4 & 5 shows that, the maximum bending moment in section 4 is increased by 20.3% (from 5120 kNm/m to 6160 kNm/m) and for section 5 by 22.07%(from 5120 kNm/m to 6250 kNm/m). The stiffness of sections 4 and 5 are greater than the stiffness of the section 1 (as shown in Table 6.1) and hence the bending moment increases in sections 4 & 5. While comparing the maximum bending moment variation within the sections 4 & 5 the rectangular pile section shared 39% $\left(\frac{2430}{6160}\times 100\right)$ of bending moment in section 4 and circular pile shared 44% $\left(\frac{2750}{6250}\times 100\right)$ of bending moment in section 5.

The study shows that when a flexible pile is introduced in a RCC section, there is a redistribution of stress, hence the bending moment show variation within the section. Out of all the anchor locations studied, the anchor at -6.0m is found to be more effective. Maximum value of Displacement and bending moment with respect to anchor location are shown in Table 6.6 & 6.7.

Table 6.6 Maximum deflection and maximum bending moment of section 4 for different anchor locations

Anchor location (m)	Max. Displacement & its location		Max. Bending Moment & its location (0.6 thick concrete)		Max. Bending Moment & its location (steel pile)	
	Displacement (m)	Location (m)	B.M (kNm/m)	Location (m)	B.M (kNm/m)	Location (m)
+4.5	-0.01131	-9.5	6160	-25	2430	-25
+2.5	-0.00961	-9.5	5760	-25	1950	-25
0.0	-0.00741	-13.0	5130	-25	1530	-25
-6.0	-0.00270	-15.0	2980	-25	1190	-25
-10.0	-0.01047	+4.5	2650	-10	980	-10

Table 6.7 Maximum deflection and maximum bending moment of section 5 for different anchor locations.

Anchor location (m)	Max. Displacement & its location		Max. Bending Moment & its location (0.6 thick concrete)		Max. Bending moment & its location (steel pile)	
	Displacement (m)	Location (m)	B.M (kNm/m)	Location (m)	B.M (kNm/m)	Location (m)
+4.5	-0.01147	-9	6250	-25	2750	-25
+2.5	-0.00976	-10.5	5860	-25	2380	-25
0.0	-0.00754	-12.8	5210	-25	2080	-25
-6.0	-0.00277	15.2	3040	-25	1125	-25
-10.0	-0.01071	+4.5	2700	-25	1081	-10

6.4.6 Analysis of section 6 & 7

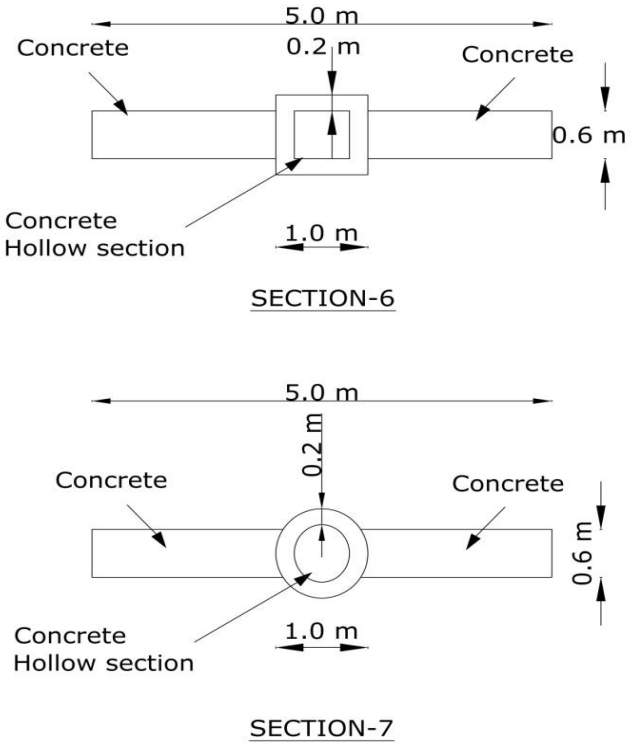

Fig. 6.19 Diaphragm wall section 6 and section 7

In order to study the performance of a hollow section with same young's modulus, the section 6 & 7 are designed as shown in Fig. 6.19. In section 6, hollow square RCC piles are used where as in section 7 circular hollow RCC piles are used in between 0.6 m thick panel as shown in Fig. 6.19. Stiffness of RCC piles are more when compared with steel piles. Fig. 6.20 and 6.21 shows the maximum displacement of wall for different anchor locations. Similarly Fig. 6.22 and 6.23 shows the maximum bending moment of wall for different anchor locations. From the analysis it is found that maximum displacement in section 6 and 7 are found to be 0.00663 m and 0.00692 m, whereas for section 1 it is 0.0046 m for anchor location -10 m at +4.5 m. Similarly maximum bending moment in section 6 & 7 are 2630 kNm/m and 3640 kNm/m for

the anchor location at +4.5 at a depth -25.0 m. This displacement and bending moment is found to be less when compared to sections 1, 2, 4, & 5, but higher than the section 3 (T section).

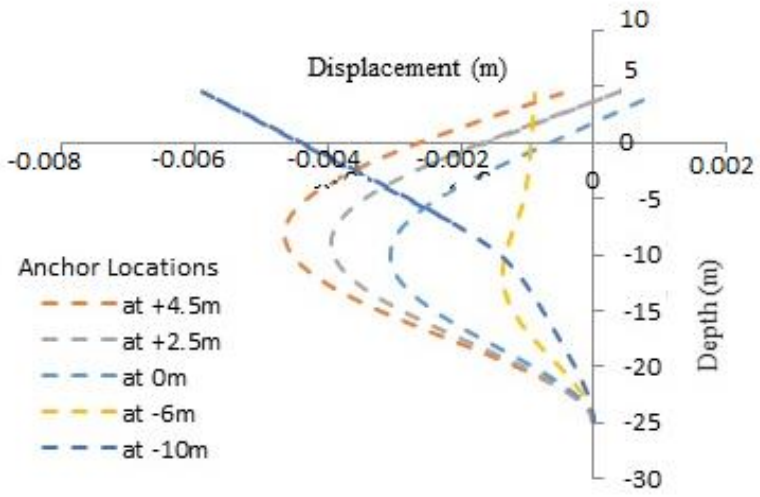

Fig. 6.20 Variation in displacement with depth for section 6

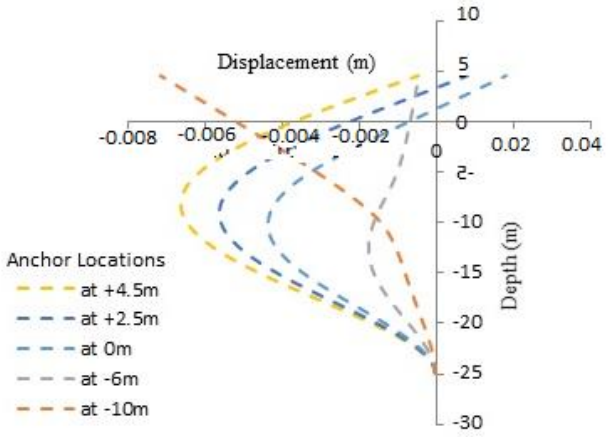

Fig. 6.21 Variation in displacement with depth for section 7

The overall reduction in bending moment for the present results when compared with section 4 & 5 may be the presence of stiff RCC section instead of steel. The performance of sections 6 & 7 are found to be better than section 4 & 5. Among section 6 and 7, section 6 is performing better.

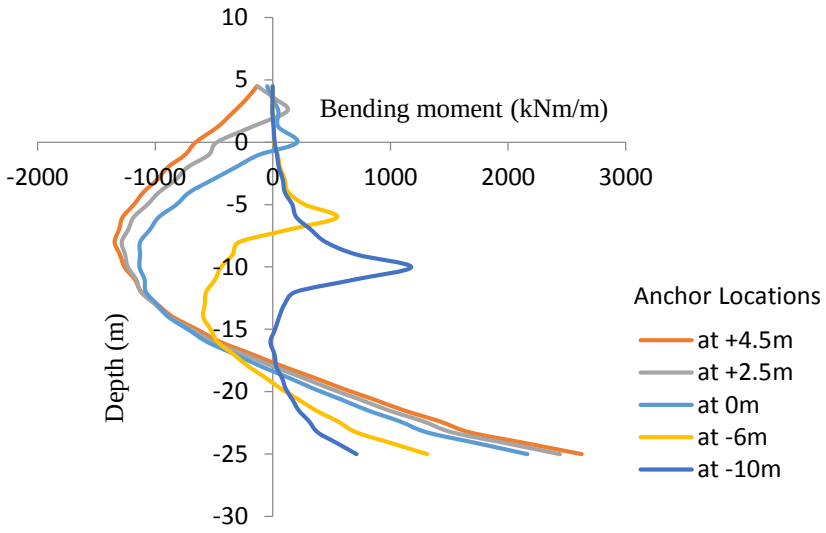

Fig. 6.22 Variation in bending moment with depth for section 6

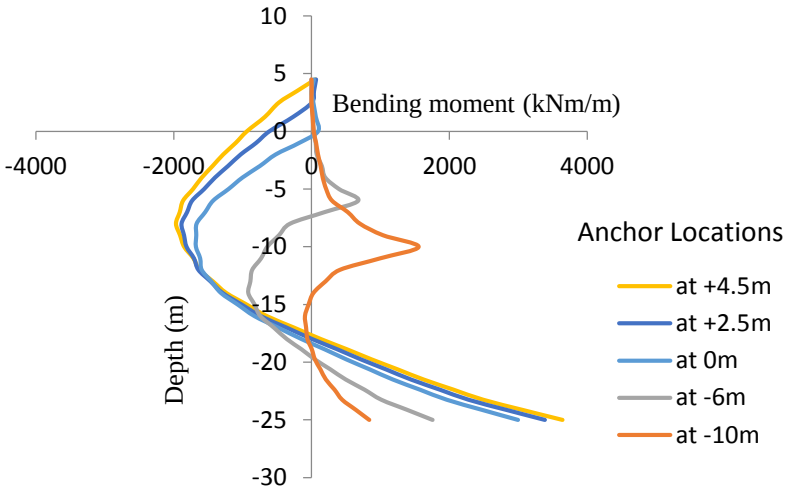

Fig. 6.23 Variation in bending moment with depth for section 7

Variation of maximum value of displacement and bending moment, with anchor location for both sections are shown in Table 6.8 and 6.9. From the study it is found that the anchor at -6m is more effective because both displacement and bending moment are minimum for this location.

Table 6.8 Maximum value of displacement and bending moment of section 6 for different anchor locations

Anchor location (m)	Max. Displacement & its location		Max. Bending moment & its location			
	Displacement (m)	Location (m)	B.M (+ ve) (kNm/m)	Location (m)	B.M (- ve) (kNm/m)	Location (m)
+4.5	-0.00663	-8	2630	-25	1285	-8
+2.5	-0.00393	-10	2440	-25	1220	-8
0.0	-0.00306	-11	2160	-25	1135	-10
-6.0	-0.00236	-14	1310	-25	591	-14
-10.0	-0.00686	+4.5	1190	-10	78	-17

Table 6.9 Maximum displacement and maximum bending moment of section 7 for different anchor locations

Anchor location (m)	Max. Displacement & its location		Max. Bending moment & its location			
	Displacement	Location	B.M (+ ve) (kNm/m)	Location (m)	B.M (- ve) (kNm/m)	Location (m)
+4.5	-0.00692	-7.5	3640	-25	1890	-8
+2.5	-0.00561	-10	3390	-25	1885	-8
0.0	-0.00433	-12	3000	-25	1676	-10
-6.0	-0.00274	-15	1760	-25	916	-14
-10	-0.00756	+4.5	1570	-10	87	-18

From the analysis of actual section, it is found that the maximum displacement of the diaphragm wall depends on the location of anchor. When the anchor is placed at + 4.5 m, the maximum displacement of the wall of 0.0057 m are obtained at -8 m. The maximum positive and negative bending moment (+9560 kNm/m & -5565 kNm/m) is obtained for the anchor location +4.5 m, at -25 m & -8 m respectively. When the stiffness of the actual section reduced by 83.77% (from 17.533 x10^6 kN-m^2 to 2.846 x 10^6 kN-m^2), the displacement increased by

70% (from 0.0057 m to 0.097 m) and bending moment is reduced by 47% (from 9750 kNm/m to 5120 kNm/m) for anchor location +4.5. From this study it is found that stiffness variation causes considerable impact on the performance of the wall. In order to analyses the behavior of varying cross-section, section 2 is designed by sandwiching 1.1 m thick panel between 0.6 m panels. The maximum bending moment at middle 1.1 m thick section 2, is 12730 kNm, (Table 6.4) which is more than that of actual section, 9560 kNm (Table 6.2), even though same thickness and same loading condition exist. The bending moment at 0.6 m thick panel of section 2, (4130 kNm/m, Table 6.4) is reduced with respect to section 1, (5120 kNm/m, Table 6.2) because a part of that transferred to adjacent thicker section thereby producing higher bending moment in section 2. The study on the effect of wall stiffness by Potts & Fourie (1986) shows, stiffer the wall, larger is the bending moment. From the present investigation it is clear that, when stiffness varies within the section there will be some rearrangement of bending moment compared with actual section having uniform stiffness. The varying stiffness of the section causes soil arching and leads to three dimensional stresses and it effects the variation in displacement and bending moment on the wall.

6.4.7 Effect of stiffness on the displacement and bending moment of diaphragm wall

Table 6.10 shows the maximum displacement and bending moment obtained by varying stiffness of the diaphragm wall. Fig 6.24 shows variation of maximum displacement with varying stiffness of sections. From the figure, it is observed that as the stiffness increases the displacement decreases. When the anchor is located at -6 m and -10 m, the stiffness vs. displacement follows logarithmic curve with correlation coefficients R^2 = 0.973 & 0.938 respectively. For the anchor locations at +4.5 m, +2.5 m and 0.0 m, the best trend is power with correlation coefficient R^2 = 0.91, 0.91 and 0.88 respectively. The variations in the curve fitting may be due to the change in trend of displacement as well as bending moment of the wall. Fig. 6.25 shows the variation of bending moment with respect to varying stiffness of the sections. The trend line shows that the bending moment increase with increase in stiffness. Stiffness vs. bending moment follows polynomial curve with correlation coefficients R^2 = 0.979, 0.88, 0.835, 0.88 and 0.82 for the anchor locations +4.5 m, +2.5 m, 0.0 m, -6.0m and -10 m respectively.

Table 6.10 Maximum displacement and maximum bending moment for diaphragm wall of different stiffness (Plaxis 3D)

Sections	Stiffness (EI) kN-m^2	Max. Displacement & its location		Max. B.M (+ve) & its location		Max. B.M (-ve) & its location	
		Displacement (m)	Location (m)	B.M (kNm/m)	Location (m)	B.M kNm/m)	Location (m)
Actual Section	17.533×10^6	-0.0057	-8	9560	-25	5565	-8
Section-1	2.846×10^6	-0.0097	-9	5120	-25	2935	-9
Section-2	5.78×10^6	-0.0076	-7	12730	-25	6880	-9
Section-3	20.52×10^6	-0.0043	-9	1660	-25	733	-8
Section-4	3.977×10^6	-0.011	-9.5	6160	-25	3246	-10
Section-5	3.074×10^6	-0.0114	-9	6250	-25	3406	-9
Section-6	4.569×10^6	-0.005	-8	2630	-25	1345	-8
Section-7	3.626×10^6	-0.0066	-7.5	3640	-25	1967	-8

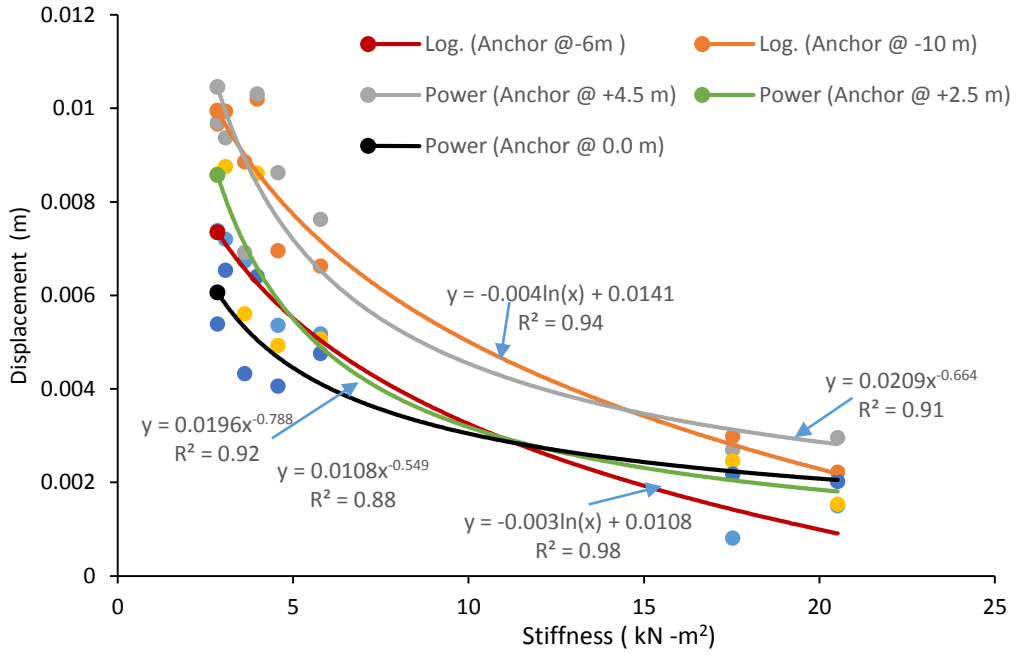

Fig. 6.24 Variation in displacement with varying stiffness of the section

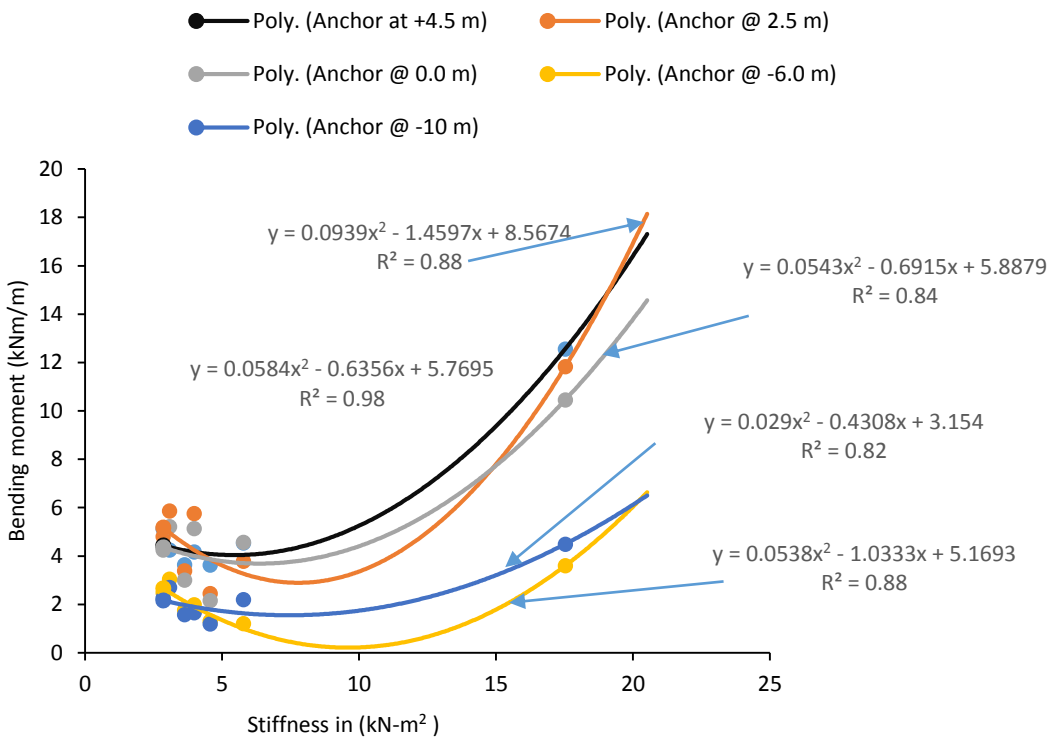

Fig. 6.25 Variation in Maximum bending moment with varying stiffness of section

6.5 SUMMARY

To study the effect of stiffness on the behavior of diaphragm wall, static analysis on non-uniform sections are considered. Seven different diaphragm wall sections having non uniform configurations are modelled and the results are compared with the actual section. The maximum displacement and bending moment of the wall for varying anchor locations are plotted with depth. Analysis is carried out to find the effect of stiffness on displacement and bending moment by choosing best curve fitting by plotting the various stiffness vs. displacement and bending moment. Analysis shows, the T section performed well compared with other sections considered for the present study.

Based on the present study, the following conclusions are drawn:

- ✓ Stiffness variation causes considerable impact on the performance of the wall.

- ✓ When the stiffness of wall is reduced, the displacement increases and bending moment decreases.
- ✓ Stiffness of section 1 (2.846×10^6 kN-m^2) is 83.77% less than that of the stiffness actual section (17.533×10^6 kN-m^2), even though the displacement for section 1 has been increased by 70.2% (from 0.0057 m to 0.0097 m), there is considerable reduction in bending moment of 46.44% (from 9560 kNm/m to 5120 kNm/m) when compared with the actual section. Maximum displacement and bending moment are found corresponding to anchor location +4.5 m. Both displacement and bending moment are found to be minimum at anchor location -6 m.
- ✓ The young's modulus of actual section and section 2 is the same. Variation of displacement and bending moment with depth follows similar trend for both actual section and section 2. But, the magnitude of bending moment is increased at 1.1thick middle section and reduced at 0.6 m thick panel of section 2. This shows there is some percentage of moment transfer from thinner to thicker section.
- ✓ While comparing the maximum bending moment of section 1 and section 2, it is found that bending moment acting at 0.6m thick panel is reduced by19.4% (from 5120kNm to 4130 kNm) when compared with section1.
- ✓ The analysis of section 4 & 5 shows that rigid concrete panel is susceptible to higher bending moment when flexible pile is introduced in between rigid RCC wall. When the two sections of different stiffness coupled to form a single section (in the case sections 2, 4, 5, 6 & 7), the stiffer member is taking higher bending moment. The magnitude of this bending moment depends on the stiffness of the thinner member.
- ✓ The displacement of the T section is reduced by 47.9%, 43.5% & 38.4% for anchor location +4.5m, +2.5m and 0 m respectively when compared to actual section. Similarly, the bending moment for T section is also reduced by 82.6%, 80.14% & 81.6% respectively, for the same anchor locations when compared with the actual section.
- ✓ In all the sections studied when anchor is placed at -6.0 m both bending moment and deflection are found to be minimum.
- ✓ When the anchor is located at -6 m and -10 m, the stiffness vs. displacement follows logarithmic curve with a correlation coefficients $R^2 = 0.97$ & 0.94 respectively. For the

anchor locations at +4.5 m, +2.5 m and 0.0 m, the best trend is power curve with correlation coefficient R^2 = 0.91, 0.91 and 0.88 respectively.

- ✓ Stiffness vs. bending moment follows polynomial curve with correlation coefficients R^2 = 0.98, 0.88, 0.84, 0.88 and 0.82 for the anchor locations +4.5 m, +2.5 m, 0.0 m, -6.0m and -10 m respectively.

CHAPTER 7

VALIDATION OF THE RESULTS OF THE PRESENT INVESTIGATION

7.1 GENERAL

In the present investigation, static and dynamic analysis are performed to assess the behavior of a diaphragm wall using Plaxis software. In 2D, static and dynamic analysis are carried out to arrive maximum displacement, shear force and bending moment of a diaphragm wall with and without anchor and the dredging effects on wall. Similarly, in Plaxis 3D, static analysis for diaphragm wall with and without anchor, construction sequence analysis, and effect of stiffness analysis by varying the stiffness of the wall sections are carried out.

7.2 VALIDATION

Validation is the process of checking whether the analysis results meets the results with analytical or numerical or experimental solutions at desired level which will be realistic in practice. Different methods of validation in general:

1. Experimental studies
2. Empirical studies
3. Case studies having analytical and numerical results
4. Case studies having filed measured data

Experimental studies are the designed methodical procedure employed for testing the physical models. The experimental studies may be the most scientific and use-full method of supporting a hypothesis or theory or any field problems (Jiali et al, 2014). In soil structure interaction problems, conducting experimental studies is relatively complicated because, SSI problems are quite complicated in nature and in some case acquiring actual field data is very difficult. In empirical studies, some empirical models are generated based on some theories or set of principles for a system based on the data collected from observations or from experience. Empirical studies can help researchers to develop a deeper or more generalized understanding of a system (Flood and Issa 2010). For complex problems the

increase in input variables makes the empirical studies quite difficult. Numerical methods based on Finite Element Method can solve complex problems with the help of software. Similarly, analytical methods involve step by step procedures to solve simple problems. The field measurement recorded on construction stages shows real behavior of the element at loading stages. Such case studies are useful to validate the analysis results.

In the present investigation validation of analysis results are carried by comparing the results obtained by empirical models, case studies having analytical and numerical results and field measured data of similar case studies.

7.2.1 Empirical Model for Wall Deflection

Clough & Rourke (1990) proposed a semi-empirical procedure for estimating wall movement at excavations in which the maximum lateral wall movement δ_{hm} is evaluated relative to factor of safety (FS) and system stiffness which is defined as follows.

System stiffness (η) = $EI/\gamma_w h^4$

Where EI is the flexural rigidity per unit width of the retaining wall, γ_w the unit weight of water and h is the average support spacing. The factor of safety (FS) is defined according to Terzaghi (1943) which is presented in Table 7.1. The system stiffness is defined as a function of the wall flexural stiffness, average vertical separation of supports, and unit weight of water, which is used as a normalizing parameter. Fig. 7.1 shows δ_{hm} plotted relative to system stiffness for various FS. From the literature, it is found that, the method is widely used for the preliminary estimation of wall movement.

Table 7.1 Some Classical Factors of Safety for Geotechnical Practice (Data from Terzaghi and Peck 1948).

Retaining Structures	F.S = 1.5 (against sliding) F.S = 1.5 (base heave) F.S = 2.0 (strut buckling)

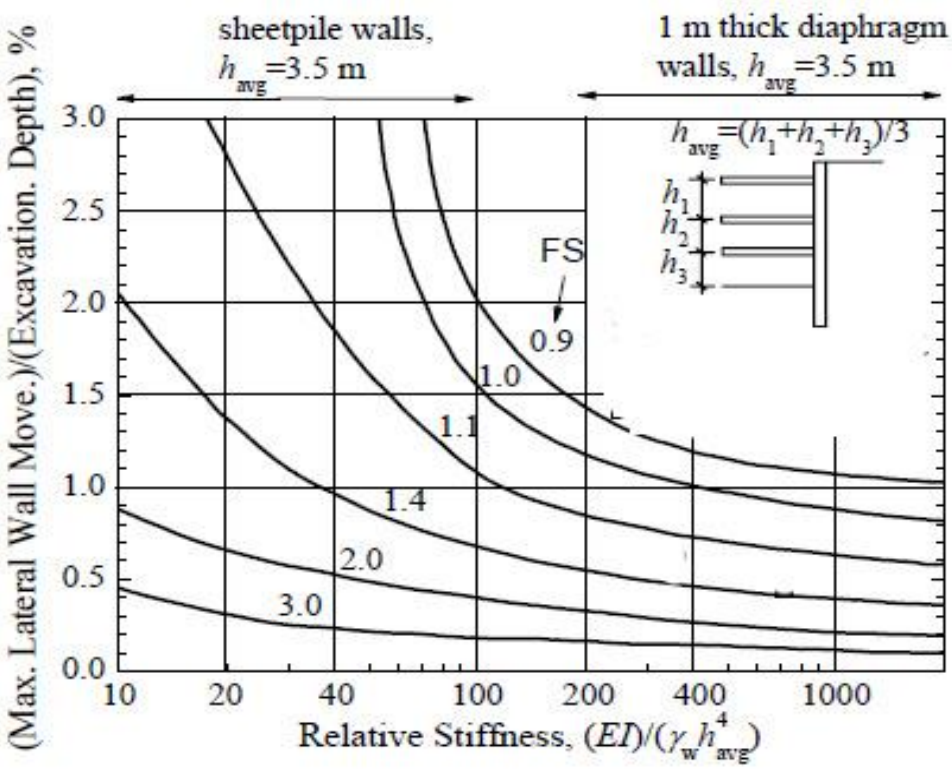

Fig. 7.1 Design chart for estimating maximum lateral wall movement in soft to medium clays (Clough and O'Rourke 1990).

He = Excavation depth = 14.5m, γ_w = 9.807 (kN/m^3)

Sample calculation for ∂h according Clough & Rourke (1990) proposed semi-empirical procedure. Fig. 7.2 and 7.3 shows the diaphragm wall with +4.5 m and +2.5 m anchor location, which are considered for the displacement calculation.

For the case 1.1 m thick wall, anchor at +4.5 m.

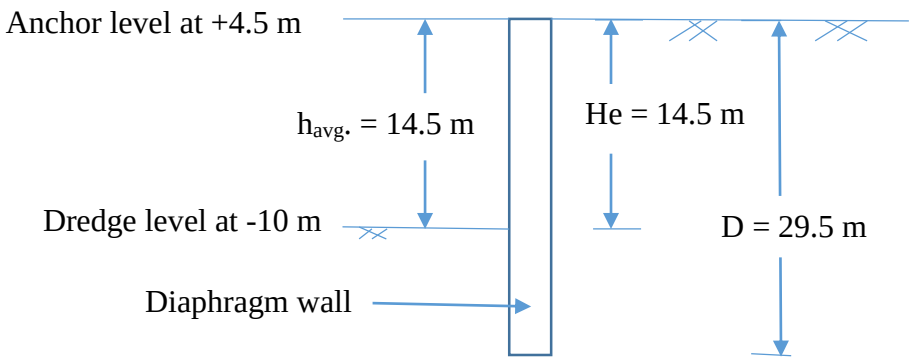

Fig. 7.2 Diaphragm wall with anchor at +4.5 m

Based on the Fig. 7.5, the $h_{avg.} = (h_1 + h_2 + h_3)/3$

Where, h_1 = the spacing between first strut from the top to the second strut.

h_2 = the spacing between second strut from the top to the third strut.

h_3 = the spacing between third strut from the top to the dredge level.

For the present study single anchor is provided in each cases and only anchor location is varied.

Factor of safety (F.S) = 2

For the case, anchor at +4.5 m, $h_{avg.} = 14.5$ m

Young's modulus, $E = 31.6 \times 10^6$ kN/m^2

Moment of Inertia, $I = 0.5545$ m^4 (Table 6.1)

$$EI/\gamma_w h^4 = (31.x10^6 \times 0.5545)/ (9.8 \times 14.5^4) = 33.52$$

From Fig. 7.5, $(\frac{\delta h}{He})$ % = 0.56

$$\delta h = 0.56 \times 14.5/100 = \underline{0.0812 \text{ m}}$$

For the case 1.1 m thick wall anchor at +2.5 m

The anchor at +2.5 m, $h_{avg.} = 12.5$ m (Fig. 7.7)

Young's modulus, $E = 31.6 \times 10^6$ kN/m^2

Moment of Inertia, $I = 0.5545$ m^4 (Table 6.1)

$EI/\gamma_w h^4 = (31.6 \times 10^6 \times 0.5545)/ (9.8 \times 12.5^4) = 73.21$

From Fig. 7.5, $(\frac{\delta h}{He})$ % = <u>0.44</u>

$$\delta h = 0.44 \times 14.5/100 = \underline{0.0638 \text{ m}}$$

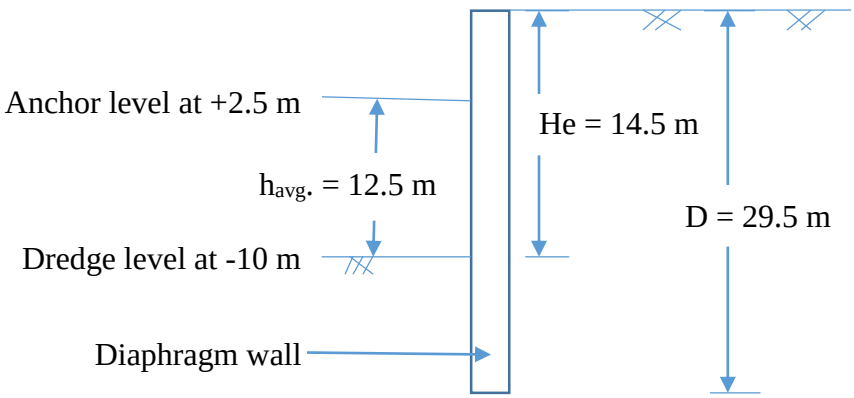

Fig. 7.3 Diaphragm wall with anchor at +2.5 m

Table 7.2 Maximum displacement (δ_h) for various wall sections obtained by design chart (Clough and Rourke, 1990), Plaxis 2D and 3D

t (m).	Anchor location (m)	h_{avg}. (m)	E (kN/ m^2)	I (m^4)	EI	$\frac{EI}{\gamma_w}$(1 /h^4)	$\frac{\partial h}{He}$ %	∂h (m)	Plaxis-2D		Plaxis-3D	
									∂h	$\frac{\partial h}{He}$ %	∂h	$\frac{\partial h}{He}$ %
1.10	+4.5	14.5	31.6 x10^6	0.5545	17.53 x10^6	33.5	0.56	0.0812	0.00599	0.041	0.0057	0.0397
1.10	+2.5	12.5	31.6 x10^6	0.5545	17.53 x10^6	73.21	0.44	0.0638	0.00492	0.0337	0.00446	0.0303
1.10	0.0	10	31.6 x10^6	0.5545	17.53 x10^6	178.75	0.4	0.058	0.00362	0.0248	0.00328	0.022
1.10	-6.0	6	31.6 x10^6	0.5545	17.53 x10^6	1380	0.2	0.029	0.00113	0.00758	0.001	0.0068
0.6	+4.5	14.5	31.6 x10^6	0.182	5.78 x10^6	13.34	0.64	0.092	-	-	0.0097	0.069
0.6	+2.5	12.5	31.6 x10^6	0.182	5.78 x10^6	24.08	0.55	0.079	-	-	0.0086	0.0593
0.6	0.0	10	31.6 x10^6	0.182	5.78x 10^6	58.97	0.42	0.0609	-	-	0.00639	0.0092
0.6	-6.0	6	31.6 x10^6	0.182	5.78x 10^6	455	0.32	0.042	-	-	0.0039	0.00565

Similarly, calculation are carried out for the anchor locations 0.0 m and -6.0 m for the diaphragm wall having thickness 1.1 m and 0.6 m and results are shown in Table 7.2.

Table 7.2 shows the lateral deflection estimated for the diaphragm wall based on design chart (Clough and Rourke, 1990) considering factor of safety 2 (as shown in Table 7.1) and the Plaxis 2-D and 3-D results. According to Clough and Rourke semi empirical procedure for estimating lateral deflection, the ratio δ_h / He varies 0.56% – 0.2% for 1.1 m thick diaphragm wall and 0.64% – 0.32% for 0.6m thick diaphragm wall which are considered for the present study. But Plaxis 2D & 3D analysis results for 1.1 thick diaphragm wall ranges between 0.041% – 0.0075% and 0.039% - 0.0068% respectively. The ratio $\delta h / He$ for 0.6 m thick wall, Plaxis 3D results 0.069 -0.013% for different anchor locations. It shows that present analysis results are within the values suggested by Clough and Rourke. Hence the study is satisfactory.

7.2.2 Case studies having analytical and numerical results

Michael Long (2001) conducted study in lateral displacement of retaining wall based on 296 individual case histories. The soil profile comprise predominantly stiff to medium soil,

sandy to gravel, stiff clay, medium to coarse sand and residual soil. The objective of the study is to arrive some relation between the lateral displacements (δ_{hm}) with respect to excavation height. The study concluded that the normalized maximum lateral displacement values, δ_{hm} are in between 0.05 to 0.5%H. According to Long value the maximum displacement of the diaphragm wall considered for the present study, for an excavation height, H (equal to 14.5 m) lies in between 0.00725 m to 0.0725 m. The maximum displacement obtained in the present study in Plaxis 2D analysis ranges from 0.00599 m to 0.0702 m and Plxis 3D results ranges from 0.0057 m to 0.0692 m. The present investigation values are very near and within the values obtained based on Long's method. Hence the study in Plaxis 2D and 3D are satisfactory.

Moormann (2004) had carried out extensive empirical studies by taking 530 case histories of retaining wall and ground movement due to excavation in soft soil (cu<75kpa). The study concluded that the maximum horizontal wall displacement (δ_{hm}) lies between 0.5% H and 1.0 % H, on average at 0.87%. In the present study the depth of excavation H is 14.5 m and undisturbed strength of soil Cu varies 30-120 Kpa. According to Moormann the δ_{hm} can vary from 0.072 to 0.145 m. But present study results for staged excavation with anchor varies from 0.01 to 0.063m and without anchor support 0.073m. Hence present study shows that the wall displacement is comparatively less than the Moormann method. It may be due to the variations in shear strength of soil.

7.2.3 Field Performance Studies of Diaphragm wall

For better understanding of the actual displacement of the diaphragm wall, a database of 19 international well-documented case histories are collected, each of which has been published in geotechnical journals, international conference proceedings, national technical reports, or dissertations. The main focus of these cases are on the deformation of walls supporting deep excavations in medium to fine sand and soft to firm clays. For each case history, relevant information was extracted and tabulated as Table 7.3.

Field measured displacement values of diaphragm wall for varying thickness, (0.6m, 1.0m and 1.1m) are collected from the case studies and plotted against the depth of excavation as shown in Fig. 7.4, 7.5 & 7.6. The trend line for the case of 0.6 m thick diaphragm wall, follows logarithmic curve fitting with a correlation coefficient R2 = 0.83. From the graph

Table 7.3 Field measured displacements of diaphragm wall for various case studies.

Sl no	Reference	Support type	Thickness of wall (m)	Soil details	H(m)	δ_{hm}(m)
1	Cunningh and Fernandez (1972)	Without anchor	0.6	Soft to stiff clay	7	0.008
2	Tait and Taylor (1975)	Anchor	0.6	Soft to stiff clay	14	0.013
3	Cunningh and Fernandez (1972)	Tieback anchor	0.6	Soft to stiff clay	9.8	0.011
4	Burland and St.john(1974)	Without anchor	0.6	Very stiff to hard clay	7.9	0.01
5	Garvin,R.& Boward (1992	Tieback anchor	0.6	Sand and gravel	8.2	0.008
6	Hsieh, et al (2011)	T-shaped wall with bracings	0.6	Sandy soil	9.6	0.009
7	Richard, N. et al (2007)	Struts	0.6	Silty sand ,silty clay/gravel	12.0	0.01
8	Cole and Burland (1972)	Rackers	1.0	Very stiff to hard clay	18.4	0.019
9	Armento (1973)	Bracing-prestressed	1.0	Soft to stiff clay	21.4	0.022
10	Teoh Yaw Poh.et al (2001)	Anchor	1.0	stiff to very stiff sandy silt	23.7	0.0217
11	Xu1,Z.H.et al (2005)	multi-propped	1.0	sandy silt, very soft clay,	16.2	0.0187
12	Teparaksa, W.(2012)	Bracings	1.0	Soft to hard clay, silty sand, silty	15.5	0.0154
13	YongTan,.and Dalong Wang (2014)	Unpro-pped circular wall	1.0	Firm silty clay to very dense silty fine sand	16.3	0.02
14	Gang Zheng,et al (2014)	No support	1.0	Silty clay, Clayey silts, Sandy silts,	12.0	0.010
15	Thomand Harlan(1973)	Bracings	1.1	Soft to hard clay	23.8	0.03
16	Hata,S.et al (1985	anchors	1.1	Soft to stiff clay	27.9	0.09
17	Schenwolf,.et al (992)	Tieback anchors	1.1	Soft to stiff clay	24.4	0.051
18	Hsieh, et al (2013	Tieback anchors	1.1	Silty clay and sand with gravel	23.6	0.18
19	Muthukkumaran, etal (2004)	Without anchor	1.1	stiff clay to hard marine silt	9.5	0.0173

H = the excavation depth, δ_{hm} = maximum horizontal displacement

It is clear that the maximum displacement value obtained in the Plaxis 3-D analysis for the present study is close to the trend line. Hence it is valid with the present study.

In the case of 1.0 m thick diaphragm wall the correlation coefficient is R^2 = 0.97 for polynomial curve fitting for order 2 (refer Fig. 7.5). From the graph it is clear that the maximum displacement value obtained in the Plaxis 3-D analysis is very close to the trend line, hence it is valid with the present study.

.

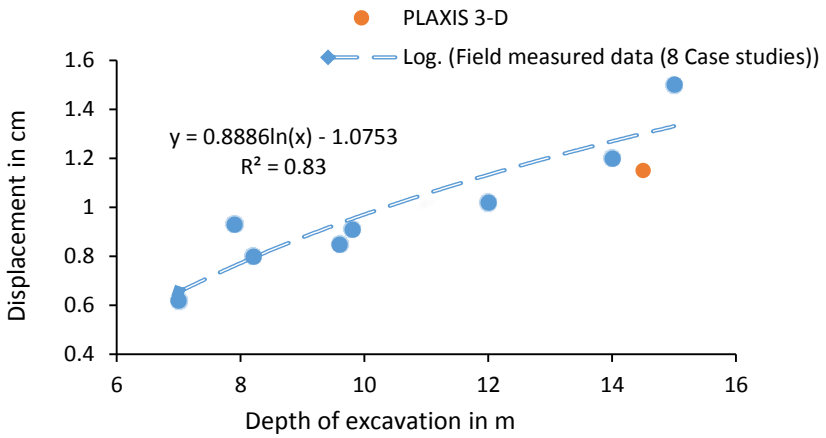

Fig. 7.4 Variation in displacement with depth of excavation for 0.6 m thick diaphragm wall

Fig. 7.6 gives the variation of diaphragm wall with depth of excavation for 1.1 m thick diaphragm wall. The trend line follows linear fitting with a correlation coefficient R^2 = 0.99. Displacement value obtained in the Plaxis 3-D analysis is very close to the trend line.

From these analysis, it is clear that the result of the present investigation matches fairly well with the results from literature. Hence the present study results are validated.

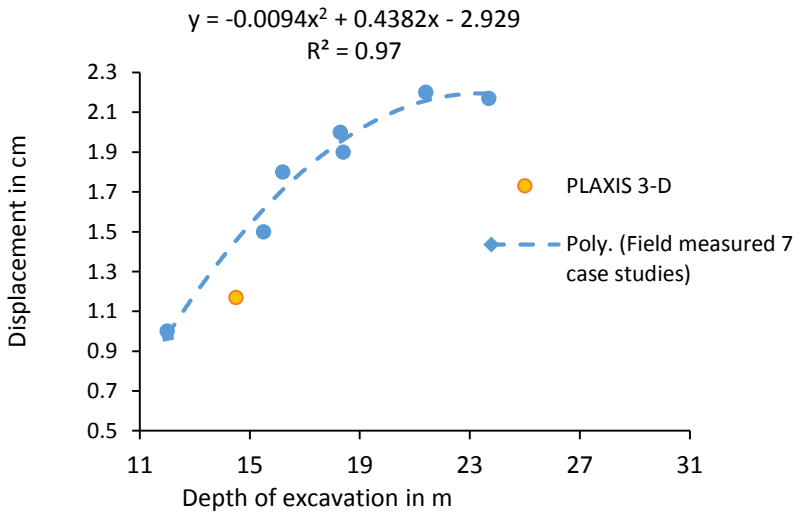

Fig. 7.5 Variation in displacement with depth of excavation for 1.0 m thick diaphragm wall

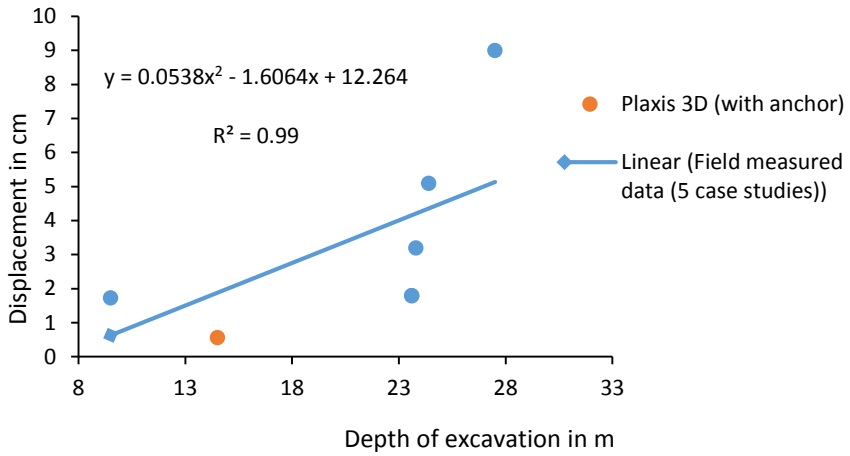

Fig 7.6 Variation in displacement with depth of excavation for 1.1 m thick diaphragm wall

7.2.4 Comparison of displacement with full scale field test of a diaphragm wall.

7.2.4.1 Case study 1 – Full scale field test conducted on berthing structure to measure the actual displacement using Inclinometer at JNPT, Mumbai.

Deflection values obtained from Plaxis for actual section are compared with the results obtained from a full scale field test conducted by Muthukumaran et.al (2004). In both cases diaphragm wall without anchors are studied. In the field test the inclinometer tubes were installed in one of the diaphragm wall panels at Jwahar lala Nehru Port Trust (JNPT), Mumbai and measurements were recorded. The thickness of the diaphragm walls are same, but the dredge levels are different. The soil layer details are tabulated in Table 7.4 for the field tested diaphragm wall 1 and in Table 3.3 of chapter 3, for diaphragm wall 2, which is considered for the present Plaxis analysis and there are variations in soil layers in these two cases. Fig. 7.7 shows the comparison of deflections of diaphragm Wall 1 & 2. From the graph it is found that, from -20 m to -25 m the measured value of deflection is in good agreement with the present Plaxis result. The trend of the graph for both cases are matching, but the deviation starts from -18 m and continues up to +4.5 m. The maximum deflections for diaphragm wall 1 & 2 are 17 mm and 69 mm at +4.5 m level respectively. The variation with the deflection values may be due: i) the dredge level of diaphragm wall 1 varies from +7.025 m to +.05 m as shown in Fig. 7.8. But the dredge level varies from +4.5 m to -10 m for the diaphragm wall 2 as shown in Fig. 3.23 (chapter 3). ii) The embedded depth of diaphragm wall 1 is +0.05 m to -25.0 m and for wall 2 is -10 m to -25m.The depth of

penetration of wall 1 is 25.05 m and wall 2 is 15 m. iii) Black to bluish clay is found from a level of -6 m to -10m and -12 m to -18 m for wall 2. But for wall 1, it is hard marine silt. Since there is 10 m soft clay for wall 2, the resistance to deflection is less. In addition, the wall 1 is socketed to the hard basalt rock giving more support and the depth of penetration of wall 1 is 1.67 times more than wall 2. Hence wall 1 is deflected less compared with wall 2 as shown in Fig. 7.7.

Table 7.4 Different soil layers at inclinometer test location for the diaphragm wall 1

Moorum fill	+7.1 m to -2.0 m
Soft marine clay	-2 m to – 6 m
Medium stiff clay	-6 m to -8 m
Very stiff clay	-8 m to -15 m
Hard marine silty clay	-15 m to -18 m
Basalt rock	-18 m and below

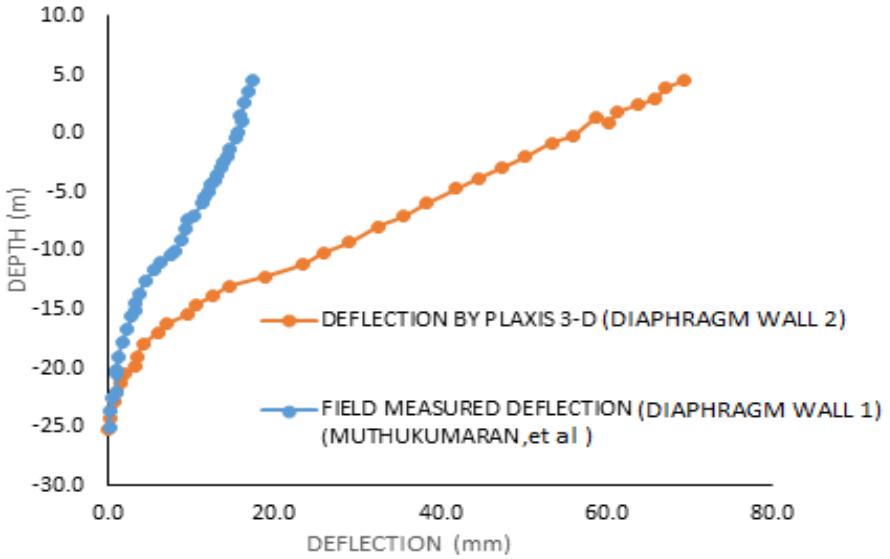

Fig. 7.7 Comparison of Measured Deflection with FEM Result for Diaphragm Wall

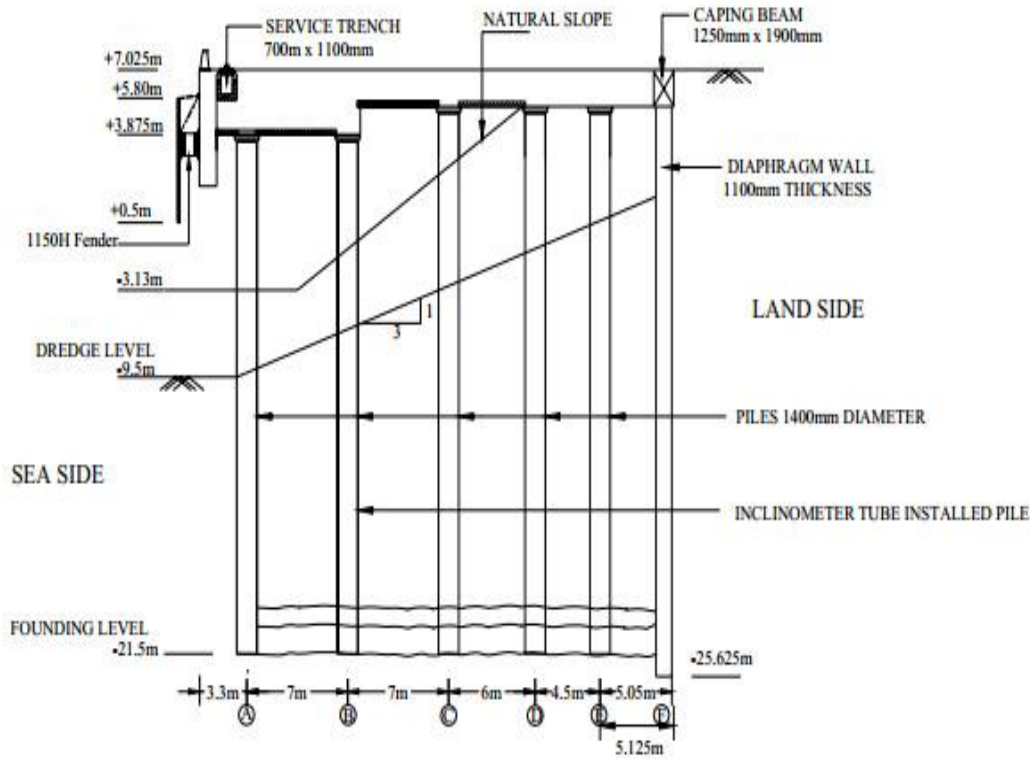

Fig. 7.8 Cross-section of berthing structure with diaphragm wall 1 at JNPT, Mumbai

7.2.4.2 Case study 2 – Full scale field test conducted on diaphragm wall to measure the actual displacement using inclinometer in construction stages at Shanghai, China.

Deflection values obtained from Plaxis for actual section are compared with the results obtained from a full scale field test conducted by Tang and Zhao (2015). In both cases displacement behavior on construction stage are studied. In the field test the inclinometer tubes were installed in the diaphragm wall of the basement floor of the Super -Tall building, Shanghai, Chaina and measurements are recorded. Top-Down construction method was adopted for construction of the building with diaphragm wall. The thickness of the diaphragm walls are the same, but the dredge levels are different. The soil layer details are tabulated in Table 7.5 for the field tested diaphragm wall 3 and Table 3.3 of chapter 3 for diaphragm wall 2, which is considered for the present study. Variations in soil layers are observed by comparing the both cases. The field measured deflection values of diaphragm wall 3, for the excavation stages from +4.5 m to -1.0 m and -1.0 m to -6.3 m are compared with the Plaxis analysis values of the diaphragm wall 2 for the excavation phases from +4.5

m to +2.5 m (phases 3), +2.5 m to 0.0 m (phase 5) and 0.0 m to -6.0 m (phase 6). Fig. 7.9 shows the comparison of deflections of diaphragm wall 2 & 3. Comparing the field measured displacement values for the excavation up to -1.0 m and the Plaxis values for the phase 3 and phase 5, the displacement variation shows similar trend, but diaphragm wall 3 shows higher displacement. The variation may be due to the difference in excavation depth (field measured excavation depth is up to -1.0 m and for Plaxis up to 0.0 m) and soil strata variation. The comparison between the displacements for the phase 6 of diaphragm wall 2 and field measured values for excavation up to - 6.3 m for diaphragm wall 3 shows similar trend up to -5.0 m and below this levels it varies. The maximum displacement obtained for diaphragm wall 2 is 53 mm and for diaphragm wall 3 is 43 mm. Diaphragm wall 2, considered for the present study shows higher displacement. It may be due to the following; 1) the depth of diaphragm wall 2 varies from +4.5 m to -25 m and whereas for diaphragm wall 3 is +4.5 m to -39 m. The depth of penetration of wall 3 is 1.73 times higher than the diaphragm wall 2, with respect to the embedded depth at -6.0 m level. 2) In Top-Down construction method the diaphragm wall and the piles are erected for full depth first and after that the basement floor is casted

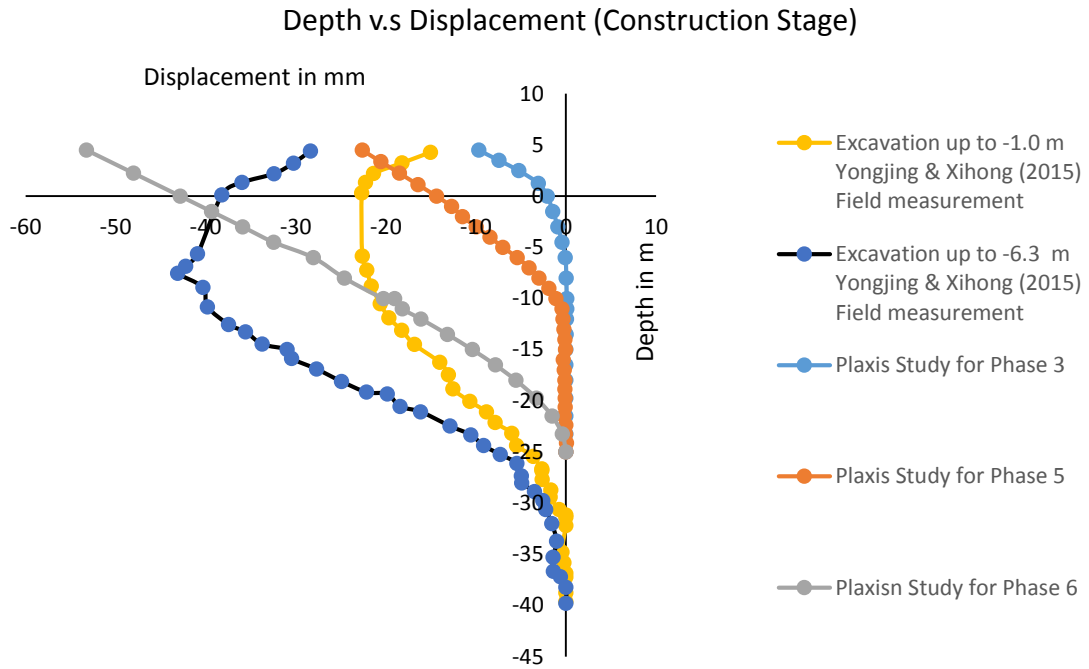

Fig. 7.9 Comparison of measured displacement for diaphragm wall 3 with Plaxis result for diaphragm wall 2.

Then the excavation starts through the opening below floor slab for the required depth. The floor gives some partial fixity to the diaphragm wall, hence the displacement is reduced in wall 3. Hence the diaphragm wall 3 show variation in displacement from -5.0 m to +4.5 m.

Table 7.5 Different soil layers at inclinometer test location for the diaphragm wall 3

Silty clay	+4.5 m to +2.2 m
Very soft silt clay	+2.2 m to –5 m
Very soft clay	-5 m to -14 m
Silty clay	-14 m to -24 m
Stiff sand and silt	-24 m to -44 m

7.3 SUMMARY

Validation of analysis results are carried out by comparing the results obtained by empirical models, case studies having analytical and numerical results and field measured data of similar case studies. The limiting displacement values obtained using the Empirical model developed by Clough & Rourke (1990) are compared with values obtained in the present study. Also the limiting displacement values suggested by Michael Long (2001) and Moormann (2004) are compared with the Plaxis 2D and 3D analysis results of present investigation. Two field measured case studies are compared with the results of present investigation.

Based on the present study, the following conclusions are drawn:

- ✓ According to Clough & Rourke (1990) semi empirical procedure for estimating lateral displacement, the ratio varies from 0.56% to 0.2% for 1.1 m thick diaphragm wall and from 0.64% to 0.32% for 0.6 m thick diaphragm wall which

are considered for the present study. But Plaxis 2D & 3D analysis gives the value for 1.1 thick diaphragm wall in the range of 0.041% to 0.0075% and 0.039% to 0.0068% respectively. The ratio for 0.6 m thick wall obtained from Plaxis 3D analysis is 0.069% to 0.013%. It shows that present analysis results are within the values suggested by Clough and Rourke. Hence the study is satisfactory.

- ✓ According to Long (2001), the maximum displacement of the diaphragm wall (0.05% to 0.5% H), which is considered for the present study for an excavation height, H equal to 14.5 m are in between 0.00725 m and 0.0725 m. The maximum displacement obtained in the present study in Plaxis 2D analysis ranges from 0.00599 m to 0.0702 m and in Plxis 3D analysis ranges from 0.0057 m to 0.0692 m. The present investigation values are within the values obtained based on Long method. Hence the study in Plaxis 2D and 3D are satisfactory.
- ✓ From the case studies, field measured displacement values plotted against the corresponding depth for 0.6 m thick diaphragm wall follows logarithmic curve with a correlation coefficient $R^2 = 0.83$. The maximum displacement value in plaxis 3D obtained for 0.6 m thick wall is close to the trend line of the above plot, hence it is valid.
- ✓ In the case of 1.0 m thick diaphragm wall, the field measured displacement values vs. depth follows polynomial curve with a correlation coefficient $R^2 = 0.97$ and the Plaxis 3D analysis values are close to the trend line. Hence the Plaxis 3D study is satisfactory.
- ✓ In the case of 1.1 m thick diaphragm wall, the field measured displacement values vs. depth follows linear fit with a correlation coefficient $R^2 = 0.99$ and the Plaxis 3D analysis values are close to the trend line. Hence the present study results are valid.
- ✓ In the case of diaphragm wall without anchors, full scale field test values (Muthukumaran et al, 2004) are satisfactorily matching up to the location of -20m and varies for greater depth. The variation may be due to the presence of different soil layers and the wall penetration depth.

- ✓ Comparison between the construction stage analysis results of diaphragm wall and full scale field test values by Tang and Zhao (2015) are satisfactorily matching and shows similar trends. The variation may be due to the variations in soil layers and the wall penetration depth. Hence the present study conducted by Plaxis 2D & 3D are satisfactory.

CHAPTER 8

SUMMARY & CONCLUSIONS

8.1 SUMMARY

The study of soil structure interaction is essential to investigate the behavior of diaphragm wall under static and dynamic loading conditions. The study of anchored wall shows the importance of anchor and its locations to reduce the displacement, shear force and bending moment when the wall is subjected to static and dynamic loads. The study helps to design an economical wall section, to understand the wall installation effects and its safer erection. The analysis in varying stiffness of wall highlights, the stiffness effects on the wall in terms of variation of displacements, bending moments and redistribution of moments.

The present investigation is focused on the behavior of a diaphragm wall under static and dynamic load conditions using Plaxis software. The soil data and structural element details considered are of the existing deep draft berth of NMPT. In Plaxis 2D, static and dynamic analysis are carried out to obtain the maximum displacement, shear force and bending moment of a diaphragm wall with and without anchor and the dredging effects on the diaphragm wall. Similarly in Plaxis 3D, static analysis is carried out to find the maximum displacement, shear force and bending moment for the diaphragm wall with and without anchor.

To study the effect of stiffness on the behavior of diaphragm wall, static analysis on non-uniform sections are carried out. Both 2D and 3D analysis are under taken. Seven different diaphragm wall sections, section1 and sections 2, 3, 4, 5, 6 & 7 having uniform and non-uniform configurations respectively, are modelled and the results are compared with the actual section. The maximum value of displacement and bending moment of the wall for varying anchor locations are investigated.

The validation of the results are carried by comparing with empirical models using standard charts, case studies and field measured data from case studies. The maximum displacement values in Plaxis 2D and 3D are compared with the values obtained from an empirical model developed by Clough & Rourke (1990), and the values suggested by Michael Long (2001) and Moormann (2004).

8.2 CONCLUSIONS

Based on the present investigation, the following conclusions are drawn.

8.2.1 2D Analysis of Diaphragm wall

- ✓ From the 2D static analysis, it is observed that the maximum displacement is reduced by 17.86% (from 0.00599 m to 0.00492 m), 39.57% (from 0.00599 m to 0.00362 m), 81.13%(from 0.00599 m to 0.00113 m) & 25.87% (from 0.00599 m to 0.00444 m) for the anchor locations +2.5 m, 0.0 m,-6 m & 10 m respectively, with respect to anchor located at +4.5 m in static analysis.
- ✓ The static analysis shows reduction in maximum positive shear forces by 4.09% (from 1720 kN/m to 1650 kN/m), 11.19% (from 1720 kN/m to 1530 kN/m) for the anchor location +2.5 m and 0.0 m respectively, with respect to the maximum shear force corresponding to anchor at +4.5 m. But the maximum negative shear force is increased by 4.3% (from 1160 kN/m to 1210 kN/m) when the anchor is shifted from -6 m to -10 m. The increase in shear force may be due to the anchor located at dredge level (-10 m) and reduction in passive resistance below dredge level.
- ✓ The maximum bending moment is reduced by 8.49% (from 10710 kNm/m to 9800 kNm/m), 21.19% (from 10710 kNm/m to 8440 kNm/m), 60.78% (from 10710 kNm/m to 4200 kNm/m) & 57.42% (from 10710 kNm/m to 4560 kNm/m) for the anchor locations +2.5 m, 0.0 m,-6 m & -10 m respectively, when compared to maximum value of bending moment corresponding to anchor at +4.5 m in static analysis.
- ✓ For anchored diaphragm wall, the maximum value of displacement, shear force and bending moment are reduced by 91.79% (from 0.073 m to 0.00599 m), 11.69% (from 1947.82 kN/m to 1720 kN/m) & 57% (from 24936 kNm/m to 10710 kNm/m) respectively, when compared with the diaphragm wall without anchor in static analysis.
- ✓ The results obtained in the dynamic analysis of anchored wall show that, the maximum value of displacement, shear force and bending moment are increased by 7.2% (from 0.00599 m to 0.0064 m), 10% (from 1720 kN/m to 1950 kN/m) & 13.5%

(from 10710 kNm/m to 11830 kNm/m) with respect to static analysis. Hence the dynamic analysis is essential for anchored wall.

8.2.2 3D Analysis of Diaphragm wall

- ✓ From 3D analysis it is found that the presence of anchor has a significant impact on the stability of diaphragm wall. In the case when no anchor is provided, the maximum displacement of the diaphragm wall is -69.3 mm whereas when an anchor is provided at an elevation of +2.5 m, the maximum displacement of the diaphragm wall is reduced to -4.46 mm which occurs at -10.0 m. The displacement is reduced by about 93.5% by placing the anchor at +2.5 m as in the actual field.
- ✓ The maximum values of displacement, shear force & bending moment obtained in Plaxis 2D are higher by 22.82% (from 0.00092 m to 0.00113 m), 15.43% (from 1490 kN/m to 1720 kN/m) & 17.58% (from 3560 kNm/m to 4200 kNm/m) respectively, when compared with Plaxis 3D results.
- ✓ From the construction stage study in Plaxis 3D, it is observed that the maximum displacement is reduced by 86% (from 0.069 m to 0.0095 m), 85.12% (from 0.069 m to 0.0102 m), 67.35% (from 0.069 m to 0.0226 m) & 23% (from 0.069 m to 0.0533 m) for the anchor locations +4.5 m, +2.5 m, 0.0 m & -6 m respectively, with respect to the maximum displacement corresponding to anchor at -10 m.
- ✓ In Plaxis 3D analysis, the maximum displacement of anchored diaphragm wall without considering the construction stage is reduced by 91.76% (from 0.0692 m to 0.0057 m) and in Plaxis 2D, 91.4% (from 0.0703 m to 0.00599 m) when compared to the maximum displacement obtained by considering the construction stage.
- ✓ The maximum bending moment obtained in Plaxis 3D analysis for anchored diaphragm wall for the case without considering the construction stage is reduced by 59.6% (from 23710 kNm/m to 9560 kNm/m) and in Plaxis 2D, it is reduced by 54.41% (from 23380 kNm/m to 10710 kNm/m) when compared to the maximum bending moment obtained by considering the construction stage.

8.2.3 3D Analysis of diaphragm wall with varying stiffness

Stiffness of section 1 (2.846×10^6 kN-m^2) is 83.77% less than that of actual section (17.533×10^6 kN-m^2). Even though the displacement for section 1 has been increased by 70.2% (from 0.0057 m to 0.0097 m), there is considerable reduction in bending moment of 46.44% (from 9560 kNm/m to 5120 kNm/m) when compared with the actual section.

- ✓ While comparing the maximum bending moment of section1 and section 2, it is found that bending moment acting at 0.6 m panel of section 2 is reduced by 19.4% (from 5120kNm/m to 4130 kNm/m) when compared with section1.
- ✓ The displacement of the T section is reduced by 47.9%, 43.5% & 38.4% for anchor location +4.5 m, +2.5 m and 0 m respectively, when compared to the actual section. Similarly, the bending moment for T section is also reduced by 82.6%, 80.14% & 81.6% respectively, for the same anchor locations.
- ✓ The analysis of section 4 & 5 shows that rigid concrete panel is susceptible to higher bending moment when flexible pile is introduced in between rigid concrete wall. When the two sections of different stiffness are coupled to form a single section (in the case of sections 2, 4, 5, 6 & 7), the stiffer member takes higher bending moment.
- ✓ When the anchor is located at -6 m and -10 m, the stiffness vs. displacement curve follows logarithmic curve with a correlation coefficients R^2 = 0.973 & 0.938 respectively. For the anchor locations at +4.5 m, +2.5 m and 0.0 m, the best trend is power curve with correlation coefficients R^2 = 0.91, 0.91 and 0.88 respectively.
- ✓ Stiffness vs. bending moment follows polynomial curve with correlation coefficients R^2 = 0.979, 0.88, 0.835, 0.88 and 0.82 for the anchor locations 4.5 m, +2.5 m, 0.0 m, -6.0m and -10 m respectively.

8.2.4 Validation of the results of the Plaxis 2D and 3D analysis of diaphragm wall

- ✓ According to Clough & Rourke (1990) semi empirical procedure for estimating lateral displacement, the ratio $\frac{\delta h}{He}$ varies from 0.56% to 0.2% for 1.1 m thick diaphragm wall and from 0.64% to 0.32% for 0.6 m thick diaphragm wall which are considered for the present study. But Plaxis 2D & 3D analysis gives the value of $\frac{\delta h}{He}$ for 1.1

thick diaphragm wall in the range of 0.041% to 0.0075% and 0.039% to 0.0068% respectively. The ratio $\frac{\delta h}{He}$ for 0.6 m thick wall obtained from Plaxis 3D analysis is 0.069% to 0.013%. It shows that present analysis results are within the values suggested by Clough and Rourke. Hence the study is satisfactory.

- ✓ According to Long (2001), the maximum displacement of the diaphragm wall (0.05% to 0.5% H), which is considered for the present study for an excavation height, H (equal to 14.5 m) lies in between 0.00725 m and 0.0725 m. The maximum displacement obtained in the present study in Plaxis 2D analysis ranges from 0.00599 m to 0.0702 m and in Plxis 3D analysis ranges from 0.0057 m to 0.0692 m. The present investigation values are within the values obtained based on Long's method. Hence the study in Plaxis 2D and 3D are satisfactory.
- ✓ According to Moormann (2004) for staged construction displacement values, δh, lies in between 0.5% H and 1.0 % H for a retaining wall. Hence, for the diaphragm wall considered for the present study, the displacement can vary from 0.072 to 0.145 m. But present study displacement results for staged excavation with anchor varies from 0.01 m to 0.063m and without anchor support it is 0.073m. Hence present study shows the wall displacement is comparatively less than the Moormann suggestion. It may be due to the variations in shear strength of soil.
- ✓ From the case studies available in literature, field measured displacement values plotted against the corresponding depth for 0.6 m thick diaphragm wall follows logarithmic curve with a correlation coefficient R^2 = 0.83. The maximum displacement value in plaxis 3D obtained for 0.6 m thick wall is close to the trend line of the above plot, hence it is valid.
- ✓ In the case of 1.0 m thick diaphragm wall, the field measured displacement values vs. depth follows polynomial curve with a correlation coefficient R^2 = 0.97 and the Plaxis 3D analysis values are close to the trend line. Hence the Plaxis 3D study is satisfactory.
- ✓ In the case of 1.1 m thick diaphragm wall, the field measured displacement values vs. depth follows linear fit with a correlation coefficient R^2 = 0.99 and the Plaxis 3D analysis values are close to the trend line. Hence the present study results are valid.

- ✓ In the case of diaphragm wall without anchors, full scale field test values (Muthukumaran et al., 2004) are satisfactorily matching up to location of -20m and for greater depth it varies. The variation may be due to the presence of different soil layers and the wall penetration depth.
- ✓ Comparison between the construction stage analysis results of diaphragm wall in the present study and full scale field test values by Tang and Zhao (2015) are satisfactorily matching and shows similar trends. The variation may be due to the variations in soil layers and the wall penetration depth. Hence the present study conducted by Plaxis 2D & 3D are satisfactory.

8.3 RECOMMENDATION

From the analysis it is found that the maximum bending moment of the sections 1, 3, 6 and 7 is reduced by 46%, 83.8%, 72.48% and 61.92% respectively, comparing with the actual section in the field. The percentage reduction in volume of concrete for the sections 1, 3, 6 and 7 is 45.45%, 32.45%, 49.45% and 51.22% respectively, comparing with the volume of concrete required for the actual diaphragm wall section.

From the above sections, for section 3 (T- section) and section 7 (compound section) it is found that the reduction in bending moment and volume of concrete required is maximum. Hence present study recommends section 3 and section 7 for the field application.

8.4 SCOPE FOR FUTURE WORK

- Similar study can be carried out for the diaphragm wall by varying the width of panel to optimize the panel size and best anchor location.
- Dynamic analysis can be performed to study the 3D effects on diaphragm wall for varying stiffness of the sections.

Anestis, S., Veletsions. and Younan Adel, H. (1997). "Dynamic response of cantilever retaining wall." *Journal of Geotechnical and Geo-environmental Engineering*, 123, 375-384.

Abraham, K. (2007). "Three dimensional behavior of retaining wall systems." *Ph.D. thesis,* Louisiana State University.

Anwar, Hossain, K. M. and Wright, H. D. (2004). "Experimental and theoretical behavior of composite walling under in plane shear for building." *Journal of Constructional Steel Research,* 60, 59-83.

Arablouei, A., Gharabaghi, A. R. M., Ghalandarzadeh, A., Abedi, K. and Ishibashi, I. (2011). "Effects of seawater-structure-soil interaction on seismic performance of caisson-type quay wall." *Computers and Structures*, 89(23-24), 2439-2459.

Cunningham, J. A. and Fernandez, J. I. (1972). "Performance of Two Slurry Wall Systems in Chicago." *Proceeding of Specialty Conference on Performance of Earth and Earth-Supported Structures, ASCE.*, 1(2), 1425-1449.

Cole, K. W. & Burland, J. B. (1972). "Observations of retaining wall movements associated with a large excavation." *Proc. 5th Eur. Conf. Soil Mech. Found. Engg,* Madrid., 445-453.

Clough, G., & O'Rourke, T. (1990). "Construction induced movements of in-situ walls." *Proceeding of Special Conference on Design and Performance of Earth Retaining Structures, ASCE.,* Cornell University, New York., 439-470.

Clough, G.W., Smith, E. W. and Sweeney, B. P. (1989). "Movement control of excavation support system by iterative design." *Foundation Engineering Current Principles and Practices,* ASCE, NY., 2, 869-882.

Clough, G. & Tsui, Y. (1974). "Performance of Tied-Back Walls in Clay." *Journal of Geotechnical Engineering Division,* ASCE, Ed., 10(12), 1259-1273.

Diao, Yu. and Zheng, Gang. (2008). "Numerical analysis of effect of friction between diaphragm wall and soil on braced excavation." *Journal of Cent. South Univ. Technol*. 15.

Deepankar, Choudhury. and Syed, Mohd, Ahmad. (2007). "Design of waterfront retaining wall for the passive case under earthquake and tsunami." *Applied Ocean Research.*, 29.

Gourvenec, S.M. and Powrie, W. (2000). “Three-dimensional finite element analyses of embedded retaining walls supported by discontinuous berms.” *Canadian Geotechnical Journal.*, 37, 1062-1077.

Garvin, R. & Boward, J. (1992). “Using slurry walls to protect a historic building: a case study.” *Slurry walls: Design, Construction and Quality Control ASTM Special Topic Publication* 11(29), 117-127.

Goldberg, D.T., Jaworski, W.E., and Gordon, M.D. (1976). “Lateral support systems and underpinning.” Rep.FHWA-RD-75-128, *Federal Highway Administration*, Washington.

Hsii, Sheng, Hsieh., Li-Hua, Wu., Ting-Mei, Lin., Jih-Cherng. and Wei-Ting, Hsu. (2011). “Performance of t-shaped diaphragm wall in a large scale excavation.” *Journal of geoengineering.*, 6, 135-144.

Hoe, N. H. (2007). “Numerical Modeling of Diaphragm Wall in Kuala Lumpur Limestone Formation.” *MSc Thesis*.

Hsieh, P. & Ou, C. (1997). “Use of the modified hyperbolic model in excavation analysis under undrained conditions.” *Geotechnical Engineering Journal.*, 28 (2), 123-150.

Ingale, S. A., Kale, S.Y., Khandekar, V. B., Maskar, A. D. and Banne, S. P. (2015). “Comparison Study of Static and Dynamic Earth Pressure behind the Retaining Wall.” *Journal of Mechanical and Civil Engineering*., 12(3), pp 77-84.

IStructE, (1989). “Soil-Structure interaction, the real behavior of structures.” *The institution of Structural Engineers*., 10.

Jacques, Monnet. and Dominique, Allagnat. (2006). “Interpretation of Pressure meter Results for Design of a Diaphragm Wall.” *Geotechnical Testing Journal*., 29.

Kavitha, P. and Sundaravadivelu, R. (2017).). “Soil Structure Interaction Analysis of a Berthing Structure Under Lateral Loading- By Numerical Approach.” ASME 2017 36th International Conference on Ocean, Offshore and Arctic Engineering, Trondheim, Norway., OMAE2017-62484.

Long, M. (2001). “Database for retaining wall and ground movements due to deep excavation.” *J. Geotech. & Geoenviron. Engg*, ASCE. 127(3), 203-224.

Lee, Jin., Kim, Jung. and Kim, Jae. Kwan. (2017). “Perfectly matched discrete layers for three-dimensional nonlinear soil-structure interaction analysis.” Computers and Structures., 165(2016), 34 - 47.

Moormann, C. (2004). “Analysis of wall and ground movement due to deep excavation in soft soil based on a new worldwide database.” *Soils and Foundations.*, 44(1), 87- 98.

Mosher, R. L. and Knowles, V. R. (1990). "Finite analysis study of tieback wall for Bonneville navigation locks." *Technical Report ITL-90-4, U.S. Army Engineer Waterways Experiment Station*, Vicksburg.

Mitew, M. (2002). "Numerical analysis of displacements of a diaphragm wall." *Warsaw University of Technology, Warsaw*, Poland.

Muthukkumaran, K., Sundaravadivelu, R. and Gandhi, S. R. (2007). "Effect of Dredging and Axial load on a berthing structure." *Internal journal of Geo engineering Case Histories.*, 1(2), 73.

Mohammad, S., Imanzadeh, S. and Bagherinia, K. H. (2003). "Characteristics of diaphragm wall lateral deformations and ground surface settlements: Case study in Iran-Ahwaz metro." *Tunnelling and Underground Space Technology.*, 35, 109-121.

Mohamed, Nageer. (2010). "Enhancement of steel sheet-piling quay walls using grouted anchors." *Journal of Soil Science and Environmental Management.*, 1(4).

Neelakantan, G., Budhu, M. and Richards, R. (1992). "Balanced Seismic design of Anchored Wall." *journal of Geotechnical Engineering.*,118, 660.

Osman, A. S. and Bolton, M. D. (2004). "A new design method for retaining walls in clay." *Can. Geotech. Journal*, 41(3), 453-469.

Ou, C., Hsieh, P. & Chion, D. (1993). "Characteristics of ground surface settlement during excavation." *Canadian Geotechnical Journal*, 30 (5), 758-767.

Orabi A.E., Sherbiny R.M.E. and Salem, A.A. (2017). "Evaluation of a proposed inverted U-shaped retaining wall". Proceedings of the Iff1 International Conference on Soil Mechanics and Geotechnical Engineering. 50 (3), 558-567.

Popa H., Batali L. and Mania, S. (2017). "Analysis of various constitutive laws for numerical modeling of a diaphragm wall". Proceedings of the 19 International

Conference on Soil Mechanics and Geotechnical Engineering., 259 (2), 367-375.

Rourke, O. D. (1993). "Base stability and ground movement prediction for excavations in soft clay." *Proceedings of the international conference on Retaining Structures,* Tomas Telford, London., 657-686.

Osman, A. S. and Bolton, M. D. (2006). "Design of braced excavations to limit ground movements. "*Proceedings of Institution of Civil Engineers-Geotechnical Engineering.*, 159 (3), 167-175.

Potts, D.M. and Day, R. A. (1991). "Effect of wall stiffness on bending moments." *Proceedings of the fourth international conference on piling and deep foundations* Stresa, Italy.

Psarropoulosa, P.N., Klonarisb, G. and Gazetasa, G. (2005). “Seismic earth pressures on rigid and flexible retaining walls.” *Soil Dynamics and Earthquake Engineering.*, 25.

Premalatha, P.V., Muthukkumaran, K. and Gandhi, S.R. (2011). “Behavior of piles supported berthing structure under lateral loads.” *Proceedings, Pan-Am CGS geotechnical conference*.

Rowe, P.W. (1957). “Anchored sheet-pile walls.” *Proceedings Institution Civil Engineers*, 27-69.

Susumu, Kurata., Hideo, Aron. and Toshiyuki, Yoki. (2000). “Earth quake resistance of anchored sheet pile bulk heads.” *Port and Harbour Technical Research Institute, Ministry of Transportation*, Japan.

Spiros, Costopoulos ,D. (1988). “Model behavior of pre stressed tie-back wall.” *Journal of geotechnical engineering.*, 114.

Sakas,K. and Tazakia, K. (2003). “Development and applications of diaphragm walling with special section steel-NS-Box.” *Tunneling and Underground Space Technology.*, 18, 283-289.

Subha, I.P. (2012). “Behavior of an open type berthing structure under earthquake condition, a numerical approach”. *International Journal of Engineering Research and Applications.*, 2(1).

Terzaghi, K. (1943). “Theoretical soil mechanics.” *Wiley*, New York.

Tschebotarioff, G.P. (1948). “Large scale earth pressure tests with model flexible bulkhead.” *Final Report, Bureau of Yards and Dock, Department of Navy* 1-112.

Tait, R. E. and Taylor, H. T. (1974). “Design, construction and performance of rigid and flexible bracing systems for deep excavation.” *Natl. meeting on water Res. Eng, Preprint*, ASCE., 2162.

Thomas, J. and Matthew, O. (1992). “Design of Tie- Back walls for Seismic Loading.” *Journal of Geotechnical Engineer*., 118, ASCE, 960.

Tuladhar, R., Maki, T. and Mutsuyoshi, H. (2008). “Cyclic behavior of laterally loaded concrete piles embedded into cohesive soil.” *Earthquake Engineering & Structural Dynamics*, 37(1), 43-59.

Vardanega, P.J. and Bolton, M.D. (2011). “Strength mobilization in clays and silts.” *Canadian Geotechnical Journal.*, 48(10), 1485-1503.

Woo S. M., Chien M. C., Hsieh H. S. and Guo G. R. (1991). “Remedial actions for a deep excavation; a case history.” *Proceedings of the Asian Regional Conference on Soil Mechanics and Foundation Engineering.*, 9.

Yegian, M. K., Chang, C. J., Mullen Chris, L. and George Mylonakis. (2001). "Soil-Structure Interaction under dynamic loading for Both Shallow and Deep Foundations." *Proceedings on Fourth International Conference on Resent Advances in Geotechnical Earth quake Engineering and Soil Dynamics and Symposium in Honor of Professor W.D. Liam Finn, San Diego*, California. Gr 6.

Ye, B., Ye, G.L., Nagaya, J. and Sugana, T. (2012). "Numerical simulation of shaking-table tests on soil-stabilized, geosynthetic-reinforced quay wall structures." *Geosynthetics International*., 19(1).

Yongjing, Tang. and Xihong , Zhao. (2015). "Field Testing and Analysis during Top-down Construction of Super-tall Buildings in Shanghai." *KSCE Journal of Civil Engineering*, 20(2), 647-661.